

Singularization of knots and closed braids

Thomas Fiedler

December 6, 2024

pour Séverine

Abstract

We give a method to construct non symmetric solutions of a global tetrahedron equation. The solutions gives rise to the first combinatorial 1-cocycles with values in the \mathbb{Z} -module of singular long knots with signed planar double points and which represent non trivial cohomology classes in the topological moduli space of long knots. The canonical resolution of the evaluation of the 1-cocycles on Hatcher's loop for a knot leads to a *wave* in the space of all long knots. Each knot invariant becomes a new invariant by evaluating it on the wave. In particular, the Kauffman-Vogel HOMFLYPT polynomial for singular knots applied to our 1-cocycles on Hatcher's loop leads to the first quantum knot polynomials which are *not multiplicative* for the connected sum of knots.

A variation of the combinatorial method produces universally defined non trivial combinatorial 1-cocycles for all closed n-braids which are knots. We use them to formulate the *entropy conjecture* for pseudo-Anosov braids, which is an analogue of the volume conjecture for hyperbolic knots, and we give some evidence for it.

1

Contents

1	Introduction and basic definitions	2
----------	---	----------

¹2000 *Mathematics Subject Classification*: 57M25 *Keywords*: singularization, 1-cocycle invariants, global tetrahedron equation, cube equations, entropy conjecture

2	Main results	23
2.1	The 1-cocycle R_1 of degree 1 for long knots	24
2.2	The 1-cocycle R_2 of degree 2 for long knots	35
2.3	The 1-cocycles R_1 and R_2 for closed n-braids	40
3	Examples and applications	50
3.1	Long knots	50
3.2	Closed braids	76
4	Proofs	83
4.1	Generalities and reductions by using singularity theory	83
4.2	Reidemeister II moves in a cusp and in a flex	94
4.3	Simultaneous Reidemeister moves	96
4.4	Tetrahedron equation	100
4.5	Cube equations	125
4.6	Moving cusps	140

1 Introduction and basic definitions

This paper contains a combinatorial counterpart of a not yet existing "embedded Kontsevich-like integral for 1-parameter families of long knots".

In the construction of the *Kontsevich integral* one considers a Morse knot K in $\mathbb{C} \times \mathbb{R}$ as a 1-parameter family of 0-dimensional links, namely the intersections of K with the horizontal planes \mathbb{C} . Each plan \mathbb{C} contains a finite number of *horizontal chords* connecting the intersection points of K with the plan. The Kontsevich integral is then the integration of some closed differential form with values in the Hopf algebra generated by abstract finite chord diagrams (corresponding to chords in different horizontal plans) modulo some relations. The resulting integral is the universal invariant of finite type and it has a natural filtration by the number d of chords, called the degree (see [37], [3]). It can be seen as a 0-cocycle with values in some Hopf algebra of chord diagrams for the space of all knots.

In this paper we consider 1-parameter families of long knots (and more generally of string links) in $\mathbb{C} \times \mathbb{R}$.

Definition 1 *A long knot K is an oriented smooth knot which coincides with the real axis in \mathbb{C} outside a compact set. A n-string link K is a n-component*

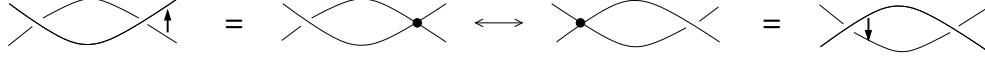


Figure 1: Forbidden move

link where each component is parallel to a long knot outside some compact set.

Examples of n -string links are n -cables of framed long knots and n -braids.

First of all we choose an abstract closure of the string link to an oriented circle and we choose a point at infinity in the boundary of the string link (in the case of long knots there aren't any choices). So, a string link is for us a circle with only a part of it embedded in 3-space and with a marked point in the remaining (abstract) part.

For each generic long knot (or string link) we have a finite number of *vertical chords* (replacing the finite number of horizontal chords in Kontsevich's approach), i.e. chords connecting points with the same \mathbb{R} -coordinate. These points correspond to the crossings for the natural projection of the knot into $\mathbb{C} \times 0$.

Definition 2 *Let K be an isotopy class of a long knot, i.e. a long knot up to smooth isotopy of long knots which is the identity outside a compact set, and let d be a natural number.*

An embedded chord diagram of degree d for K is a trivalent graph obtained from a generic diagram for K together with exactly d vertical chords. The chords are oriented from the undercross to the overcross and they are signed by the usual writhe of the corresponding crossing. An isotopy of an embedded chord diagram is a smooth isotopy of the trivalent graph and such that the vertical chords stay vertical all the time.

In particular, each embedded chord diagram decomposes in a canonical way into a knot part and into the chords. If we contract the vertical chords and we drop the sign then we obtain a *singular knot* in the usual sense (see e.g. [33]). However, our notion of isotopy is a refinement of the usual notion of isotopy for singular knots, namely we do *not* allow the move which corresponds to reversing the orientation of a vertical chord. We illustrate the forbidden move in Fig. 1. So, it is natural to call the double points *planar*.

To each embedded chord diagram corresponds an underlying abstract chord diagram in the following way: the knot is an oriented circle with a

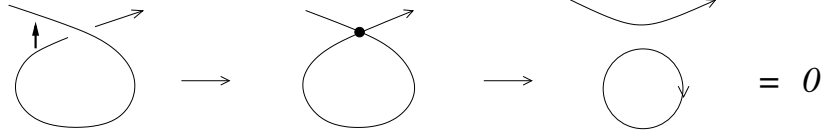


Figure 2: Smoothing link and embedded 1T-relation

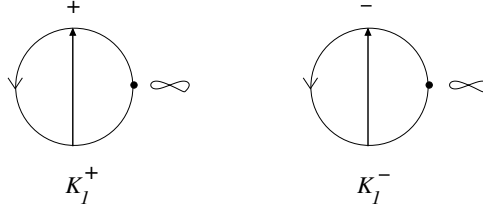


Figure 3: Underlying Gauss diagrams for K_1

marked point, which corresponds to the point at infinity, and oriented signed arrows which connect points on the circle and which correspond to the oriented signed vertical chords. This is usually called a *Gauss diagram of K* if all crossings of K are considered (see [42], [14]). So, the underlying abstract chord diagram is a sub-diagram of a Gauss diagram. We will shortly call it the *underlying Gauss diagram*.

In the first part of this paper we consider embedded chord diagrams of degree 1. Contracting the chord and smoothing the double point with respect to the orientation leads to an oriented link with one more component, which we call the *smoothing link*. We show an example in Fig. 2.

Let K be an isotopy class of a long knot (or n -string link).

Definition 3 K_1 is the free \mathbb{Z} -module generated by all isotopy classes of embedded chord diagrams of degree 1 for K with the underlying Gauss diagrams shown in Fig. 3 modulo the following embedded 1T-relation: an embedded chord diagram is 0 in K_1 if and only if the corresponding smoothing link is a split link which contains a closed trivial knot as a component (e.g. as in Fig. 2). Let $K_1 = K_1^+ \oplus K_1^-$ denote the natural splitting of K_1 with respect to the sign of the double points.

Instead of a 0-cocycle with values in some algebra of abstract chord diagrams (the Kontsevich integral) we construct now a 1-cocycle, called R_1 ("R" stands for Reidemeister), with values in K_1 . Instead of integrating

a differential form we introduce a *discrete combinatorial integration*: in a generic 1-parameter family of diagrams only a finite number of Reidemeister moves appear and we associate an element of K_1 to each (co-oriented) Reidemeister move of type III and of type II (see e.g. [11] for the definition of Reidemeister moves). Instead of showing that a differential form is closed we show in a combinatorial way (and by using some global singularity theory for projections of knots into the plan) that the sum of the contributions of the Reidemeister moves does not change when non generic diagrams (as e.g. quadruple crossings or crossings in an auto-tangency) occur in a generic deformation of the 1-parameter family.

The value of R_1 on a loop in the *topological moduli space* M_K , i.e. the space of all string links isotopic to K , is an invariant of the homology class of the loop. In order to obtain an isotopy invariant of K itself we need a canonical choice of a loop in M_K . There are two canonical loops associated to each long knot and which are homologically non trivial for non trivial knots: Gramain's loop, denoted by $rot(K)$, and Hatcher's loop, denoted by $hat(K)$. *Gramain's loop* is induced by the rotation of the 3-space around the long axes of the long knot (see [25]). *Hatcher's loop* is defined as follows: one puts a pearl (i.e. a small 3-ball B) on the closure of the long framed knot K in the 3-sphere. The part of K in $S^3 \setminus B$ is a long knot. Pushing B once along the knot with respecting the framing induces Hatcher's loop in M_K (see [27]). The homology class of $rot(K)$ does not depend on the framing of K and changing the framing of K adds multiples of $rot(K)$ to $hat(K)$. Notice that Hatcher's loop has a canonical orientation induced by the orientation of the long knot. The same loops are still well defined and non trivial for those n -string links which are n -cables of a non trivial framed long knot.

The complement in \mathbb{R}^3 of a general n -string link T for $n > 1$ does not contain any incompressible torus and its topological moduli space is contractible. In this case we consider the string link T as a tangle in a cube I^3 and we chose a partial closure σ of T outside the cube as shown e.g. in Fig. 4. We consider now the resulting tangle $T \cup \sigma$ of one component again as a long knot in 3-space and we can apply Hatcher's loop to it. R_1 of this loop is an isotopy invariant of the string link T (but which depends of course of the chosen closure σ).

Gramain's and Hatcher's loop have nice geometric realizations. Gramain's loop can be represented by pushing the knot through a curl as shown in Fig. 5 (see [47]). Hatcher's loop corresponds to the following loop: we go on K from ∞ to the first crossing. If we arrive at an undercross then we

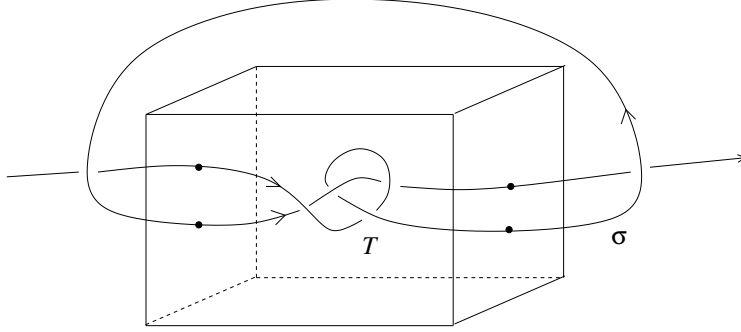


Figure 4: A partial closure of a tangle to a long knot

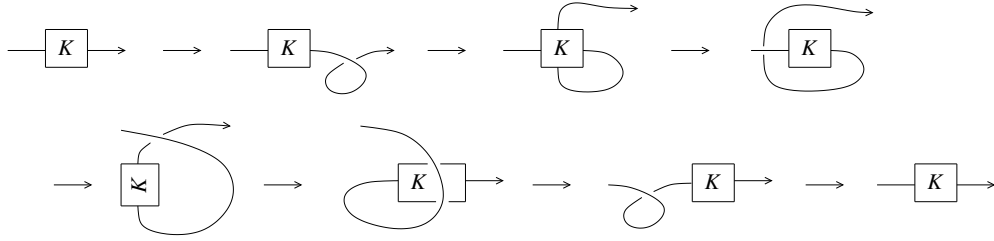


Figure 5: Nice realization of Gramain's loop

move the branch of the overcross over the rest of the knot up to the end of K . If we arrive at an overcross then we move the branch of the undercross under the rest of the knot up to its end. We continue the process up to the moment when we obtain a diagram which is isotopic to our initial diagram of K (see [27]), see Section 3.1 for examples. We can of course consider the analog loops for cables of long framed knots. (In Gramain's loop we have just at the end to push a full twist of the n -strands back through the knot and in Hatcher's loop we move bunches of n strands.)

We prove that $R_1(\text{rot}(K)) = 0$ for each long knot K . So, the interesting loop is Hatcher's loop and $R_1(\text{hat}(K))$ does not depend on the framing of K . Notice that Hatcher has proven that $\text{rot}(K)$ and $\text{hat}(K)$ represent linearly dependent homology classes in $H_1(M_K; \mathbb{Q})$ if and only if K is a torus knot (see [27]). (It is well known that the isotopy classes of long knots are in 1-1 correspondence to the isotopy classes of closed knots in S^3 .) Consequently, $R_1(\text{hat}(K)) = 0$ for all torus knots K too.

We have calculated that for the figure-eight knot $R_1(\text{hat}(4_1)) = 0$ but already for the connected sum $R_1(\text{hat}(4_1 \# 4_1)) \neq 0$ (we use the standard



Figure 6: $R_1(\text{hat}(4_1 \# 4_1))$

notations for knots from the *knot atlas* but we distinguish a knot from its mirror image). Its precise value is given in Fig. 6, where as usual in the figures vertical chords are contracted. Notice that the embedded 1T-relation does not annihilate R_1 because the compact knot in the smoothing links is not the trivial knot and note also that the value in K_1 would vanish in this example without the signs of the double points. (In fact, it comes from the symmetry of 4_1 that Hatcher's loop is in this case the double covering of our loop.)

But already $R_1(\text{hat}(5_2^+))$ (which we give in Fig. 7, where the "+" denotes the knot 5_2 which has a diagram with only positive crossings) is highly non trivial. In particular, each summand is an irreducible singular knot. Notice that all four summands are easily distinguished by the sign of the double point together with the linking number of the two components of the smoothing link. This linking number vanishes only for the last summand in K_1^+ , but one easily shows with e.g. the Conway polynomial that the smoothing link is not a split link and hence the embedded 1T-relation does not apply to it.

The above examples show that the induced map

$$\pi_0(\Pi_K M_K) \rightarrow R_1(\text{hat}(K)) \in K_1 = K_1^+ \oplus K_1^-$$

is non trivial.

We can fix now any standard 2-tangle, e.g. any 2-braid with a fixed odd number of crossings, and replace all double points in K_1^+ or in K_1^- by this 2-tangle. For example, we could replace each positive double point by a negative crossing and each negative double point by a positive crossing. Let us call this the *canonical resolution of $R_1(\text{hat}(K))$* . The result is an integer combination of ordinary long knots and each invariant derived from this combination of knots is an invariant of our original knot K . Moreover, we could iterate our construction and apply $R_1(\text{hat})$ to each of the new knots. The result is the *canonical wave of K* in $\Pi_K M_K$ which starts from the given

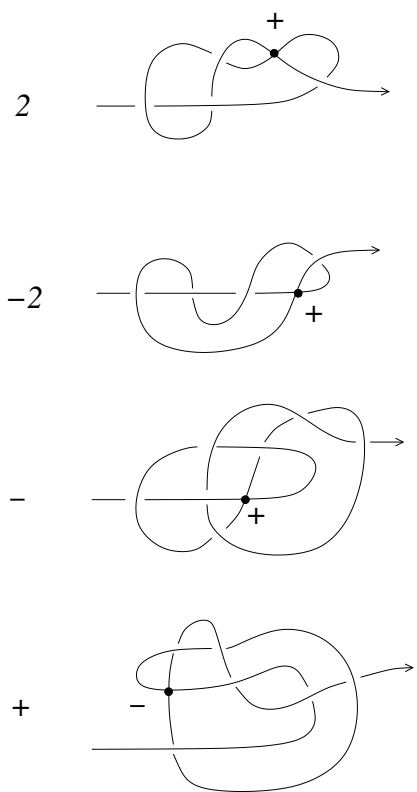


Figure 7: $R_1(\hat{5}_2^+)$

knot K . For example, $R_1(\text{hat}(5_2^+)) \in K_1^-$ consists of a single singular knot. If we replace the double point by a negative crossing then we get back of course our original knot 5_2^+ . But if we replace it by a positive crossing then we obtain the knot 7_3^+ . This looks to us already as a candidate for a complete invariant of the knot 5_2^+ even without the use of any iterations of our construction. More precisely:

Question 1 *Let K be a knot such that $R_1(\text{hat}(K)) \in K_1^-$ consists of a single knot with coefficient $+1$ and which becomes the knot 7_3^+ under a positive resolution of its double point. Does this imply that the negative resolution and hence $K = 5_2^+$?*

Replacing the positive double points by negative crossings for $R_1(\text{hat}(5_2^+)) \in K_1^+$ leads to a linear combination of the knots 3_1^+ , 0_1 and 8_{20} (with writhe $w = +2$ for a minimal diagram), more precisely to $2(3_1^+) - 2(0_1) - 8_{20}$. The wave is *contracting* (i.e. ends with the element 0) for all torus knots and for the knot 4_1 but as shown above it seems very likely that it is *expanding* (i.e. contains knots with arbitrary high crossing number) already starting from the knot 5_2^+ .

It is well known (see [1]) that the couple of Vassiliev invariants $(v_2(K), v_3(K))$ is a complete invariant for torus knots (and it distinguishes also 4_1 from all torus knots). *A optimistic conjecture would be that (v_2, v_3) evaluated on the canonical wave of K (i.e. each iteration gives an unordered linear combination of couples (v_2, v_3)) separates already all knots.* We show the beginning of the wave $(v_2(K), v_3(K))$ for 5_2^+ in figure Fig. 8. Notice that even the trivial invariant, which associates 1 to each knot, becomes an interesting invariant when it is evaluated on the canonical wave because it distinguishes already 4_1 from 5_2 (the augmentation is -1 in K_1^+ and $+1$ in K_1^- for the knot 5_2 and two times 0 for the knot 4_1).

Notice also that cabling a framed knot defines another well known wave in the space of all knots. However, quantum knot invariants are dominated by finite type invariants (see e.g. [3]) but the latter behave functorial under cabling and twisted cabling (see e.g. [5]). Hence this wave does not lead to new knot invariants.

The above examples suggest that the augmentation of $R_1(\text{hat}(K))$ in K_1 is always 0, but we have no proof for this.

In order to obtain numerical knot invariants from the Kontsevich integral one has to use weight systems [3]. In our case, in order to obtain calculable and very powerful knot invariants from $R_1(\text{hat}(K))$ we use quantum

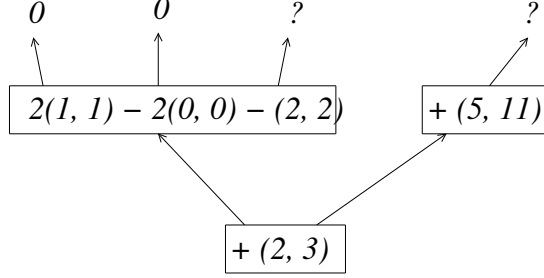


Figure 8: The wave (v_2, v_3) generated by $R_1(\text{hat})$ starting from 5_2^+

polynomials for singular links. We replace each singular knot in $R_1(\text{hat}(K))$ (or even of its restriction to K_1^+ or to K_1^-) by a quantum invariant for singular links, e.g. the HOMFLYPT polynomial P for singular links defined by Kauffman-Vogel (see [33]). We recall its skein relations in Fig. 9. It is an invariant of regular isotopy for singular links and it becomes an isotopy invariant after normalization with $v^{-w(K)}$, where $w(K)$ is the usual writhe of the diagram of the singular knot K . The double points come with a sign in our case. There is an evident refinement of the Kauffman-Vogel invariant by replacing A and B by A^+ respectively B^+ for a positive double point and by A^- respectively B^- for a negative double point. Indeed, at most one double point enters into a skein relation and hence Kauffman-Vogel's proof extends word for word. But the former relation $A - B = z$ splits now into two relations $A^+ - B^+ = z$ and $A^- - B^- = z$.

We denote by $PR_1(\text{hat}(K))$ the resulting quantum invariant of K .

Instead of refining the Kauffman-Vogel invariant we could of course also simply split $PR_1(\text{hat}(K))$ into

$$P(R_1(\text{hat}(K)) \in K_1^+) \oplus P(R_1(\text{hat}(K)) \in K_1^-).$$

(Notice that instead of the HOMFLYPT invariant for singular links we could also use the refined Kauffman polynomial for singular links [33] and the Alexander or Jones polynomial for singular links via state sum models [17].)

Using the relations $A^- = z + B^-$ and $B^+ = A^+ - z$ the invariant $PR_1(\text{hat}(K))$ becomes a Laurent polynomial in $\mathbb{Z}[A^+, B^-, z, z^{-1}, v, v^{-1}]$. Let $\delta = (v - v^{-1})/z$ denote the HOMFLYPT polynomial of the trivial 2-component link. One easily calculates from $R_1(\text{hat}(4_1 \# 4_1))$ that

$$PR_1(\text{hat}(4_1 \# 4_1)) = (A^+ - B^- - z)\delta P_{4_1}^2,$$

$$\begin{aligned}
& \text{Crossing with dot on top-left} = \text{Crossing} - A \text{ Crossing with dot on top-right} \\
& \text{Crossing with dot on bottom-left} = \text{Crossing} - B \text{ Crossing with dot on bottom-right} \\
& \text{Loop with dot on top} = v \text{ Crossing} \\
& \text{Loop with dot on bottom} = 1 \\
& \text{Crossing} - \text{Crossing with dot on top-left} = z \text{ Crossing with dot on top-right}
\end{aligned}$$

Figure 9: Kauffman-Vogel skein relations for HOMFLYPT of singular links

where P_{4_1} is the usual HOMFLYPT polynomial of the figure eight knot.
(The invariant changes the sign if we change the orientation of the loop.)

Remark 1 *This example shows that the quantum knot polynomial $PR_1(\text{hat}(K \# K'))$ is not always determined by $PR_1(\text{hat}(K))$ and $PR_1(\text{hat}(K'))$, in contrast to all other known quantum knot polynomials (which make no explicit use of the knot group)!*

One easily calculates from $R_1(\text{hat}(5_2^+))$ that

$$PR_1(\text{hat}(5_2^+)) = (v^{-1} - v)P_{5_2^+} + A^+v^{-4}[z^{-1}(v - v^{-1}) + z(v^{-1} - v + 2v^3) - z^3v] - B^-v^{-4}[z^{-1}(v - v^{-1}) + z(-v^{-3} + v^{-1} + 2v) + z^3(v^{-1} + v)]$$

(For comparison, the HOMFLYPT polynomial $P_{5_2^+} = -v^{-6} + v^{-4} + v^{-2} + z^2(v^{-4} + v^{-2}).$)

Remark 2 *An easy calculation shows that for the substitution $A = vz/(v - v^{-1})$ and $B = v^{-1}z/(v - v^{-1})$ into PR_1 the embedded 1T-relation disappears for each string link, i.e. the invariant of the corresponding singular string link from the embedded 1T-relation is 0.*

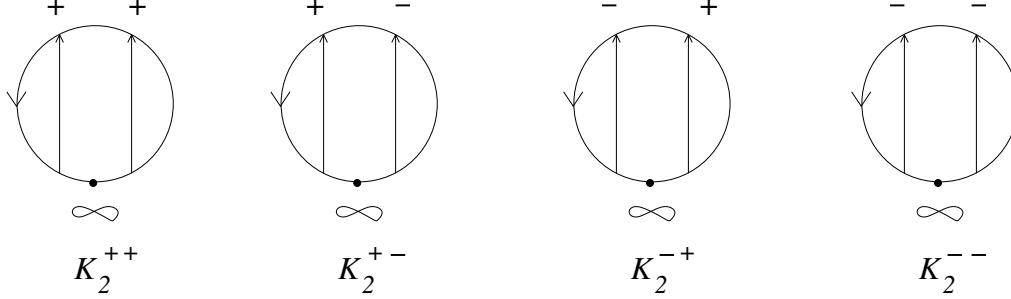


Figure 10: Underlying Gauss diagram for R_2 in K_2

Remark 3 $R_1(\text{hat}(K))$ is not an invariant of finite type even for long knots. Indeed, switching a crossing of K leads in general to a new knot K' . $R_1(\text{hat}(K))$ takes its values in K_1 and $R_1(\text{hat}(K'))$ in K'_1 . But the intersection of these two modules is 0 if K is not isotopic to K' . Indeed, even if a singular knot is in the intersection of K_1 with K'_1 the double points have necessarily different signs. Hence no non trivial combination of the invariants could sum up to 0.

We call $R_1(\text{hat}(K))$ and all derived quantum invariants *1-cocycle invariants of degree 1* for K . But notice that our notion of a degree (compare Definition 2) is very different from Vassiliev's notion, see [50] and also [26].

We consider now embedded chord diagrams of degree 2 and we construct 1-cocycle invariants of degree 2. The underlying Gauss diagrams (together with their notations) are shown in Fig. 10.

Definition 4 K_2 is the free \mathbb{Z} -module generated by all isotopy classes of embedded chord diagrams of degree 2 for K with the underlying Gauss diagrams shown in Fig. 10 modulo the generalized embedded 1T-relation: an embedded chord diagram is 0 in K_2 if and only if at least one of the two corresponding smoothing links is a split link which contains a closed trivial (non singular) knot as a component. Let $K_2 = K_2^{++} \oplus K_2^{+-} \oplus K_2^{-+} \oplus K_2^{--}$ denote the natural splitting of K_2 with respect to the signs of the double points.

Using the same techniques as for the construction of R_1 we construct a 1-cocycle R_2 of degree 2 with values in K_2 . We have calculated only very few examples by hand because of their complexity: $R_2(\text{rot}(3_1^+)) = R_2(\text{rot}(4_1)) = 0$. But $R_2(\text{hat}(4_1))$ is already highly non trivial. It is given in Fig. 11, where knots in the same line are in the same submodule. We have calculated

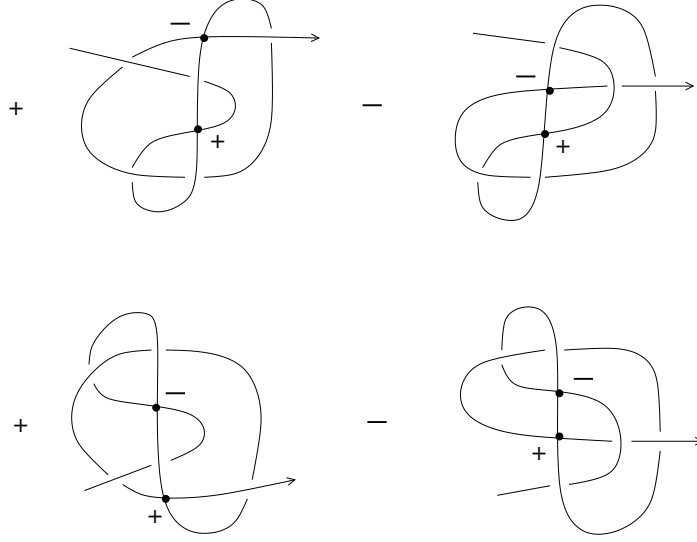


Figure 11: $R_2(\text{hat}(4_1))$

just the part of $PR_2(\text{hat}(4_1))$ in K_2^{+-} , which we denote by $PR_2^{+-}(\text{hat}(4_1))$.

$$PR_2^{+-}(\text{hat}(4_1)) = A_+B_-(v^{-2}\delta(\delta + zv) - (\delta + zv)(\delta - zv^{-1})) - B_-(v^{-1}\delta + z - v(\delta + zv) + zv^{-2}(-1 - z^2 + v^2 + v^{-2}))$$

where δ denotes as usual the HOMFLYPT polynomial of the trivial link of two components.

Notice the apparent symmetry of the value of $R_2(\text{hat}(4_1))$, which seems to reflect the fact that the knot 4_1 is amphichiral. The canonical resolutions do not lead to interesting new knots, but a partial canonical resolution (i.e. exactly for one of the double points we take the resolution which corresponds to its sign) leads e.g. to the knot 6_1 .

It is amazing that we can construct another 1-cocycle of degree 2 by using the underlying Gauss diagrams shown in Fig. 12. However, in all examples it has turned out to be trivial and therefore we will not give it in this paper. Notice that if we take the product of the two signs and we sum up over all such sub-diagrams in the Gauss diagram of a knot K then we obtain exactly one of the Polyak-Viro formulas for the Vassiliev invariant $v_2(K)$ (see [42], [43]). In contrast to that the Gauss diagrams shown in Fig. 10 do not lead to a 0-cocycle for knots even for regular isotopy (but they lead to a non trivial 1-cocycle).

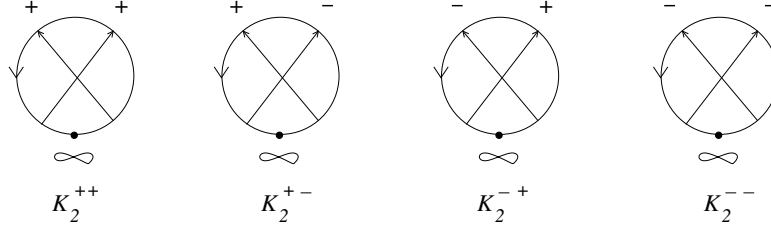


Figure 12: Underlying Gauss diagram for the trivial 1-cocycle of degree 2

Our philosophy, which is at the origin of this paper, is that for *classifying a topological object one has to use the topology of its topological moduli space*. For most knots in 3-manifolds the topological moduli space is just a contractible space. The most interesting cases of knots with a non contractible topological moduli space are non trivial long knots in 3-space and knots in the solid torus which are not contained in a 3-ball neither isotopic to the core of the solid torus. A particular interesting (and well studied) case of such knots in the solid torus are closed n -braids. Therefore we adapt our approach also to the case of those closed n -braids which are knots in the solid torus.

Let V be the standard solid torus in $\mathbb{C} \times \mathbb{R}$ which intersects $\mathbb{C} \times 0$ in an annulus around the origin. There are two 1-parameter families of diffeomorphisms of the solid torus: one is induced by the rotation of the 3-space around the axes $0 \times \mathbb{R}$ and it is called $rot(V)$. The other is induced by the rotation of V around its core $\{|z| = 1\} \times 0$ and it is called $hat(V)$. Given a knot $\hat{\beta}$ in the solid torus which is a closed braid (i.e. its projection into $\mathbb{C}^* \times 0$ is transverse to the fibers of the function $arg(z) : \mathbb{C}^* \rightarrow S^1$) the families $rot(V)$ and $hat(V)$ induce two loops, called $rot(\hat{\beta})$ and $hat(\hat{\beta})$, in the topological moduli space $M_{\hat{\beta}}$ of all closed braids isotopic to $\hat{\beta}$ in V (here $\hat{\beta}$ denotes as usual the standard closure of the braid in the solid torus). It is well known that closed braids are isotopic as knots in V if and only if they are isotopic as closed braids in V , see e.g. [40].

In the Gauss diagram of a closed braid there is no longer a marked point at infinity. But we can attach a natural number to each arrow. This number corresponds to the homology class in $H_1(V; \mathbb{Z}) \cong \mathbb{Z}$ represented by the loop which consists of the arrow together with the part of the closed braid which goes from the head of the arrow to its foot. We define now $\hat{\beta}_1$ completely analog to K_1 besides that we don't need any embedded $1T$ -relation and that the underlying Gauss diagrams are those given in Fig. 13.



Figure 13: Underlying Gauss diagram for $\hat{\beta}_1$

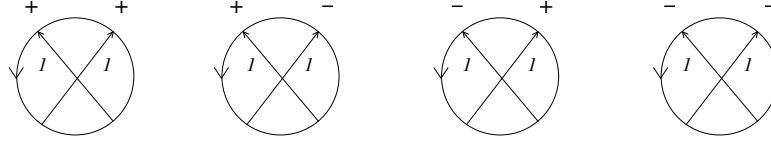


Figure 14: Underlying Gauss diagram for $\hat{\beta}_2$

$\hat{\beta}_2$ is also analog to K_2 besides that the underlying Gauss diagrams are those given in Fig. 14. However, we have to take the quotient of $\hat{\beta}_2$ by some new relation. Let us call *head arc* the arc in the underlying Gauss diagram which connects the two heads of the arrows.

Definition 5 *An embedded chord diagram is called trivial if the two chords have different signs and if the 2-component link which is obtained from contracting the chords and smoothing both double points against the orientation leads to an (unoriented) split link for which the component which contains the head arc is a trivial knot in V . The embedded 2T-relation is now: an embedded chord diagram in $\hat{\beta}_2$ is 0 if and only if it is trivial.*

We give an example in Fig. 15.

Using the techniques from the previous parts we construct a 1-cocycle R_2 with values in $\hat{\beta}_2$ and an almost 1-cocycle R_1 with values in $\hat{\beta}_1$. The 1-cochain R_1 is a 1-cocycle only in the complement of all braid diagrams with an ordinary self-tangency in an ordinary flex (compare Section 4.2). These 1-cocycles are universally defined for all closed n-braids which are knots.

Hatcher has proven a result for closed braids which is analog to his result for long knots: $rot(\hat{\beta})$ and $hat(\hat{\beta})$ represent linearly dependent homology

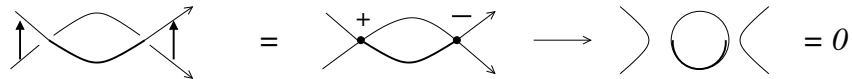


Figure 15: Embedded 2T-relation

classes in $H_1(M_{\hat{\beta}}; \mathbb{Q})$ if and only if $\hat{\beta}$ is isotopic to a torus knot in ∂V (personal communication, see also Section 3.2). On the other hand, it is well known that a braid β , which closes to a knot, is *periodic* if and only if $\hat{\beta}$ is isotopic to a torus knot in ∂V (see e.g. [7]).

We see immediately that $R_1(\text{rot}(\hat{\beta})) = 0$ and $R_2(\text{rot}(\hat{\beta})) = 0$ for all closed n -braids because $\text{rot}(\hat{\beta})$ is just an isotopy of diagrams without any Reidemeister moves at all. Hence $\text{hat}(\hat{\beta})$ is again the interesting loop (justifying its notation). It corresponds to pushing a full twist $\Delta^2 = (\sigma_1 \sigma_2 \dots \sigma_{n-1})^n$ through the closed braid (we use the standard notations from e.g. [6]).

It follows now from Hatcher's result that $R_2(\text{hat}(\hat{\beta})) = 0$ for each periodic n -braid which closes to a knot.

Given $\hat{\beta}$ as a cyclic braid word $R_1(\text{hat}(\hat{\beta}))$ is invariant under Reidemeister III moves but it can change under certain Reidemeister II moves of $\hat{\beta}$, see Section 4.2. Therefore we have to fix $\hat{\beta}$ up to Reidemeister III moves.

$R_1(\text{hat}(\hat{\beta}))$ for the 3-braid $\sigma_1 \sigma_2^{-1}$ and for the 4-braid $\sigma_1 \sigma_2 \sigma_3^{-1}$ are given in Fig. 16 and Fig. 17. $R_2(\text{hat}(\hat{\beta}))$ for the 3-braid $\sigma_1 \sigma_2^{-1}$ is given in Fig. 18, where each line corresponds to a different sub-module. (We do not draw the standard closure. The singular knots in the same sub-module are easily distinguished just by linking numbers of components of certain smoothings of the double points. The embedded 2T-relation does not annihilate the two singular closed braids with double points of different signs in Fig. 18 because the smoothings do not lead to a split link.)

The Nielsen-Thurston classification says that a braid which is not periodic (i.e. some power of it is isotopic to a power of the full twist) neither composite (i.e. there is a not boundary parallel incompressible torus in the complement of its closure in V) is of pseudo-Anosov type (see e.g. [13]). The *entropy* $h(\beta)$ of a pseudo-Anosov braid is known to be equal to $\log(\lambda_\beta)$, where $\lambda_\beta > 1$ is the *stretching factor* of one of the two transverse invariant measured foliations associated to β (see [13]). The foliation is called *transverse orientable* if no arc transverse to the foliation intersects a leaf positively and negatively (or equivalently, if the invariant foliations have odd order singularities at all punctures and all interior singularities are of even order, see e.g. [2], [36]).

We consider now the quantum invariant $PR_1(\text{hat}(\hat{\beta}))$ in the HOMFLYPT skein module of the solid torus (for the definition of skein modules see [44], [49]) as in the case of string links, which is obtained from $R_1(\text{hat}(\hat{\beta}))$ by applying the Kauffman-Vogel skein relations (here we do not need to normalize because Reidemeister I moves do not appear in an isotopy of closed braids and moreover we set $A = A^+ = A^-$ and $B = B^+ = B^-$). Setting

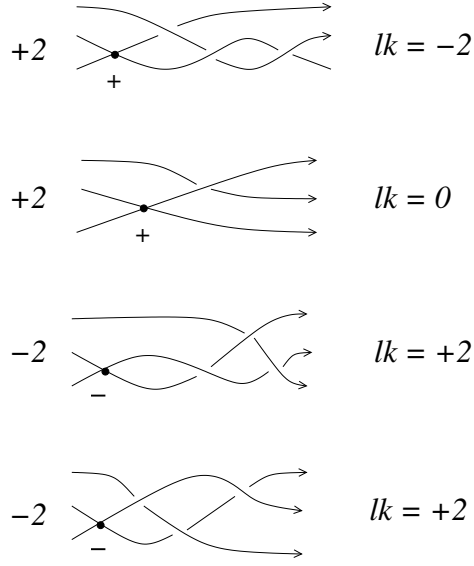


Figure 16: $R_1(\hat{hat}(\sigma_1 \hat{\sigma}_2^{-1}))$

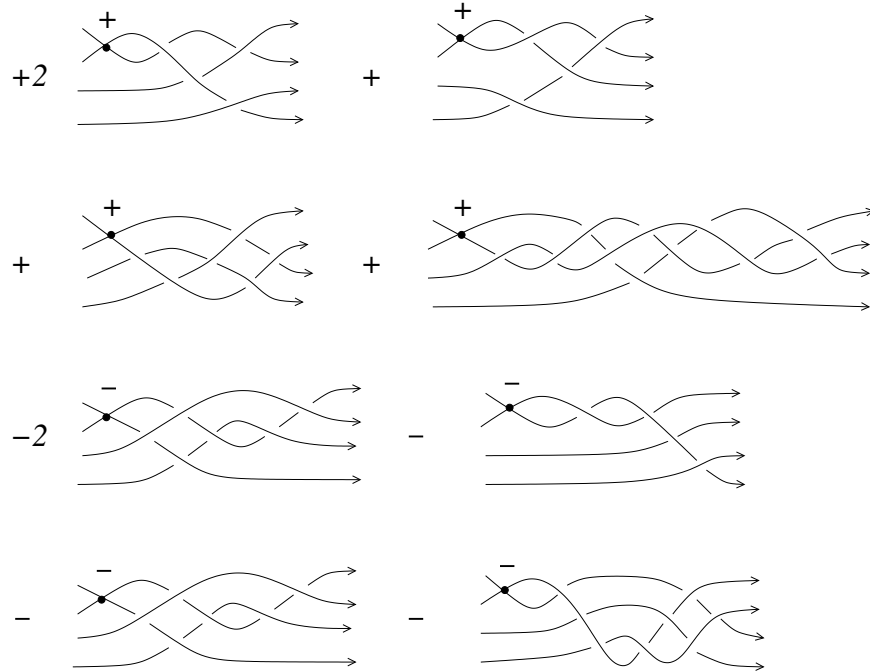


Figure 17: $R_1(\hat{hat}(\sigma_1 \hat{\sigma}_2 \sigma_3^{-1}))$

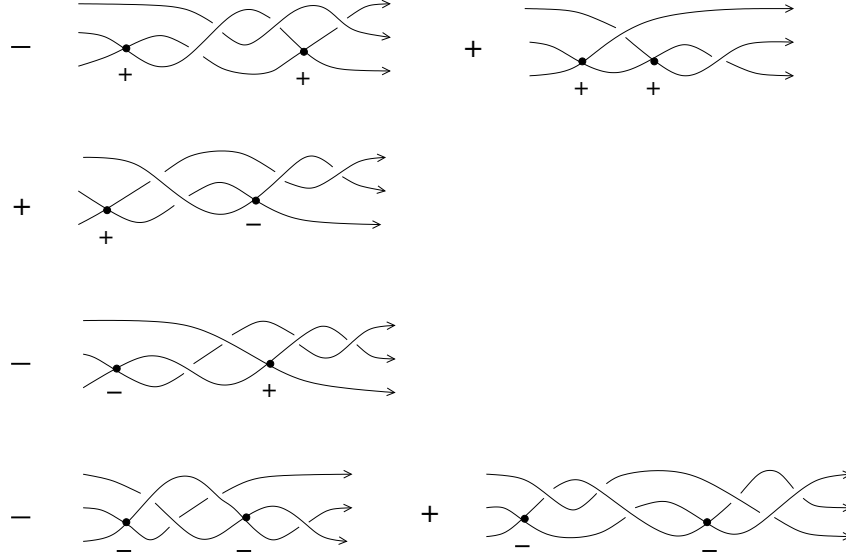


Figure 18: $R_2(\text{hat}(\sigma_1 \hat{\sigma}_2^{-1}))$

$v = 1$ and substituting $z = t^{1/2} - t^{-1/2}$ we obtain an element $\Delta R_1(\text{hat}(\hat{\beta}))$ in the Alexander skein module of the solid torus. Using skein relations we express $\Delta R_1(\text{hat}(\hat{\beta}))$ in the standard basis of the Alexander skein module, namely the isotopy classes in V of all those closed positive permutation braids which stay permutation braids under cyclic permutations. Each closed permutation braid $\hat{\sigma}$ is now replaced by its 2-variable Alexander polynomial $\Delta_{\hat{\sigma} \cup L}(u, t) = \det(u \text{Id} - B_{\sigma}^r(t))$. Here $L = (0 \times \mathbb{R}) \cup \infty \subset S^3$ is the braid axes and $B_{\sigma}^r(t)$ is the reduced Burau matrix for σ . (The variable u corresponds to the meridian of L and the variable t corresponds to the meridian of $\hat{\sigma}$.) The result of the substitution $\Delta R_1(\text{hat}(\hat{\beta}))(A, B, t, u)$, with $A - B = t^{1/2} - t^{-1/2}$, is a Laurent polynomial in $t^{1/2}$ and a polynomial in u of degree $n - 1$. We specialize the invariant by $t = -1$ and by the *magic relation* $A + B = 1$. The result is a polynomial in u of degree $n - 1$ which we denote shortly by $\Delta R_1(\text{hat}(\hat{\beta}))(u)$. Let u_{β} denote the zero of $\Delta R_1(\text{hat}(\hat{\beta}))(u)$ with the greatest absolute value.

Given $\hat{\beta}$ as the closure of a braid word we define the iteration $\hat{\beta}^m$ for each $m \in \mathbb{N}$ as the closure of the braid which is obtained by repeating m times the given braid word. We are now ready to formulate the *entropy conjecture*.

Conjecture 1 *Let β be a braid word which represents a pseudo-Anosov n -*

braid which closes to a knot. Then

$$\lim_{m \rightarrow \infty} \log |u_{\beta^{mn+1}}| / (mn + 1) = h(\beta).$$

So, in particular the asymptotic should not depend on the chosen braid word.

Moreover, if the associated invariant measured foliation is transverse orientable and the cyclical braid word is the shortest amongst all cyclical braid words which represent the isotopy class of $\hat{\beta}$ then already

$$\log |u_{\beta}| = h(\beta).$$

The conjecture needs some explanations. We do not consider all iterations of β but only a subsequence because our invariant is only defined for those braids which close to a knot. Following Artin, a n -braid can be considered as an automorphism of the free group F_n (in fact, the fundamental group of the n -punctured disc with the base point on the boundary of the disc). One fixes a system of generators x of F_n and one defines the *growth rate* of β by

$$GR(\beta) = \sup_{x \in F_n} \lim_{k \rightarrow \infty} |\beta^k(x)|^{1/k}$$

where $|\cdot|$ denotes the reduced word length with respect to the generators x and their inverses. It is well known that $GR(\beta) = \lambda_{\beta}$ for a pseudo-Anosov braid β (for all this see [13], [2], [36], [34]). Moreover, it is known that the invariant measured foliation is transverse orientable if and only if there do not occur accidental reductions of the word length $|\beta^k(x)|$ and hence $GR(\beta) = \sup_{x \in F_n} |\beta(x)|$. In this case it is known that λ_{β} is the greatest real zero of $\Delta_{\hat{\beta} \cup L}(u, t = -1) = \det(uId - B_{\beta}^r(-1))$ (see [35], [34], [2]).

It is well known that the measured invariant foliation is transverse orientable for all pseudo-Anosov 3-braids (see [34]). In particular, for $\beta = \sigma_1 \sigma_2^{-1}$ (which is evidently a shortest representative of its conjugacy class) the stretching factor λ_{β} is the greatest real zero of $\Delta_{\hat{\beta} \cup L}(u, -1) = u^2 - 3u + 1$.

We have calculated

$$\begin{aligned} \Delta R_1(\text{hat}(\hat{\beta}))(A, B, t, u) = & u^2(-4z + 2z(A + B) + 2z^2 - 2z^2(A + B)) + \\ & u(-4z(t - 1) + 2z(A + B)t - 4z^2 - 2z^2(A + B)(t - 1)) + (4zt + 2z(A + B)t^2 + \\ & 2z^2 + 2z^2(A + B)t) \end{aligned}$$

(where $z = A - B = t^{1/2} - t^{-1/2}$).

Substituting $t = -1$ and $A + B = 1$ gives then

$$\Delta R_1(\text{hat}(\hat{\beta}))(u) = u^2 - 3u + 1 = \Delta_{\hat{\beta} \cup L}(u, -1).$$

It is known that for the pseudo-Anosov 4-braid $\beta = \sigma_1\sigma_2\sigma_3^{-1}$ the measured invariant foliation is not transverse orientable and in fact $\Delta_{\hat{\beta} \cup L}(u, -1) = (u - 1)^3$. The stretching factor $\lambda_\beta \approx 2.2966$ is the greatest real zero of $u^4 - 2u^3 - 2u + 1$ (obtained from the action of β on the corresponding train track, see e.g. [36], [34]).

We have calculated

$$\Delta R_1(\text{hat}(\hat{\beta}))(u) = i(u - 1)(u^2(16 + 17i) + u(-54 - 22i) + 16 + 17i)/2.$$

It turns out that $|u_\beta|/\lambda_\beta = 1.00143\dots$

Calculating iterations by hand is too complicated, but we see that already $m = 0$ gives a very good approximation!

Notice that our invariant $\Delta R_1(\text{hat}(\hat{\beta}^{mn+1}))(u)$ has the right property of an invariant which could give a perturbative approximation of a geometric invariant: it is not determined by $\Delta R_1(\text{hat}(\hat{\beta}))(u)$ together with the number mn .

Remark 4 *The volume conjecture for hyperbolic knots says that*

$$\lim_{n \rightarrow \infty} \log |J_{K,n}(\exp(2\pi i/n))|/n = \text{Vol}(S^3 \setminus K)/2\pi$$

where $J_{K,n}$ is the n -colored Jones polynomial of the knot K (see [29], [41]). An important feature for this conjecture is the fact that $J_{K,n}$ is not determined by the usual Jones polynomial $J_{K,2}$ together with the number n . The same is true in general with respect to iterations for $|\beta^k(x)|$ and for our 1-cocycle invariants, compare Remark 1 (here we consider connected sums of the same knot naturally as iterations). Notice also that our 1-cocycle invariants are all 0 for torus knots (which have simplicial volume 0) and for periodic braids (which have entropy 0) if they are represented by positive braid words. The entropy conjecture suggests that there could be perhaps also an alternative volume conjecture with cablings (corresponding to colorings) replaced by connected sums and the colored Jones polynomial by the quantum 1-cocycle invariant $PR_1(\text{hat})$. But for the moment we lack calculations of examples.

Notice, that it would be also interesting to find a conjecture which relates the hyperbolic volume of the mapping torus $\text{Vol}(S^3 \setminus (L \cup \hat{\beta}))$ with the asymptotics of the quantum 1-cocycle $PR_1(\text{hat}(\hat{\beta}^{mn+1}))$, where $m \rightarrow \infty$, for pseudo-Anosov braids $\beta \in B_n$. So, even if there is no direct relation between the hyperbolic volume $\text{Vol}(S^3 \setminus (L \cup \hat{\beta}))$ and the entropy $h(\beta)$ of a pseudo-Anosov braid $\beta \in B_n$, it could well be that there is a relation between them as

different asymptotics of the same quantum 1-cocycle $PR_1(\text{hat}(\hat{\beta}^{mn+1}))$ in the complement of braid diagrams with an ordinary self-tangency in an ordinary flex.

Let us mention that our 1-cocycles allow sometimes to answer in the negative a very difficult question: *given two loops in M_K by sequences of Reidemeister moves of diagrams, are the two loops homologous in M_K ?* For example, R_1 shows that the loop shown in Fig. 65 up to Fig. 74, see Section 3.1, is not homologous to any loop $\text{rot}(K)$.

Notice also that our invariants can not be extended to singular knots neither to virtual knots in contrast to the usual quantum knot invariants. Indeed, the loop $\text{hat}(K)$ can not be defined for singular knots (each double point would have to move over infinity which would change the isotopy type of the long singular knot) in contrast to the loop $\text{rot}(K)$. Non of these loops can be defined for virtual knots because they would contain lots of forbidden moves for virtual knots, see e.g. [32].

The present paper is a continuation of the preprint [18], but for the convenience of the reader we have made it self-contained. The preprint [18] contains already the essential combinatorial features but we have missed the main point: the *singularization*. Most of the results of [18] can be obtained directly from the present paper just by replacing a double point by its smoothing with respect to the orientation. But the inverse operation contains a lot of new information. For example, smoothing the double points in $R_1(\text{hat}(4_1 \# 4_1))$ without using the refined Kauffman-Vogel skein relations leads to the HOMFLYPT polynomial 0.

Finally, let us mention that the topology of knot spaces was much studied in [27], [8], [9], [10], [52]. It seems that the Teiblum-Turchin 1-cocycle v_3^1 and its lift to \mathbb{R} by Sakai are the only other known 1-cocycles for long knots which represent a non trivial cohomology class. The Teiblum-Turchin 1-cocycle is an integer valued 1-cocycle of degree 3 in the sense of Vassiliev's theory. Its reduction mod 2 has a combinatorial description and can be calculated (see [50], [51] and [47]). Sakai has defined a \mathbb{R} valued version of the Teiblum-Tourchine 1-cocycle via configuration space integrals (see [45]). Moreover, he has shown that the value of his 1-cocycle on $\text{rot}(K)$ is equal to the Vassiliev invariant $v_2(K)$. Another formula for an integer valued 1-cocycle for long knots which extends $v_3^1 \bmod 2$ is contained in [39].

Integer valued 1-cocycles of all degrees for closed braids were constructed in the unpublished paper [15]. They are already sufficient to detect that

the braids $\sigma_1\sigma_2^{-1}$ and $\sigma_1\sigma_2\sigma_3^{-1}$ are not periodic, because they distinguish the loops $rot(\hat{\beta})$ and $hat(\hat{\beta})$.

The relation between the topology and the geometry of knots was discovered by W. Thurston, see e.g. [46]. Far reaching generalizations of the volume conjecture are contained in [20] and in [12]. Relations of quantum topology with the geometry of knots other than the volume conjecture are studied e.g. in [21], [22], [23], [24], [38].

Let us finish this introduction by formulating some interesting questions and which allow perhaps to put our approach into a larger perspective:

Do there exist non trivial combinatorial 1-cocycle invariants of higher degrees? (In the construction it is essential that each Reidemeister II move contributes only for the diagram which has two new crossings and not for the difference of the two diagrams at different sides of the discriminant. Otherwise the 1-cocycle turns out to be trivial. Unfortunately, starting from degree 3 it seems to be very complicated to find non trivial solutions of the global tetrahedron equation in a combinatorial way.)

Can the approach of Futer-Kalfagianni-Purcell [21] be combined with our approach by studying loops of embedded surfaces bounded by the long knots in the loop $hat(K)$ (question due to Vladimir Turaev)?

Can our approach perhaps be combined with the work of Fuji-Gukov-Sulkovski [20]? (Notice that for a diagram of an oriented long knot there is a canonical choice for a base point in its complement and hence there is a canonical peripheral system. Consequently, loops in the topological moduli space M_K induce automorphisms of the peripheral system and hence an action on the algebraic curve which is used in the definition of the A -polynomial.)

Does $PR_1(hat(\sharp_m K))$ satisfy some non-trivial linear recursion relation with respect to m similar to that for the colored Jones polynomial (see e.g. [24])?

Does there exist a representation theory for loops in conjugacy classes of braids? (It should associate to each Reidemeister move of type III or II in a 1-parameter family of n -braids some linear operator such that the trace of their composition depends only on the homology class of the loop.)

Does our 1-cocycle $R_2(hat(\hat{\beta}))$ have an extension to a 1-cocycle for all knots K in the solid torus?

Most importantly, does our combinatorial approach have some differential geometric counterpart, in a similar way to the Kontsevich integral or to Witten's construction of the Jones polynomial (see [53])? Such an approach could perhaps lead to 1-cocycle invariants of arbitrarily high degree (but for

each given knot there are of course only non trivial 1-cocycle invariants for a finite number of degrees, e.g. for the knot 4_1 they would be all 0 starting from degree 7, see Section 3.1). Notice that our 1-cocycle invariants of degree 1 and 2 transform knots into a much more rigid object, namely linear combinations of singular long knots up to isotopy which does not flip over the planar double points. The (not yet existing) non trivial 1-cocycle invariant of the highest degree for a given knot K could perhaps be a linear combination of 4-valent graphs with signed vertices and with a marked edge on the 2-sphere, a completely rigid object. Each of these graphs on the 2-sphere determines already the knot. To compare two knots we would have only to pick up one of these graphs and to see whether or not we find it (necessarily with the same coefficient) amongst the graphs of the other knot. This would be a complete knot invariant.

But we think that it will be not easy to find such a differential geometric counterpart because all our constructions have some global flavor: we make heavy use of the point at infinity, of the non trivial homology classes in the case of closed braids and of the global type of Reidemeister III moves (see the next section). This is not by accident because Hatcher has shown that if a closed knot K in S^3 is not a satellite then $H_1(M_{K \subset S^3}; \mathbb{Q}) = 0$ and hence there aren't any non trivial 1-cocycles with values in a torsion free module in this case (see [27]).

Acknowledgments

I have started this work in 2006. Over the years I have profited from the help of many people, in particular: Dror Bar-Natan, Christian Blanchet, Ryan Budney, Karen Chu, Alan Hatcher, Vitaliy Kurlin, Gregor Masbaum, Arnaud Mortier, Hugh Morton, Hitoshi Murakami, Victor Turchin. I wish to thank all of them. Finally, let me mention that without Séverine, who has created all the figures, this paper wouldn't exist.

2 Main results

We split our main result into four theorems corresponding to the four different non trivial 1-cocycles. Each of our four 1-cocycles determines of course "dual" 1-cocycles by applying the obvious symmetries as e.g. replacing all our constructions by their mirror images.

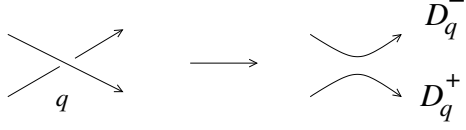


Figure 19: Two ordered knot diagrams associated to a crossing q

2.1 The 1-cocycle R_1 of degree 1 for long knots

To each Reidemeister move of type III corresponds a diagram with a *triple crossing* p : three branches of the knot (the highest, middle and lowest with respect to the projection $pr : \mathbb{C} \times \mathbb{R} \rightarrow \mathbb{C}$) have a common point in the projection into the plane. A small perturbation of the triple crossing leads to an ordinary diagram with three crossings near $pr(p)$.

Definition 6 *We call the crossing between the highest and the lowest branch of the triple crossing p the distinguished crossing of p and we denote it by d . The crossing between the highest branch and the middle branch is denoted by hm and that of the middle branch with the lowest is denoted by ml . Smoothing a crossing q with respect to the orientation splits the closure of K into two oriented and ordered circles. We call D_q^+ the component which goes from the under-cross to the over-cross at q and by D_q^- the remaining component (compare Fig. 19).*

In a Reidemeister move of type II both new crossings are considered as distinguished and we often identify them.

A *Gauss diagram* of K is an oriented circle with oriented chords and a marked point. There exists an orientation preserving diffeomorphism from the oriented line to oriented the knot K such that each chord connects a pair of points which are mapped onto a crossing of $pr(K)$ and infinity is mapped to the marked point. The chords are oriented from the preimage of the under crossing to the pre-image of the over crossing (here we use the orientation of the \mathbb{R} -factor). The circle of a Gauss diagram in the plan is always equipped with the counter-clockwise orientation.

A *Gauss diagram formula* of degree k is an expression assigned to a knot diagram which is of the following form:

$$\sum \text{function}(\text{ writhes of the crossings})$$

where the sum is taken over all possible choices of k (unordered) different crossings in the knot diagram such that the chords arising from these crossings in the knot diagram of K build a given sub-diagram with given marking. The marked sub-diagrams are called *configurations*. If the function is (as usual) the product of the writhes of the crossings in the configuration, then we will denote the sum shortly by the configuration itself. There are exactly eight local types of Reidemeister III moves and four local types of Reidemeister II moves. We show them in Fig. 20 and Fig. 21. (We attach numbers to the local types of Reidemeister III moves for shorter writing.) The sign in the figures denotes the local side of the diagram with respect to the discriminant of diagrams with a triple crossing or respectively with an auto-tangency in the projection (see Section 4.1).

Definition 7 *The sign of a Reidemeister move p , denoted by $\text{sign}(p)$, is equal to $+1$ if the move is from the negative side to the positive side and -1 otherwise.*

For example, a positive Reidemeister III move of type 1 corresponds to an application of a local braid relation $\sigma_1\sigma_2\sigma_1 \rightarrow \sigma_2\sigma_1\sigma_2$.

Let us consider the *Gauss diagram of a triple crossing* p , but without taking into account the writhe of the crossings. In the oriented circle K we connect the preimages of the triple point $pr(p)$ by arrows which go from the under-cross to the over-cross and we obtain a triangle. The distinguished crossing d is always drawn by a thicker arrow.

There are exactly six different *global types* of triple crossings with a point at infinity. We give names to them and show them in Fig. 22. (Here "r" indicates that the crossing between the middle and the lowest branch goes to the right and "l" indicates that it goes to the left.)

Definition 8 *An ordinary crossing q in a diagram K is of type 1 if $\infty \in D_q^+$ and is of type 0 otherwise.*

Let $K(p)$ be a generic diagram with a triple crossing or a self-tangency p and let d be the distinguished crossing for p . In the case of a self-tangency we identify the two distinguished crossings. We assume that the distinguished crossing d is of type 0.

Definition 9 *A crossing q of $K(p)$ is called a f-crossing if q is of type 1 and the under cross of q is in the oriented arc from ∞ to the over cross of d in K .*

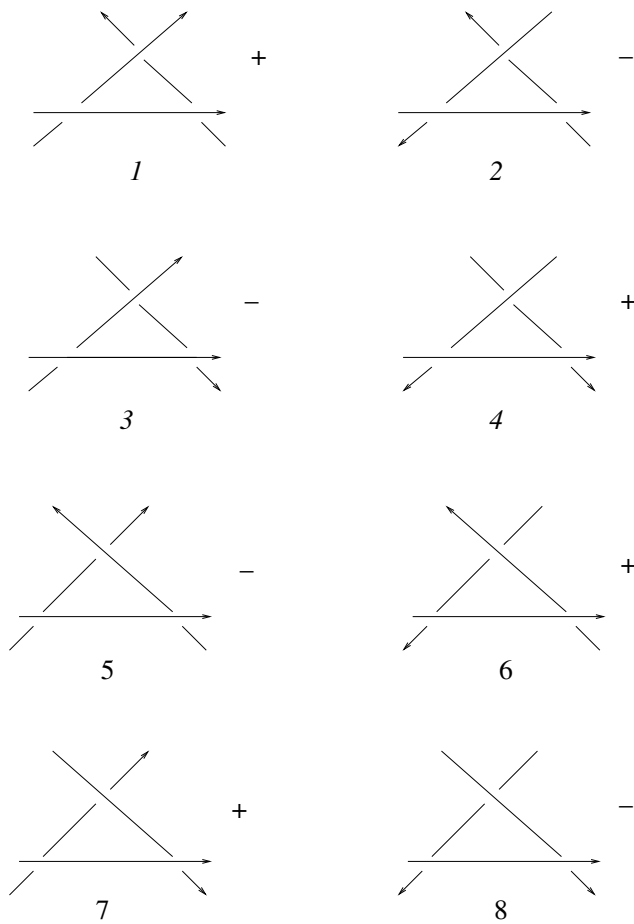


Figure 20: Local types of a triple crossing

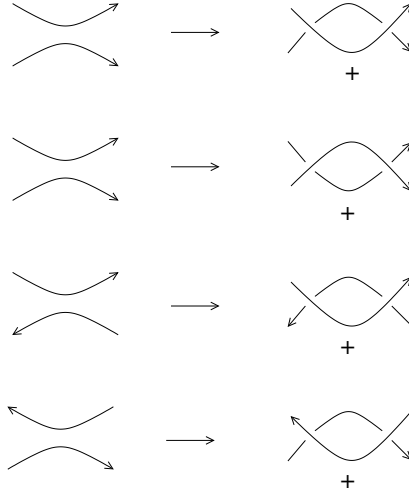


Figure 21: Local types of Reidemeister II moves

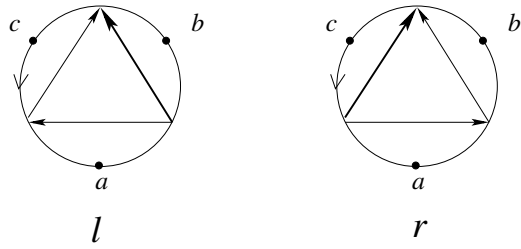


Figure 22: The six global types of triple crossings

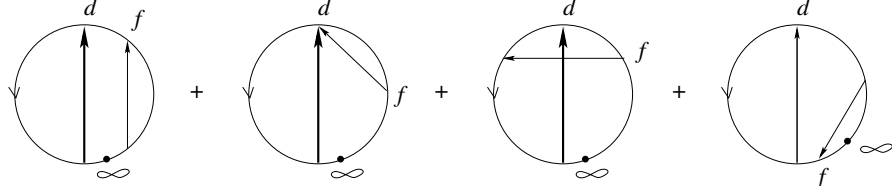


Figure 23: The f -crossings for R_1

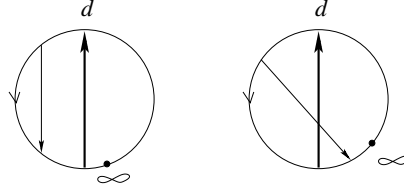


Figure 24: Crossings of type 1 that are not f -crossings

In other words, the "foot" of q in the Gauss diagram is in the sub arc of the circle which goes from ∞ to the head of d and the head of q is in the sub arc which goes from the foot of q to ∞ . We illustrate this in Fig. 23 and Fig. 24. (The letter "f" stands for "foot" or "Fuß" and not for "fiedler".) Notice that we make essential use here of the fact that no crossing can ever move over the point at infinity.

Definition 10 The quadratic weight $W_2(p)$ is defined by the Gauss diagram formula shown in Fig. 25. Here f denotes an f -crossing of p and r denotes an arbitrary crossing with a position as shown in the configurations.

(Remember that with our conventions the formula in Fig. 25 says that $W_2(p)$ is the sum of $w(f)w(r)$ over all couples of crossings (f, r) in $K(p)$ which form one of the configurations from Fig. 25.)

The second (degenerate) configuration in Fig. 25 can of course not appear for a self-tangency p . Notice that the crossing r is always of type 0.

The crossings r in Fig. 25 are called the r -crossings.

Definition 11 Let p be a triple crossing of one of the global types r_a or l_c shown in Fig. 26. The linear weight $W_1(p)$ is defined as the sum of the writhes of the crossings r in $K(p)$ which form one of the configurations shown in Fig. 27.

$$W_2(p) = \begin{array}{c} \text{Diagram 1} \end{array} + \begin{array}{c} \text{Diagram 2} \end{array}$$

Figure 25: The quadratic weight W_2

$$r_a = \begin{array}{c} \text{Diagram 1} \end{array} \quad l_c = \begin{array}{c} \text{Diagram 2} \end{array}$$

Figure 26: The global types for which the linear weight $W_1(p)$ appears

$$W_1(p) = \begin{array}{c} \text{Diagram 1} \end{array} + \begin{array}{c} \text{Diagram 2} \end{array}$$

Figure 27: The linear weight W_1

The linear weight $W_1(p)$ is defined with respect to the single f-crossing hm (normally we should denote it by $W_1(p, hm)$). Notice that we do not multiply it by $w(hm)$.

The above weights $W_1(p)$ and $W_2(p)$ correspond to positive triple crossings, i.e. of local type 1. There is a correction by +1 or -1 for certain other local types but only for the global type r_a . We are now ready to define the contributions $R_1(p)$ of a Reidemeister move p . They depend on the local and of the global type of p . The local type is given by the number from Fig. 20 and the global type by the notation from Fig. 22. Each term in the contribution is an integer multiple of a diagram for K with just one crossing transformed into a double point.

Definition 12 *The contributions $R_1(p)$ are defined in Fig. 28-32. The sign of each double point is equal to the sign of the underlying crossing which can be found in Fig. 20. All other Reidemeister moves contribute 0.*

Notice that the two singular knots, which are associated to the distinguished crossing d , are even globally not isotopic (they can be distinguished by the linking number of the smoothing link). The double point of the contributions with coefficient W_1 corresponds always to the crossing ml . The singular knot on the positive side of the triple crossing is even locally isotopic to the singular knot on the negative side of the triple crossing. Notice that the contributions of the Reidemeister II moves do not depend on the local type.

The boundary ∂K of a string link is an ordered set in the marked circle (which depends of course of the chosen abstract closure of the string link).

Definition 13 *Let q be the underlying crossing of a double point. The grading of a double point is the intersection of D_q^+ (compare Definition 6) with the boundary ∂K .*

Definition 14 *Let γ be an oriented generic arc in M_K (for the precise definition of "generic" we need the stratification of M_K , see Section 4.1). The 1-cochain $R_1(\gamma)$ is defined as*

$$\sum_p \text{sign}(p) R_1(p)$$

where the sum is taken over all Reidemeister moves p in γ with the same fixed chosen grading for all double points.

type 1

$$r_a, r_b, l_b \quad W_2 \left(\begin{array}{c} \nearrow \\ \text{---} \bullet \text{---} \nearrow \\ \nwarrow \end{array} d \quad - \quad \begin{array}{c} \nearrow \\ \text{---} \bullet \text{---} \nearrow \\ \nwarrow \end{array} d \right)$$

$$r_a, l_c \quad W_1 \quad \begin{array}{c} \nearrow \\ \text{---} \bullet \text{---} \nearrow \\ \nwarrow \\ ml \end{array}$$

type 2

$$r_b, l_b \quad W_2 \left(\begin{array}{c} \nearrow \\ \text{---} \bullet \text{---} \nearrow \\ \nwarrow \end{array} d \quad - \quad \begin{array}{c} \nwarrow \\ \text{---} \bullet \text{---} \nwarrow \\ \nearrow \end{array} d \right)$$

$$r_a \quad (W_2 + 1) \left(\begin{array}{c} \nearrow \\ \text{---} \bullet \text{---} \nearrow \\ \nwarrow \end{array} d \quad - \quad \begin{array}{c} \nwarrow \\ \text{---} \bullet \text{---} \nwarrow \\ \nearrow \end{array} d \right)$$

$$l_c \quad W_1 \quad \begin{array}{c} \nearrow \\ \text{---} \bullet \text{---} \nearrow \\ \nwarrow \\ ml \end{array}$$

$$r_a \quad (W_1 - 1) \quad \begin{array}{c} \nearrow \\ \text{---} \bullet \text{---} \nearrow \\ \nwarrow \\ ml \end{array}$$

Figure 28: Contributions $R_1(p)$ for the local types 1 and 2

type 3

$$r_a, r_b, l_b \quad W_2 \left(\begin{array}{c} \nearrow \\ \text{---} \bullet d \\ \searrow \end{array} - \begin{array}{c} \nearrow d \\ \text{---} \bullet \\ \searrow \end{array} \right)$$

$$r_a, l_c \quad W_1 \begin{array}{c} \nearrow \\ \text{---} \bullet ml \\ \searrow \end{array}$$

type 4

$$r_b, l_b \quad W_2 \left(\begin{array}{c} \nearrow \\ \text{---} \bullet d \\ \searrow \end{array} - \begin{array}{c} \nearrow d \\ \text{---} \bullet \\ \searrow \end{array} \right)$$

$$r_a \quad (W_2 - 1) \left(\begin{array}{c} \nearrow \\ \text{---} \bullet d \\ \searrow \end{array} - \begin{array}{c} \nearrow \\ \text{---} \bullet d \\ \searrow \end{array} \right)$$

$$l_c \quad W_1 \begin{array}{c} \nearrow \\ \text{---} \bullet ml \\ \searrow \end{array}$$

$$r_a \quad (W_1 + 1) \begin{array}{c} \nearrow \\ \text{---} \bullet ml \\ \searrow \end{array}$$

Figure 29: Contributions $R_1(p)$ for the local types 3 and 4

type 5

$$r_b, l_b \quad W_2 \left(\begin{array}{c} \nearrow \\ \text{---} \diagup \bullet \diagdown \text{---} \\ \searrow \end{array} \begin{array}{c} d \\ \bullet \end{array} \begin{array}{c} \nearrow \\ \text{---} \end{array} - \begin{array}{c} \text{---} \diagup \bullet \diagdown \text{---} \\ \searrow \end{array} \begin{array}{c} d \\ \bullet \end{array} \begin{array}{c} \nearrow \\ \text{---} \end{array} \right)$$

$$r_a \quad (W_2 - 1) \left(\begin{array}{c} \nearrow \\ \text{---} \diagup \bullet \diagdown \text{---} \\ \searrow \end{array} \begin{array}{c} d \\ \bullet \end{array} \begin{array}{c} \nearrow \\ \text{---} \end{array} - \begin{array}{c} \text{---} \diagup \bullet \diagdown \text{---} \\ \searrow \end{array} \begin{array}{c} d \\ \bullet \end{array} \begin{array}{c} \nearrow \\ \text{---} \end{array} \right)$$

$$l_c \quad W_1 \quad \begin{array}{c} \nearrow \\ \text{---} \diagup \bullet \diagdown \text{---} \\ \searrow \end{array} \begin{array}{c} ml \\ \bullet \end{array} \begin{array}{c} \nearrow \\ \text{---} \end{array}$$

$$r_a \quad (W_1 - 1) \quad \begin{array}{c} \nearrow \\ \text{---} \diagup \bullet \diagdown \text{---} \\ \searrow \end{array} \begin{array}{c} ml \\ \bullet \end{array} \begin{array}{c} \nearrow \\ \text{---} \end{array}$$

type 6

$$r_b, l_b \quad W_2 \left(\begin{array}{c} \nearrow \\ \text{---} \diagup \bullet \diagdown \text{---} \\ \searrow \end{array} \begin{array}{c} d \\ \bullet \end{array} \begin{array}{c} \nearrow \\ \text{---} \end{array} - \begin{array}{c} \text{---} \diagup \bullet \diagdown \text{---} \\ \searrow \end{array} \begin{array}{c} d \\ \bullet \end{array} \begin{array}{c} \nearrow \\ \text{---} \end{array} \right)$$

$$r_a \quad (W_2 + 1) \left(\begin{array}{c} \nearrow \\ \text{---} \diagup \bullet \diagdown \text{---} \\ \searrow \end{array} \begin{array}{c} d \\ \bullet \end{array} \begin{array}{c} \nearrow \\ \text{---} \end{array} - \begin{array}{c} \text{---} \diagup \bullet \diagdown \text{---} \\ \searrow \end{array} \begin{array}{c} d \\ \bullet \end{array} \begin{array}{c} \nearrow \\ \text{---} \end{array} \right)$$

$$l_c \quad W_1 \quad \begin{array}{c} \nearrow \\ \text{---} \diagup \bullet \diagdown \text{---} \\ \searrow \end{array} \begin{array}{c} ml \\ \bullet \end{array} \begin{array}{c} \nearrow \\ \text{---} \end{array}$$

$$r_a \quad (W_1 + 1) \quad \begin{array}{c} \nearrow \\ \text{---} \diagup \bullet \diagdown \text{---} \\ \searrow \end{array} \begin{array}{c} ml \\ \bullet \end{array} \begin{array}{c} \nearrow \\ \text{---} \end{array}$$

Figure 30: Contributions $R_1(p)$ for the local types 5 and 6

type 7

$$r_a, r_b, l_b \quad W_2 \left(\begin{array}{c} \nearrow \\ \diagdown \\ \bullet \\ \nearrow \\ d \end{array} - \begin{array}{c} \diagdown \\ \nearrow \\ \bullet \\ \diagdown \\ d \end{array} \right)$$

$$r_a, l_c \quad W_1 \begin{array}{c} \nearrow \\ \diagdown \\ \bullet \\ \nearrow \\ ml \end{array}$$

type 8

$$r_a, r_b, l_b \quad W_2 \left(\begin{array}{c} \diagdown \\ \nearrow \\ \bullet \\ \diagdown \\ d \end{array} - \begin{array}{c} \nearrow \\ \diagdown \\ \bullet \\ \nearrow \\ d \end{array} \right)$$

$$r_a, l_c \quad \begin{array}{c} \nearrow \\ \diagdown \\ \bullet \\ \nearrow \\ ml \end{array}$$

Figure 31: Contributions $R_1(p)$ for the local types 7 and 8

$$\begin{array}{c} \nearrow \\ \diagdown \\ \bullet \\ \nearrow \\ d \end{array} \quad W_2 \left(\begin{array}{c} \nearrow \\ \diagdown \\ \bullet \\ \nearrow \\ + \end{array} - \begin{array}{c} \diagdown \\ \nearrow \\ \bullet \\ \diagdown \\ - \end{array} \right)$$

$$\begin{array}{c} \nearrow \\ \diagdown \\ \bullet \\ \nearrow \\ d \end{array} \quad W_2 \left(\begin{array}{c} \nearrow \\ \diagdown \\ \bullet \\ \nearrow \\ + \end{array} - \begin{array}{c} \diagdown \\ \nearrow \\ \bullet \\ \diagdown \\ - \end{array} \right)$$

Figure 32: Contributions $R_1(p)$ for self-tangencies independant of their local type

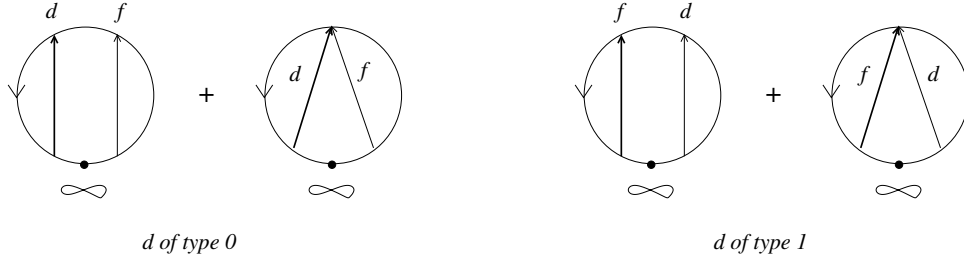


Figure 33: The f -crossings for R_2 with d of type 0, and with d of type 1

(It follows immediately from our definitions that the gradings of all double points in $R_1(\gamma)$ are the empty set in the particular case of long knots and we can ignore them.)

We are now ready to formulate the first part of our main result.

Theorem 1 *The graded 1-cochain $R_1(\gamma)$ with values in K_1 is a 1-cocycle and gives rise to a in general non trivial cohomology class $R_1 \in H^1(M_K; K_1)$.*

(Remember that the only relation in K_1 is the embedded 1T-relation, compare the Introduction.)

The theorem applied to the loop $\text{hat}(K)$ gives the first *singularization* of knots and of cables of long knots.

2.2 The 1-cocycle R_2 of degree 2 for long knots

We have to symmetrize slightly our construction in the case of 1-cocycles of degree 2 and to consider both distinguished crossings of type 0 and of type 1 (but they are still not invariant under e.g. taking the mirror image of everything).

Definition 15 *The f -crossings for a distinguished crossing d of type 0 (or type 1) are given in Fig. 33*

Notice that the f -crossings for d of type 0 are a subset of the f -crossings in the degree 1 case and that in the new definition f -crossings and distinguished crossings d become interchangeable.

Definition 16 *The contributions $R_2(p)$ are defined in Fig. 34-38. The sign of each double point is equal to the sign of the underlying crossing which can be found in Fig. 20. All other Reidemeister moves contribute 0.*

type 1

all global types $w(f) = \left(\text{diagram 1} - \text{diagram 2}, \text{diagram 3} \right)$

$r_a = \text{diagram 4}$

$l_a = - \text{diagram 5}$

type 2

all global types $w(f) = \left(\text{diagram 6} - \text{diagram 7}, \text{diagram 8} \right)$

$r_a = \text{diagram 9}$

$l_a = - \text{diagram 10}$

Figure 34: Contributions $R_2(p)$ for the local types 1 and 2

type 3

all global types

$$w(f) = \left(\text{diagram 1} - \text{diagram 2}, \text{diagram 3} \right)$$

Diagram 1: A vertex with four half-edges. The top-left half-edge is labeled d . The top-right half-edge is labeled d . The bottom-left half-edge is labeled d . The bottom-right half-edge is labeled d .

Diagram 2: A vertex with four half-edges. The top-left half-edge is labeled d . The top-right half-edge is labeled d . The bottom-left half-edge is labeled d . The bottom-right half-edge is labeled d .

Diagram 3: A vertex with four half-edges. The top-left half-edge is labeled d . The top-right half-edge is labeled d . The bottom-left half-edge is labeled d . The bottom-right half-edge is labeled d .

type 4

all global types $w(f) \left(\begin{array}{c} \diagup \\ \bullet \\ \text{\tiny d} \end{array}, -\begin{array}{c} \diagdown \\ \bullet \\ \text{\tiny d} \end{array}, \begin{array}{c} \diagup \\ \bullet \\ \text{\tiny f} \end{array} \right)$

$$l_a - \begin{array}{c} \nearrow \\ \bullet \\ \text{hm} \\ \leftarrow \bullet \leftarrow \\ d \end{array}$$

Figure 35: Contributions $R_2(p)$ for the local types 3 and 4

type 5

all global types $w(f) \left(\begin{array}{c} \diagup \quad \diagdown \\ \hline \quad \quad \quad \bullet \quad d \\ \diagdown \quad \diagup \end{array} \right. - \begin{array}{c} \quad \quad \quad \bullet \quad d \\ \hline \diagup \quad \diagdown \\ \diagdown \quad \diagup \end{array}, \begin{array}{c} \diagup \quad \diagdown \\ \bullet \\ \diagdown \quad \diagup \\ f \end{array} \right)$

$r_a \quad \begin{array}{c} \quad \quad \quad \bullet \quad hm \\ \hline \diagup \quad \diagdown \\ \diagdown \quad \diagup \\ d \end{array}$

$l_a \quad - \quad \begin{array}{c} \quad \quad \quad \bullet \quad d \\ \hline \diagup \quad \diagdown \\ \diagdown \quad \diagup \\ hm \end{array}$

type 6

all global types $w(f) \left(\begin{array}{c} \diagup \quad \diagdown \\ \bullet \\ \hline \quad \quad \quad d \\ \diagdown \quad \diagup \end{array} \right. - \begin{array}{c} \diagup \quad \diagdown \\ \hline \bullet \quad d \\ \diagdown \quad \diagup \end{array}, \begin{array}{c} \diagup \quad \diagdown \\ \bullet \\ \diagdown \quad \diagup \\ f \end{array} \right)$

$r_a \quad \begin{array}{c} \quad \quad \quad \bullet \quad d \\ \hline \diagup \quad \diagdown \\ \diagdown \quad \diagup \\ hm \end{array}$

$l_a \quad - \quad \begin{array}{c} \quad \quad \quad \bullet \quad hm \\ \hline \diagup \quad \diagdown \\ \diagdown \quad \diagup \\ d \end{array}$

Figure 36: Contributions $R_2(p)$ for the local types 5 and 6

type 7

$$\text{all global types} \quad w(f) \left(\begin{array}{c} \diagup \diagdown \\ \bullet \\ \hline \diagdown \diagup \\ d \end{array} - \begin{array}{c} \diagup \diagdown \\ \hline \bullet \\ \diagdown \diagup \\ d \end{array}, \begin{array}{c} \diagup \diagdown \\ \bullet \\ \diagdown \diagup \\ f \end{array} \right)$$

$$r_a \quad \begin{array}{c} \diagup \diagdown \\ \hline \bullet \\ \diagdown \diagup \\ hm \end{array}$$

$$l_a \quad - \begin{array}{c} \diagup \diagdown \\ \bullet \\ \hline \diagdown \diagup \\ d \end{array}$$

type 8

$$\text{all global types} \quad w(f) \left(\begin{array}{c} \diagup \diagdown \\ \hline \bullet \\ \diagdown \diagup \\ d \end{array} - \begin{array}{c} \diagup \diagdown \\ \bullet \\ \hline \diagdown \diagup \\ d \end{array}, \begin{array}{c} \diagup \diagdown \\ \bullet \\ \diagdown \diagup \\ f \end{array} \right)$$

$$r_a \quad \begin{array}{c} \diagup \diagdown \\ \bullet \\ \hline \bullet \\ \diagdown \diagup \\ hm \end{array}$$

$$l_a \quad - \begin{array}{c} \diagup \diagdown \\ \hline \bullet \\ \diagdown \diagup \\ hm \end{array}$$

Figure 37: Contributions $R_2(p)$ for the local types 7 and 8

$$\begin{array}{c} \diagup \diagdown \\ \bullet \\ \diagdown \diagup \end{array} \quad w(f) \left(\begin{array}{c} \diagup \diagdown \\ \bullet \\ \diagup \diagdown \\ + \end{array} - \begin{array}{c} \diagup \diagdown \\ \bullet \\ \diagdown \diagup \\ - \end{array}, \begin{array}{c} \diagup \diagdown \\ \bullet \\ \diagdown \diagup \\ f \end{array} \right)$$

$$\begin{array}{c} \diagup \diagdown \\ \bullet \\ \diagdown \diagup \end{array} \quad w(f) \left(\begin{array}{c} \diagup \diagdown \\ \bullet \\ \diagdown \diagup \\ + \end{array} - \begin{array}{c} \diagup \diagdown \\ \bullet \\ \diagdown \diagup \\ - \end{array}, \begin{array}{c} \diagup \diagdown \\ \bullet \\ \diagdown \diagup \\ f \end{array} \right)$$

Figure 38: Contributions $R_2(p)$ for self-tangencies independant of their local and global type

In these contributions we singularize simultaneously a distinguished crossing d and a f-crossing. Sometimes the crossing hm is a f-crossing too. Instead of weights we have just the usual writhe $w(f)$ of the f-crossing. Instead of only singularizing the crossing ml in R_1 we have sometimes to singularize now both the crossings d and hm , namely when at one side of the triple crossing their underlying Gauss diagram is one of those shown in Fig. 33. In fact, for the global type r_a we have to take always the diagram where the crossing hm is connected by the knot in the local picture to the crossing d . For the global type l_a it is just the inverse and with a negative sign. For the convenience of the reader we indicate in the figures which crossing is at the origin of the double point. Notice that all underlying Gauss diagrams are among those given in Fig. 33. We can distinguish the two arrows in the underlying Gauss diagrams and we can fix a grading for each of the two arrows as in the degree 1 case.

Definition 17 *Let γ be an oriented generic arc in M_K . The 1-cochain $R_2(\gamma)$ is defined as*

$$\sum_p \text{sign}(p) R_2(p)$$

where the sum is taken over all Reidemeister moves p in γ with fixed chosen gradings for all double points.

We are now ready to formulate the second part of our main result.

Theorem 2 *The graded 1-cochain $R_2(\gamma)$ with values in K_2 is a 1-cocycle and gives rise to a in general non trivial cohomology class $R_2 \in H^1(M_K; K_2)$.*

Remember that the only relation in K_2 is the generalized embedded 1T-relation.

It turns out that $R_2(\text{hat}(4_1))$ is already non trivial in contrast to $R_1(\text{hat}(4_1))$, compare Section 3.1.

2.3 The 1-cocycles R_1 and R_2 for closed n-braids

Let V be the standard solid torus. We identify $H_1(V; \mathbb{Z})$ with \mathbb{Z} by sending the oriented closed 1-braid to +1. Let β be a n-braid which closes to a knot and let q be a crossing of β . We assume $n > 2$.

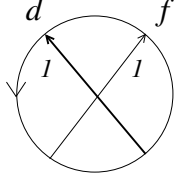


Figure 39: f -crossings for R_1 in the case of closed braids

Definition 18 *The homological marking of q in $\{1, 2, \dots, n-1\}$ is the homology class represented by D_q^+ . We write it as a number on the left side of the corresponding arrow.*

Evidently, for isotopies of closed braids only six of the local types of Reidemeister III moves, namely the types 1, 3, 4, 5, 7, 8, and only the two local types of Reidemeister II moves with equal tangent direction can occur.

Definition 19 *Let p be a Reidemeister III or II move for which the distinguished crossing d has homological marking 1. We identify here the two distinguished crossings in a Reidemeister II move (which have always the same marking). A f -crossing is a crossing with the homological marking 1 and which intersects the distinguished crossing d from the left to the right as shown in Fig. 39.*

Definition 20 *The linear weight $W(p)$ is defined as the sum of all writhes of the f -crossings.*

(Notice that according to our convention a new crossing from a Reidemeister II move is never a f -crossing with respect to the other new crossing from the same move. There will be a correction term -1 exactly for the local types 3, 4, 8. Notice that the local types 3, 4 and 8 are exactly those with a negative distinguished crossing d .)

It follows directly from our definitions that a Reidemeister III move with a distinguished crossing with marking 1 is necessarily of global type r and that the crossings hm and ml have each a marking strictly greater than 1.

Definition 21 *The contributions $R_1(p)$ are defined in Fig. 40-43. The sign of each double point is equal to the sign of the underlying crossing which can be found in Fig. 20. All other Reidemeister moves contribute 0.*

type 1

$$\begin{array}{c} \text{triangle in circle} \end{array} \quad W \left(\begin{array}{c} \text{triangle} \end{array} - \begin{array}{c} \text{triangle} \end{array} \right)$$

$$\begin{array}{c} \text{triangle in circle} \end{array} \quad \begin{array}{c} \text{triangle} \end{array}$$

type 3

$$\begin{array}{c} \text{triangle in circle} \end{array} \quad (W - I) \left(\begin{array}{c} \text{triangle} \end{array} - \begin{array}{c} \text{triangle} \end{array} \right)$$

$$\begin{array}{c} \text{triangle in circle} \end{array} \quad \begin{array}{c} \text{triangle} \end{array}$$

Figure 40: Contributions $R_1(p)$ for the local types 1 and 3 in the braid case

type 4

$$\begin{array}{c} \text{triangle with } 1 \end{array} \quad (W - 1) \left(\begin{array}{c} \text{triangle with } d \end{array} - \begin{array}{c} \text{triangle with } d \end{array} \right)$$

$$\begin{array}{c} \text{triangle with } 1, 2, 1 \end{array} \quad \begin{array}{c} \text{triangle with } ml \end{array}$$

type 5

$$\begin{array}{c} \text{triangle with } 1 \end{array} \quad W \left(\begin{array}{c} \text{triangle with } d \end{array} - \begin{array}{c} \text{triangle with } d \end{array} \right)$$

$$\begin{array}{c} \text{triangle with } 1, 2, 1 \end{array} \quad \begin{array}{c} \text{triangle with } ml \end{array}$$

Figure 41: Contributions $R_1(p)$ for the local types 4 and 5 in the braid case

type 7

$$\begin{array}{c} \text{triangle with 1 on left side} \end{array} \quad W \left(\begin{array}{c} \text{crossing with dot on top-right strand} \\ d \end{array} - \begin{array}{c} \text{crossing with dot on bottom-left strand} \\ d \end{array} \right)$$

$$\begin{array}{c} \text{triangle with 1 on left side, 2 on right side, 1 on bottom side} \end{array} \quad \begin{array}{c} \text{crossing with dot on top-right strand} \\ ml \end{array}$$

type 8

$$\begin{array}{c} \text{triangle with 1 on left side} \end{array} \quad (W - I) \left(\begin{array}{c} \text{crossing with dot on top-right strand} \\ d \end{array} - \begin{array}{c} \text{crossing with dot on bottom-left strand} \\ d \end{array} \right)$$

$$\begin{array}{c} \text{triangle with 1 on left side, 2 on right side, 1 on bottom side} \end{array} \quad \begin{array}{c} \text{crossing with dot on bottom-left strand} \\ ml \end{array}$$

Figure 42: Contributions $R_1(p)$ for the local types 7 and 8 in the braid case

$$\begin{array}{c} \text{circle with vertical line and dot, and a crossing above} \\ I \end{array} \quad W \left(\begin{array}{c} \text{crossing with dot on top-right strand} \\ - \end{array} - \begin{array}{c} \text{crossing with dot on bottom-left strand} \\ + \end{array} \right)$$

Figure 43: Contributions $R_1(p)$ for self-tangencies in the braid case

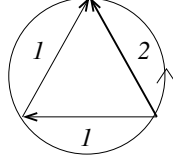


Figure 44: The only triple crossing of global type l having a distinguished crossing with marking 2

The homological markings of hm and ml are allowed to be arbitrary in the case of d with marking 1 (but they satisfy of course an evident linear relation). The R III move in Fig. 44 is the only move of global type l and with a distinguished crossing with marking 2. This comes from the obvious fact that each of the three arcs in the circle represents a positive homology class in the solid torus. The Definition 21 says now that the crossing ml becomes singular independent of the local type of the move. Notice that in all cases only crossings with marking 1 could become singular.

Definition 22 *Let γ be an oriented generic arc in $M_{\hat{\beta}}$. The 1-cochain $R_1(\gamma)$ is defined as*

$$\sum_p \text{sign}(p) R_1(p)$$

where the sum is taken over all Reidemeister moves p in γ .

Let $\bar{\Sigma}_{self-flex,1}^{(2)} \subset M_{\hat{\beta}}$ be the closure of the union of all diagrams of closed n -braids which have an ordinary self-tangency in an ordinary flex, and such that the distinguished crossing of the self-tangency has the homological marking 1, compare Section 4.1.

We are now ready to formulate the third part of our main result.

Theorem 3 *The 1-cochain $R_1(\gamma)$ with values in $\hat{\beta}_1$ is a 1-cocycle and gives rise to a in general non trivial cohomology class $R_1 \in H^1(M_{\hat{\beta}} \setminus \bar{\Sigma}_{self-flex,1}^{(2)}; \hat{\beta}_1)$.*

Remember that there aren't any relations in $\hat{\beta}_1$.

In order to construct a 1-cocycle of degree 2 we have again to symmetrize.

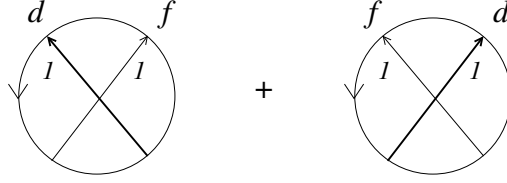


Figure 45: f -crossings for R_2 in the case of closed braids

Definition 23 Let p be a Reidemeister III or II move for which the distinguished crossing d has homological marking 1. We identify here again the two distinguished crossings in a Reidemeister II move. A f -crossing is a crossing with the homological marking 1 and which intersects the distinguished crossing d as shown in Fig. 45.

Definition 24 The contributions $R_2(p)$ are defined in Fig. 46-49. The sign of each double point is equal to the sign of the underlying crossing which can be found in Fig. 20. All other Reidemeister moves contribute 0.

(We use in the figures the same conventions as in the case of long knots.)

Definition 25 Let γ be an oriented generic arc in $M_{\hat{\beta}}$. The 1-cochain $R_2(\gamma)$ is defined as

$$\sum_p \text{sign}(p) R_2(p)$$

where the sum is taken over all Reidemeister moves p in γ .

There is no need here to take out $\bar{\Sigma}_{self-flex,1}^{(2)}$ and we can now formulate the last part of our main result.

Theorem 4 The 1-cochain $R_2(\gamma)$ with values in $\hat{\beta}_2$ is a 1-cocycle and gives rise to a in general non trivial cohomology class $R_2 \in H^1(M_{\hat{\beta}}; \hat{\beta}_2)$.

Remember that the only relation in $\hat{\beta}_2$ is the embedded 2T-relation, compare the Introduction.

type 1

$$\begin{array}{c} \text{triangle with 1 on left edge} \end{array} \quad w(f) \left(\begin{array}{c} \text{triangle with } d \text{ on top edge} \\ \text{triangle with } d \text{ on bottom edge} \end{array} - \begin{array}{c} \text{triangle with } f \text{ on top edge} \end{array} \right)$$

$$\begin{array}{c} \text{triangle with 1 on left edge, 2 on right edge, 1 on bottom edge} \end{array} \quad \begin{array}{c} \text{triangle with } ml \text{ on left edge, } hm \text{ on right edge} \end{array}$$

type 3

$$\begin{array}{c} \text{triangle with 1 on left edge} \end{array} \quad w(f) \left(\begin{array}{c} \text{triangle with } d \text{ on top edge} \\ \text{triangle with } d \text{ on bottom edge} \end{array} - \begin{array}{c} \text{triangle with } f \text{ on top edge} \end{array} \right)$$

$$\begin{array}{c} \text{triangle with 1 on left edge, 2 on right edge, 1 on bottom edge} \end{array} \quad \begin{array}{c} \text{triangle with } hm \text{ on left edge, } ml \text{ on right edge} \end{array}$$

Figure 46: Contributions $R_2(p)$ for the local types 1 and 3 in the braid case

type 4

$$\begin{array}{c} \text{triangle with edges } 1, 1, 1 \end{array} \quad w(f) \left(\begin{array}{c} \text{crossing with } d \end{array} - \begin{array}{c} \text{triangle with } d \end{array}, \begin{array}{c} \text{crossing with } f \end{array} \right)$$

$$\begin{array}{c} \text{triangle with edges } 1, 2, 1 \end{array} \quad \begin{array}{c} \text{crossing with } ml, hm \end{array}$$

type 5

$$\begin{array}{c} \text{triangle with edges } 1, 1, 1 \end{array} \quad w(f) \left(\begin{array}{c} \text{crossing with } d \end{array} - \begin{array}{c} \text{triangle with } d \end{array}, \begin{array}{c} \text{crossing with } f \end{array} \right)$$

$$\begin{array}{c} \text{triangle with edges } 1, 2, 1 \end{array} \quad \begin{array}{c} \text{crossing with } hm, ml \end{array}$$

Figure 47: Contributions $R_2(p)$ for the local types 4 and 5 in the braid case

type 7

$$\begin{array}{c} \text{triangle with arrows and label } l \end{array} \quad w(f) \left(\begin{array}{c} \text{diagram 1} \end{array} - \begin{array}{c} \text{diagram 2} \end{array}, \begin{array}{c} \text{diagram 3} \end{array} \right)$$

$$\begin{array}{c} \text{triangle with arrows and labels } l, 2, l \end{array} \quad \begin{array}{c} \text{diagram with labels } ml, hm \end{array}$$

type 8

$$\begin{array}{c} \text{triangle with arrows and label } l \end{array} \quad w(f) \left(\begin{array}{c} \text{diagram 1} \end{array} - \begin{array}{c} \text{diagram 2} \end{array}, \begin{array}{c} \text{diagram 3} \end{array} \right)$$

$$\begin{array}{c} \text{triangle with arrows and labels } l, 2, l \end{array} \quad \begin{array}{c} \text{diagram with labels } ml, hm \end{array}$$

Figure 48: Contributions $R_2(p)$ for the local types 7 and 8 in the braid case

$$\begin{array}{c} \text{circle with vertical arrow and label } l \end{array} \quad w(f) \left(\begin{array}{c} \text{diagram 1} \end{array} - \begin{array}{c} \text{diagram 2} \end{array}, \begin{array}{c} \text{diagram 3} \end{array} \right)$$

Figure 49: Contributions $R_2(p)$ for self-tangencies in the braid case

3 Examples and applications

We give some examples in much detail in the hope that it will make it easier for the reader to become familiar with the new invariants.

3.1 Long knots

Let us start by showing that the loop $rot(K)$ is not really interesting for us (this is not too surprising because the loop is just induced by a rotation of the whole 3-space which doesn't depend on the knot at all).

Proposition 1 *Let K be a long knot. Then $R_1(rot(K)) = 0$.*

Proof. Let us represent $rot(K)$ by pushing K through a curl with positive writhe and positive Whitney index as shown in Fig. 50. In the first half of the loop we move for each Reidemeister move from the overcross of the distinguished crossing d to ∞ and in the second half we move from ∞ to the undercross of d . It follows that all distinguished crossings d are of type 1. Consequently, only Reidemeister III moves of global type l_c could contribute non trivially to $R_1(rot(K))$ (compare Definition 12). However, the arc from the overcross of d to ∞ goes over everything in the first half of the loop and hence there are no r-crossings for hm at all. It follows that $W_1(p) = 0$. In the second half of the loop we move always directly from ∞ to the undercross of d . It follows that all Reidemeister III moves are of global type r_c or l_a and do not contribute at all. \square

Remark 5 *It is amazing that not only the value of R_1 on the homology classes represented by $rot(K)$ and $rot(\hat{\beta})$ vanishes but that these classes can be represented by such loops for which the 1-cocycle itself vanishes, i.e. R_1 is identical 0 on each arc in the loop. This suggests that in a future differential geometric approach the differential 1-form should vanish along these loops in M_K respectively $M_{\hat{\beta}}$.*

As a warm-up for the reader we calculate now $R_1(rot(3_1^+))$ by pushing the knot through a curl with positive writhe but negative Whitney index. The loop is shown in Fig. 51 (where as usual we attach numbers to the moves). The relevant signs, types and weights are shown in Fig. 52 and $R_1(rot(3_1^+))$ is calculated in Fig. 53. We see that the 1-cocycle is not identical 0 here and that its value on the loop vanishes only because of the embedded 1T-relation.

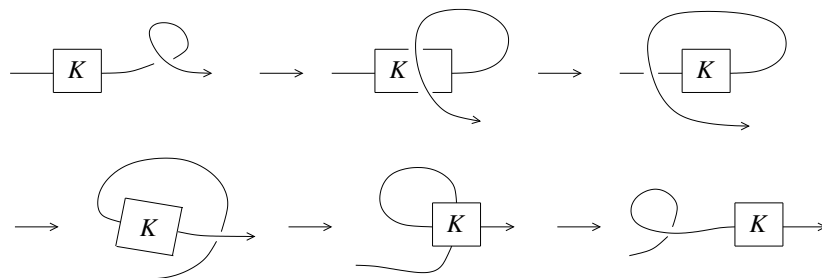


Figure 50: A representative of Gramain's loop for which R_1 is identical 0

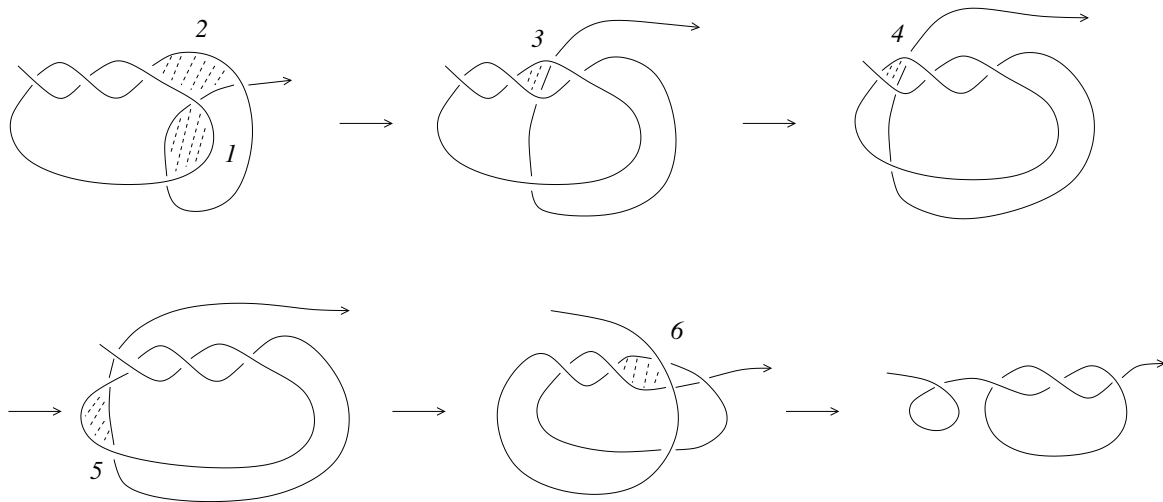


Figure 51: A representative of Gramain's loop for the trefoil

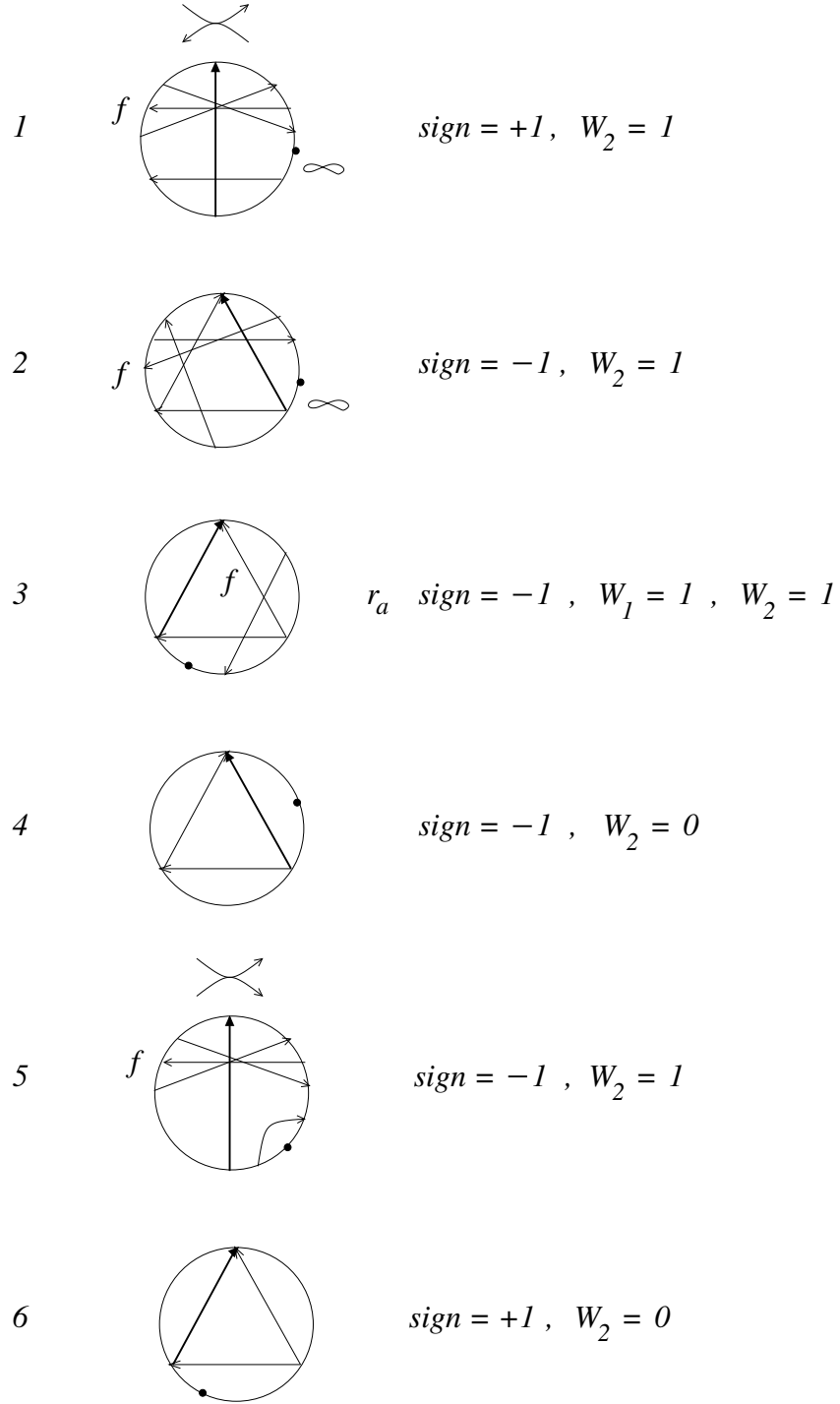


Figure 52: Gauss diagrams and weights of the moves which could a priori contribute to $R_1(rot(3_1^+))$

$$\begin{aligned}
R_1(\text{rot}(3_1^+)) &= + \left(\text{diagram}_1 - \text{diagram}_2 \right) \\
&- \left(\text{diagram}_3 - \text{diagram}_4 \right) \\
&- \left(\text{diagram}_5 - \text{diagram}_6 \right) \\
&- \text{diagram}_7 \\
&- \left(\text{diagram}_8 - \text{diagram}_9 \right) \\
&= - \text{diagram}_{10} = 0
\end{aligned}$$

The diagrams are oriented knot diagrams of the trefoil knot 3_1 . Each diagram consists of a single closed curve with an arrow indicating orientation. A dot on the curve is marked with a '+' or '-' sign, representing a rotation. The diagrams are arranged in a sequence that shows the algebraic manipulation of these rotations, ultimately leading to the zero result.

Figure 53: calculation of $R_1(\text{rot}(3_1^+))$

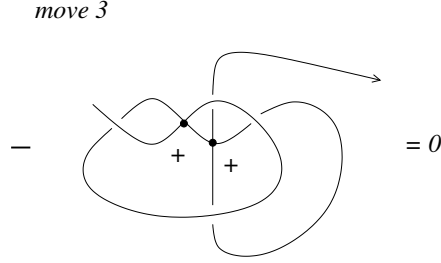


Figure 54: $R_2(\text{rot}(3_1^+)) = 0$

Remark 6 *The embedded 1T-relation is forced from the moving cusps, compare Section 4.6. In [18] (which doesn't contain any singularization) we have considered instead of the embedded 1T-relation some correction term $V^{(1)}$, which is of relative finite type (for the definition compare [18]). So, it seems that the Teiblum-Turchin 1-cocycle on $\text{rot}(K)$ corresponds just to this correction term and in R_1 we quotient out in fact finite type 1-cocycles in Vassiliev's sens.*

For the calculation of $R_2(\text{rot}(3_1^+))$ we use the signs, types and f-crossings from Fig. 52. Exactly one triple crossing is of the right global type and it contributes with the simultaneous singularization of the crossings hm and d , see Fig. 54. But its contribution is annihilated by the generalized embedded 1T-relation.

The above demonstration of the proposition does no longer work in order to show that in general $R_2(\text{rot}(K)) = 0$, because distinguished crossings of type 1 can contribute now too.

Question 2 *Is $R_2(\text{rot}(K)) = 0$ for any long knot K ?*

In Fig. 55 we show the loop $\text{hat}(4_1 \# 4_1)$, where the dot corresponds to another copy of the knot 4_1 . The signs, types, the relevant parts of the Gauss diagrams and the weights (already with taking into account the correction term) of the moves in $\text{hat}(4_1)$ are given in Fig. 56-59. The calculation of $R_1(\text{hat}(4_1))$ is given in Fig. 60-63. It is amazing that for most cancellations we have just to slide the double point over or under branches of the knot. However, in the last step of the calculation we use a non regular isotopy as shown in Fig. 62.

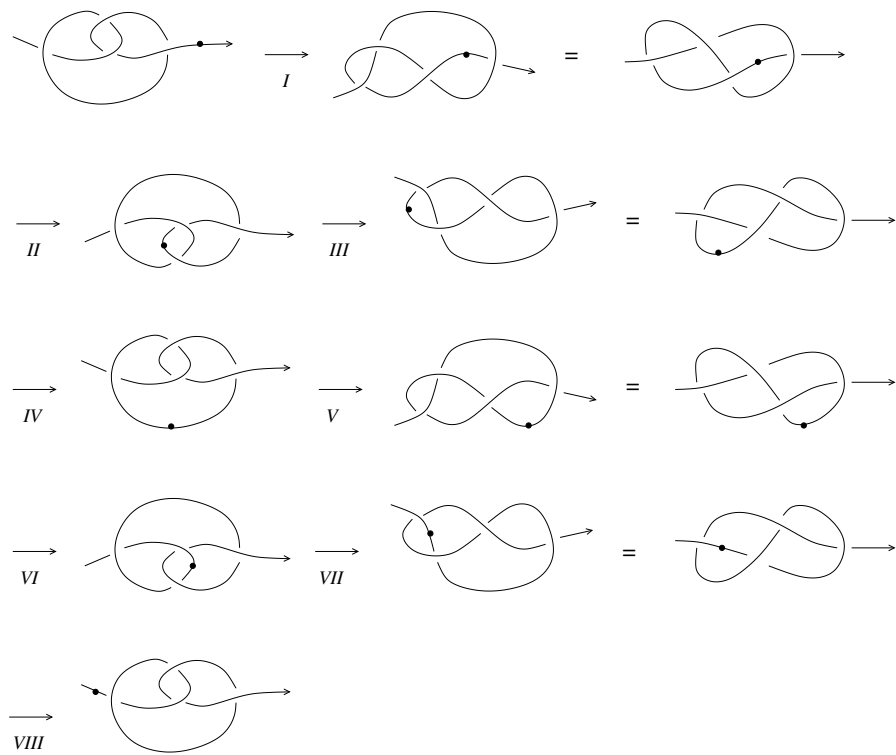


Figure 55: The loop $\hat{4}_1 \# 4_1$

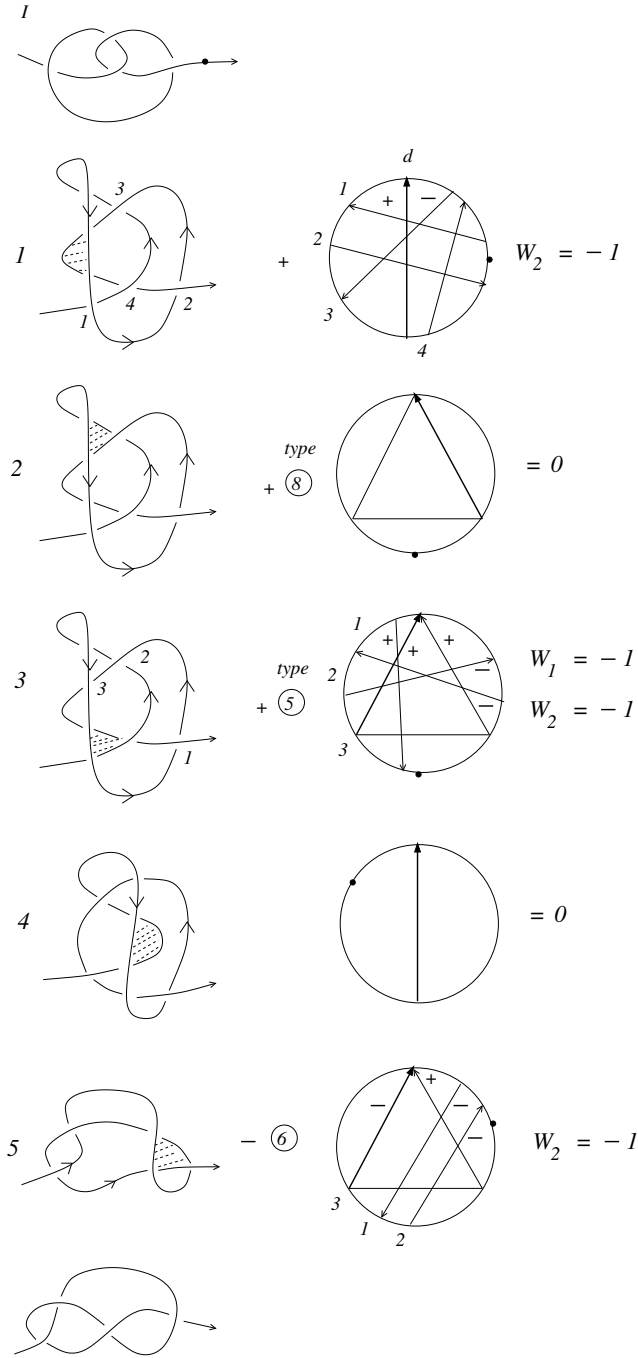


Figure 56: The Reidemeister moves of type II and III together with their signs, types and weights in part I of $\hat{hat}(4_1)$

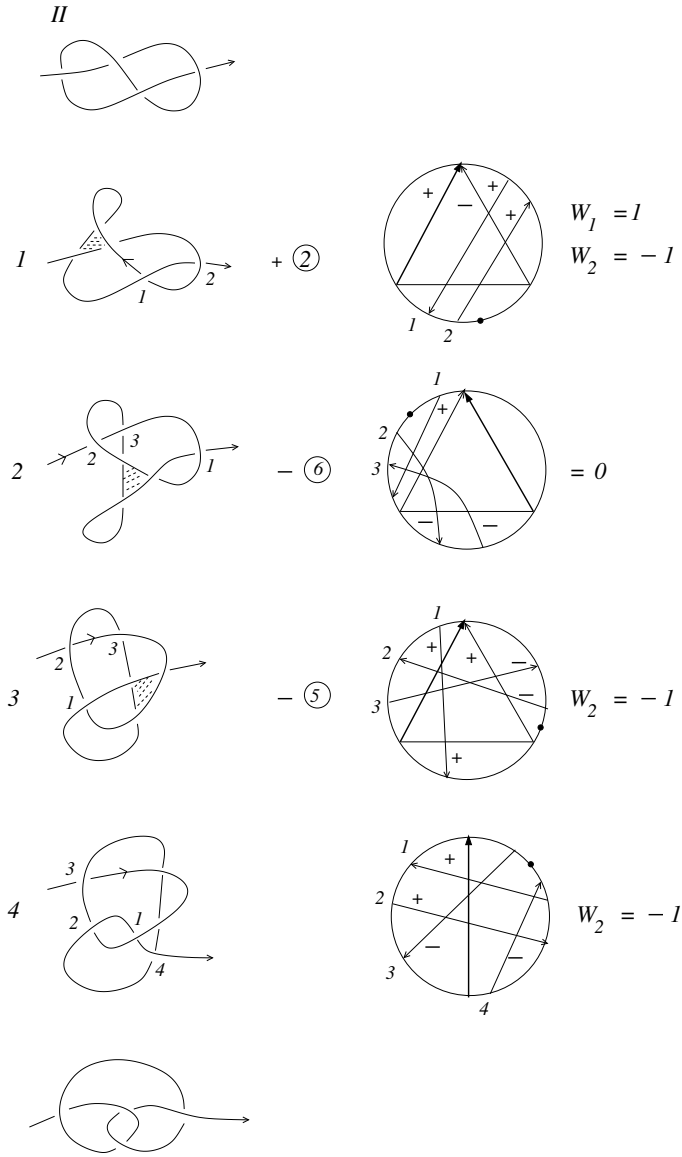


Figure 57: The moves in part II of $\hat{hat}(4_1)$

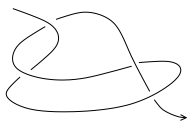
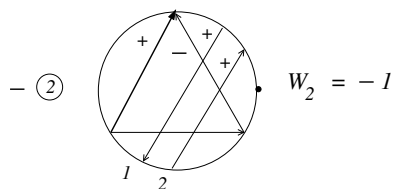
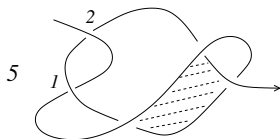
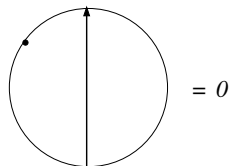
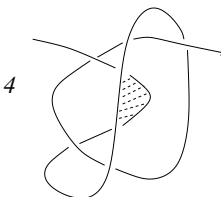
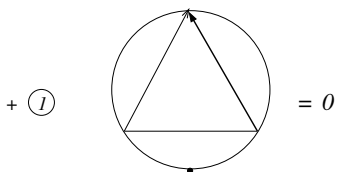
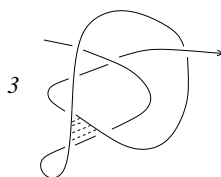
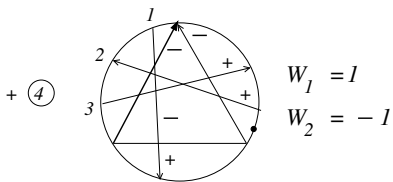
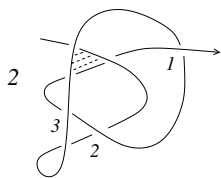
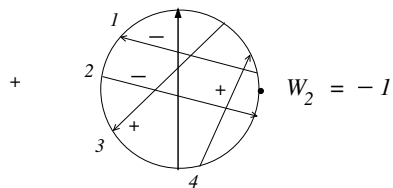
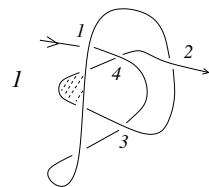


Figure 58: The moves in part III of $\hat{hat}(4_1)$

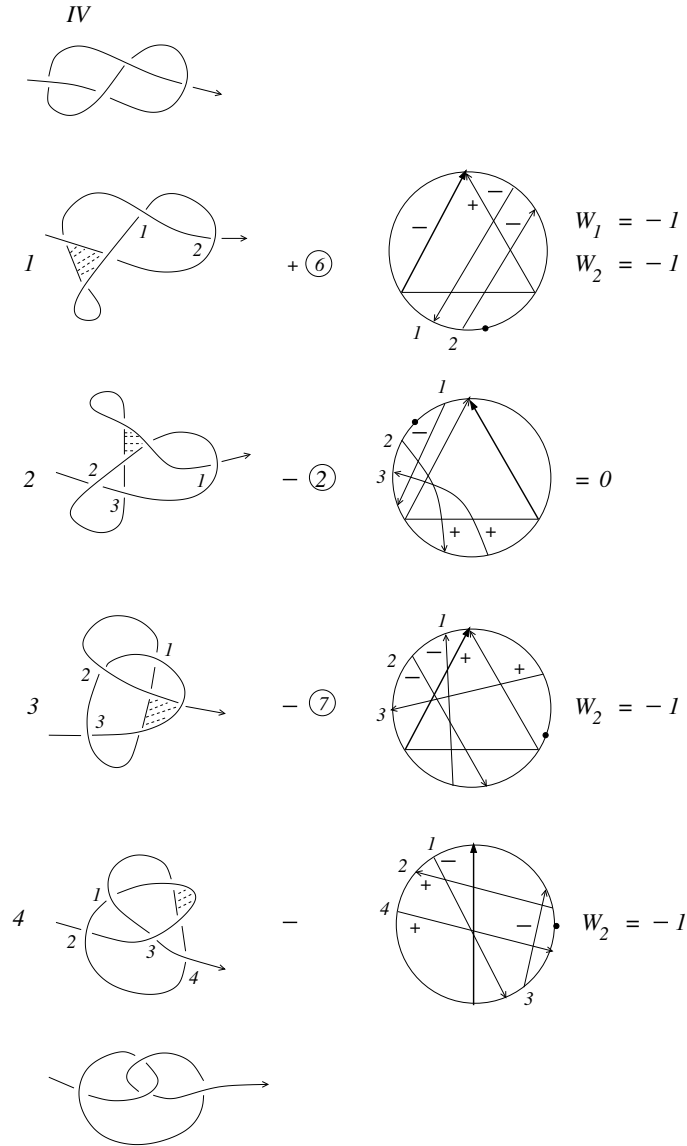


Figure 59: The moves in part IV of $\hat{hat}(4_1)$

$$\begin{aligned}
I_1 &= (\text{diagram 1} - \text{diagram 2}) \\
I_3 &= (\text{diagram 3} - \text{diagram 4}) - \text{diagram 5} \\
I_5 &= + (\text{diagram 6} - \text{diagram 7}) \\
II_1 &= (\text{diagram 8} - \text{diagram 9}) + \text{diagram 10} \\
II_3 &= + (\text{diagram 11} - \text{diagram 12}) \\
II_4 &= + (\text{diagram 13} - \text{diagram 14})
\end{aligned}$$

The diagrams are oriented links with arrows. Some regions are shaded with dots. Signs (+, -) are placed near crossings. Labels 1, 2, 0 are placed below some diagrams.

Figure 60: Calculation of $R_1(\text{hat}(4_1))$ for part I and part II

$$\begin{aligned}
III_1 &= - \left(\text{diagram}_1 - \text{diagram}_2 \right) \\
III_2 &= - \left(\text{diagram}_3 - \text{diagram}_4 + \text{diagram}_5 \right) \\
III_5 &= + \left(\text{diagram}_6 - \text{diagram}_7 \right) \\
IV_1 &= - \left(\text{diagram}_8 - \text{diagram}_9 \right) - \text{diagram}_{10} \\
IV_3 &= + \left(\text{diagram}_{11} - \text{diagram}_{12} \right) \\
IV_4 &= + \left(\text{diagram}_{13} - \text{diagram}_{14} \right)
\end{aligned}$$

Figure 61 shows the calculation of $R_1(\hat{4}_1)$ for part III and part IV. The figure consists of six rows of knot diagrams, each representing a term in the calculation. The diagrams are labeled III_1 , III_2 , III_5 , IV_1 , IV_3 , and IV_4 . Each row shows a combination of diagrams with signs (+, -) and parentheses. The diagrams are oriented with arrows and some have shaded regions. The labels 3 , 0 , and 4 are placed below some diagrams, indicating their values or weights.

Figure 61: Calculation of $R_1(\hat{4}_1)$ for part III and part IV

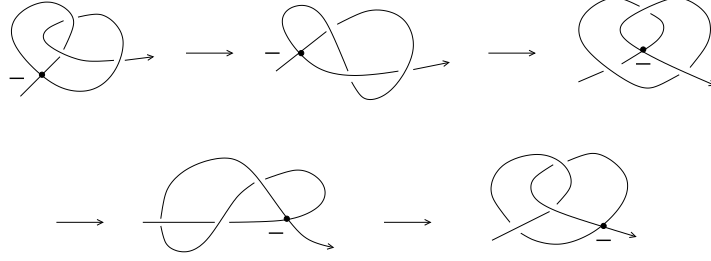


Figure 62: A non-regular isotopy of singular knots used in the calculation of $R_1(\text{hat}(4_1))$

$$\begin{array}{ccccccc}
 + & \text{[Diagram 1]} & - & \text{[Diagram 2]} & + & \text{[Diagram 3]} & - & \text{[Diagram 4]} & = 0
 \end{array}$$

Figure 63: Calculation of $R_1(\text{hat}(4_1))$

The calculation of $R_1(\text{hat}(4_1 \# 4_1))$ is very long. Notice that not all crossings intersect the distinguished crossing d (compare Definition 9). Therefore the small summand 4_1 could contribute to the weight $W_2(p)$ of a Reidemeister move p of the big knot 4_1 . Consequently, the place of the small summand 4_1 in the diagram of the big knot 4_1 is important. There were 18 Reidemeister moves (of type III and II) in $\text{hat}(4_1)$, corresponding to the pieces of the loop I up to IV. There are 36 Reidemeister moves in $\text{hat}(4_1 \# 4_1)$, corresponding to I up to VIII which have all a knot 4_1 as a summand. But pushing the strands over or under this summand leads to another 64 Reidemeister moves of type III and II. There are lots of cancellations (we use here often the obvious fact that the composition of a singular long knot with a non-singular long knot is commutative). The only two contributions which do not cancel out come from sliding branches under respectively over a small summand 4_1 . We indicate the place in the isotopy together with the relevant Reidemeister III move in Fig. 64. We left the verification of the details to the reader.

It is amazing that in both examples the knots in K_1^+ are just the mirror images of those in K_1^- and with opposite sign.

Question 3 *Let K be an amphicheral knot. Is it true that $R_1(\text{hat}(K)) \in K_1^+$*

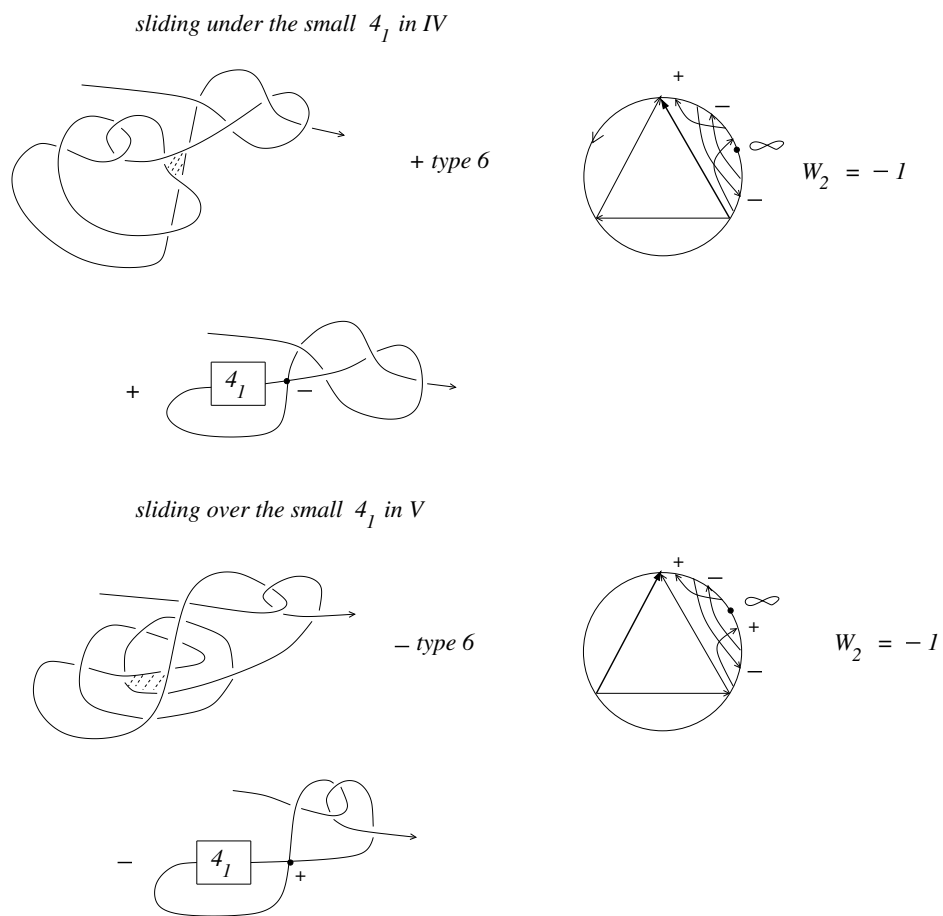


Figure 64: Calculation of $R_1(\text{hat}(4_1 \sharp 4_1))$

is equal to minus the mirror image of $R_1(\text{hat}(K)) \in K_1^-$?

We give only some indications for the calculation of $R_1(\text{hat}(5_2^+))$. There is no symmetry and the loop is much longer. The loop $\text{hat}(5_2^+)$ together with its 54 Reidemeister moves and the numbers of the crossings for each move are shown in Fig. 65-74. The signs, types and weights of the 37 Reidemeister moves which could a priori contribute non trivially to R_1 can be derived from the figures. The calculation of $R_1(\text{hat}(5_2^+))$ leads then to the invariant given in Fig. 7 (see the Introduction), by using isotopies of singular knots, but we leave the details to the reader. Notice that for all four knots in $R_1(\text{hat}(5_2^+))$ the compact knot of the smoothing link is a trivial knot. The linking numbers are 0, 1 and 2 respectively. The one with linking number 0 is evidently not a split link and hence the embedded 1T-relation does not apply. The two knots with linking number 2 are distinguished by the sign of the double point.

It would be extremely interesting to calculate $PR_1(\text{hat})$ for iterations of the knot 5_2^+ , compare Remark 4. Notice that in the calculation of $PR_1(\text{hat}(K))$ one can skip the sometimes difficult part in the calculation of $R_1(\text{hat}(K))$, namely to decide whether or not two singular knots are isotopic.

Because of its importance we give the calculation of $R_2(\text{hat}(4_1))$ in all details in Fig. 75, where we use the signs, types and f-crossings from Fig. 56-59.

Let us introduce an easily defined knot invariant, which will perhaps become important in the future.

Let K_t be a generic diagram of a long knot and let $c(K_t)$ denote its number of crossings.

Definition 26 *The 1-parameter crossing number $c_H(K)$ of a knot type K is defined as*

$$c_H(K) = \min(\max(c(K_t)))$$

where \max is over all generic knots K_t in Hatcher's loop $\text{hat}(K)$, and such that the projection of the diagram of K_t does not contain any loops neither any bigons with vertices which have different signs, and \min is over all generic representatives $\text{hat}(K)$ of Hatcher's loop for the knot type K . (We do not fix the framing of K .)

Proposition 2 $c_H(3_1) = 4$ and $c_H(4_1) = 6$.

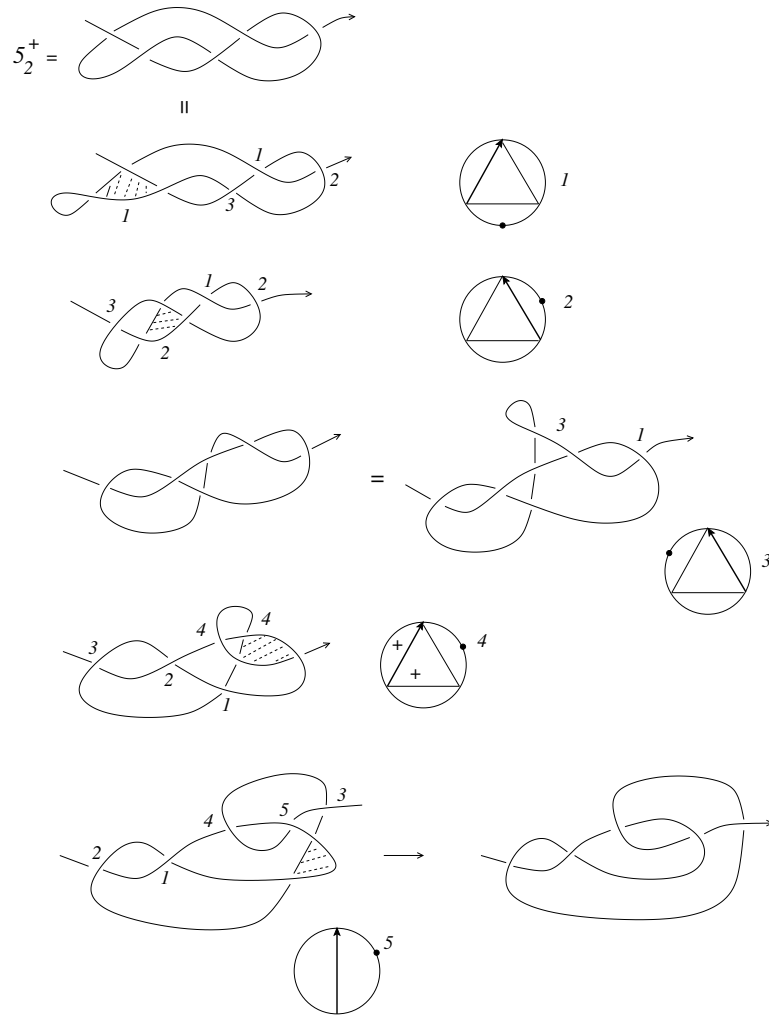


Figure 65: The loop $\hat{5}_2^+$ with the global types of the Reidemeister moves, one

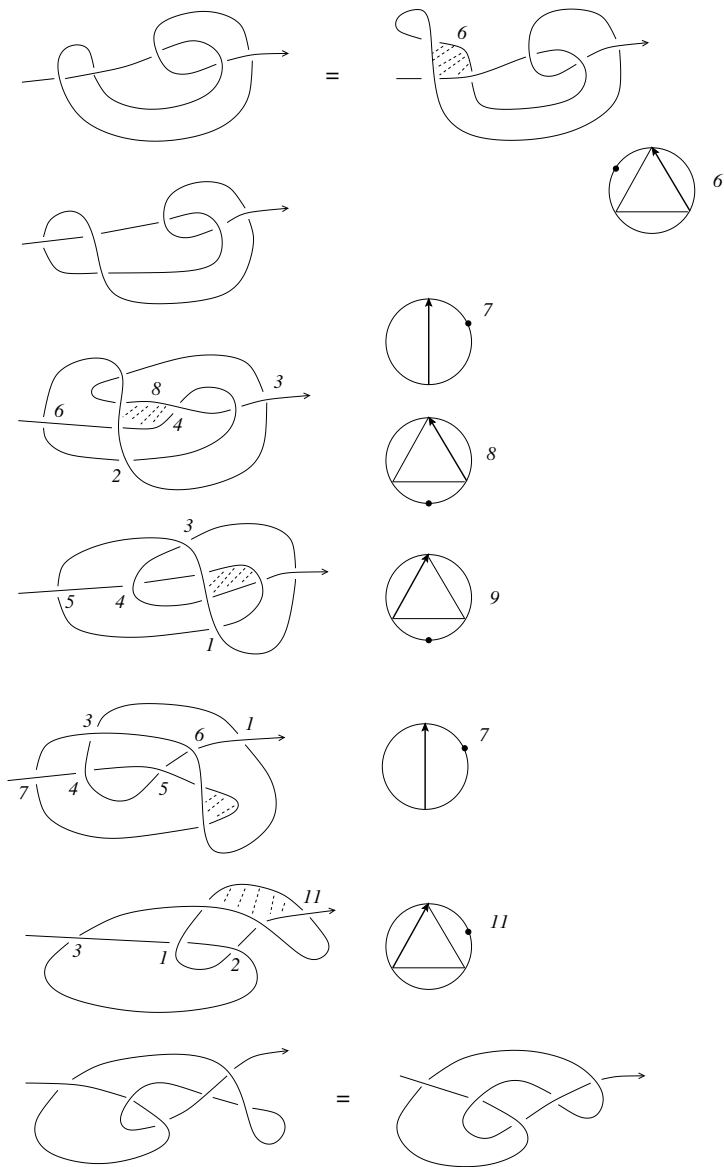


Figure 66: The loop $\hat{hat}(5_2^+)$ with the global types of the Reidemeister moves, two

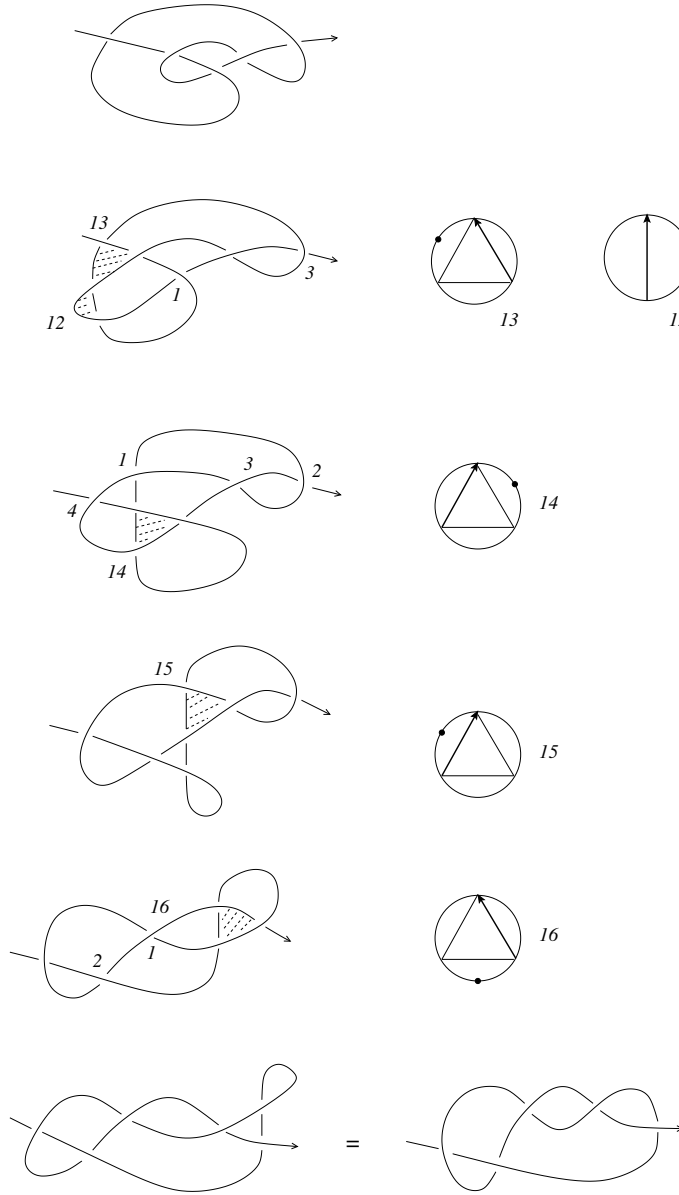


Figure 67: The loop $\text{hat}(5_2^+)$ with the global types of the Reidemeister moves, three

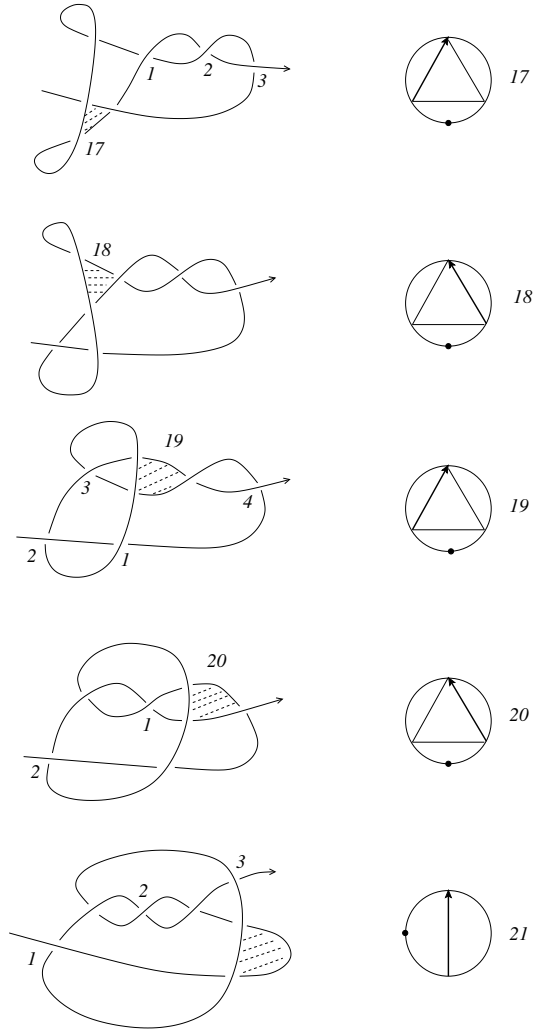


Figure 68: The loop $\text{hat}(5_2^+)$ with the global types of the Reidemeister moves, four

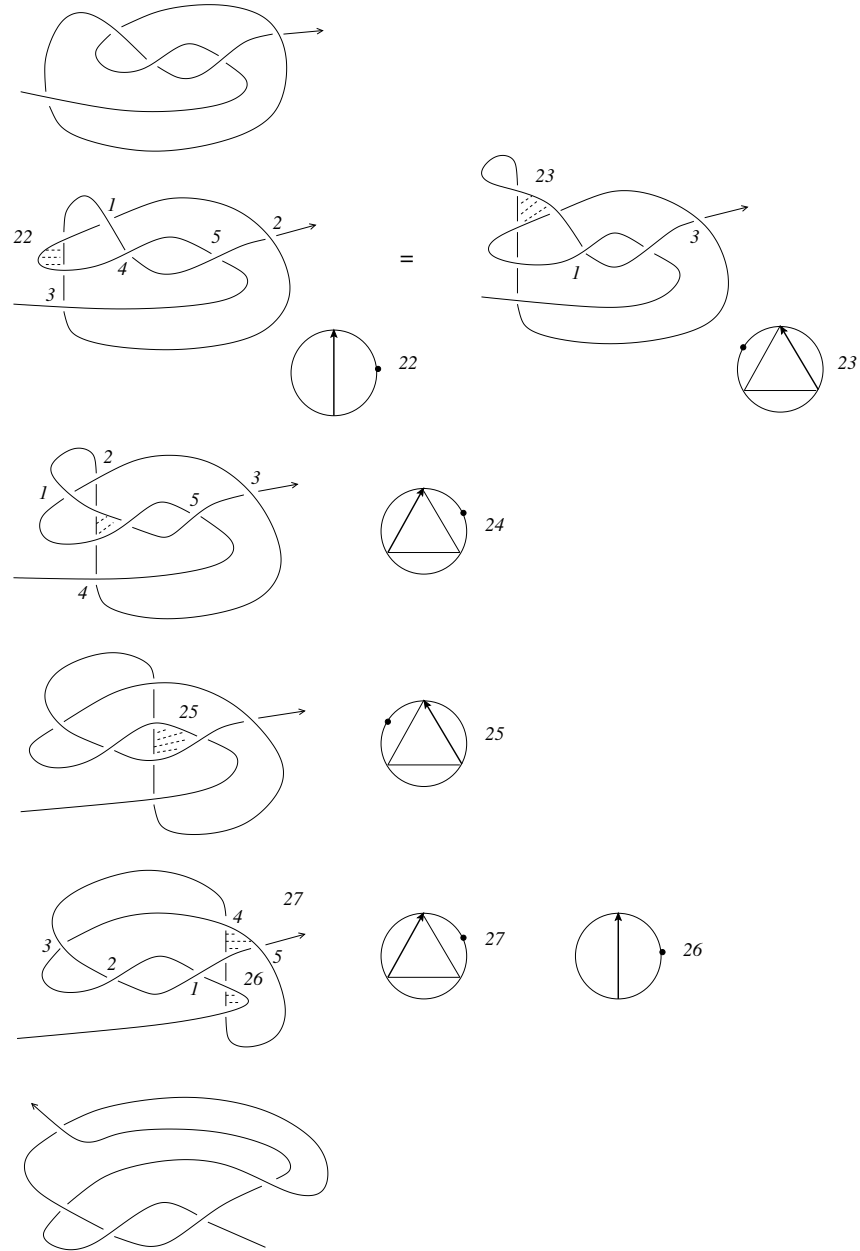


Figure 69: The loop $\text{hat}(5_2^+)$ with the global types of the Reidemeister moves, five

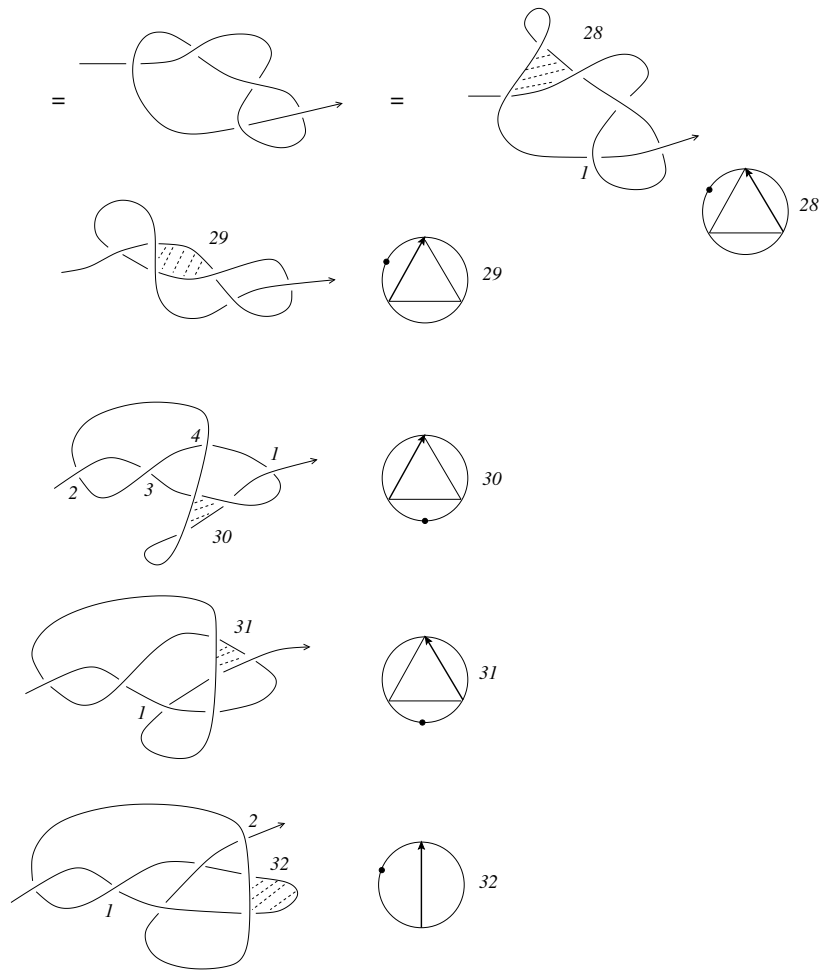


Figure 70: The loop $\hat{hat}(5_2^+)$ with the global types of the Reidemeister moves, six

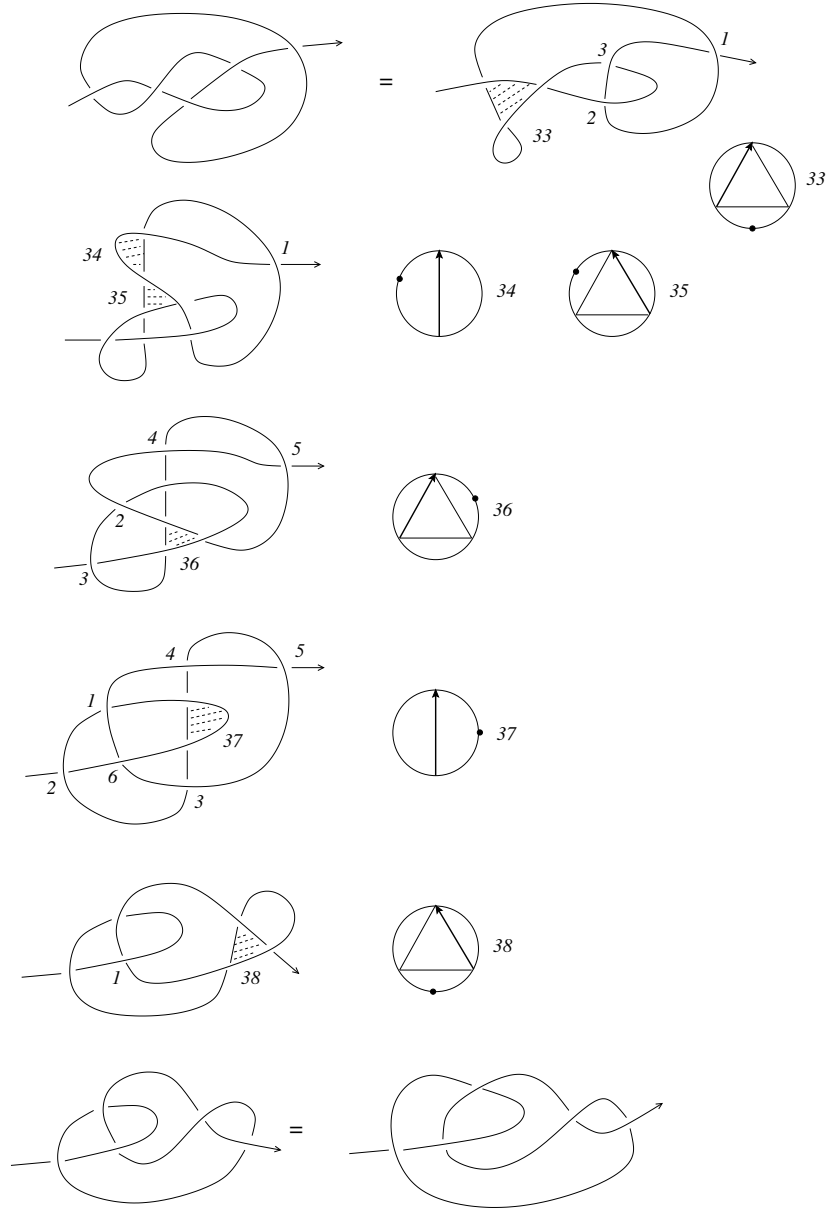


Figure 71: The loop $\hat{hat}(5_2^+)$ with the global types of the Reidemeister moves, seven

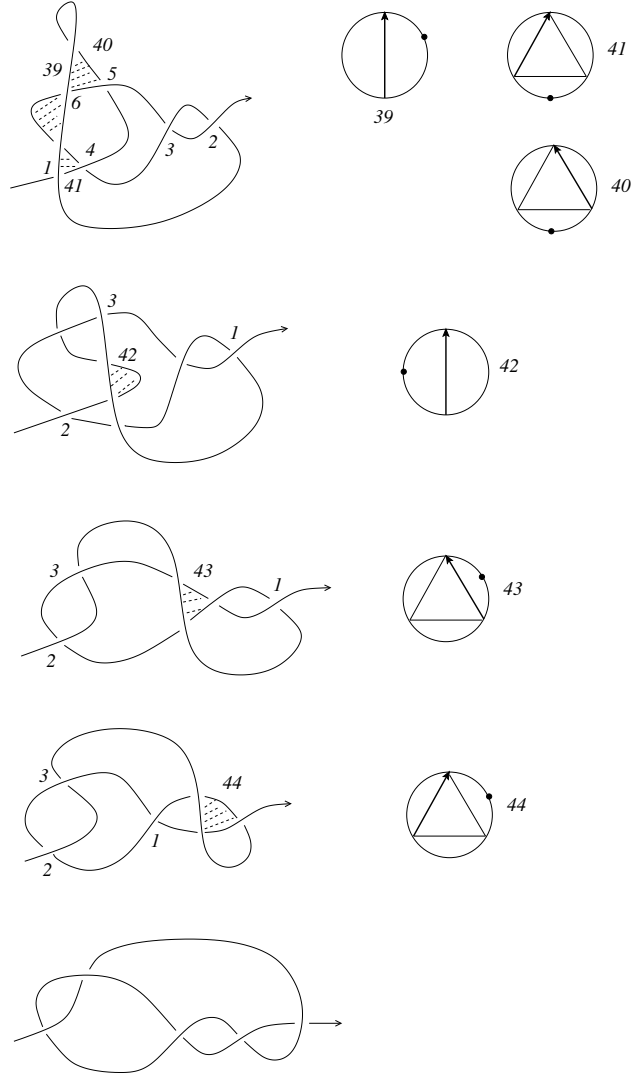


Figure 72: The loop $\hat{hat}(5_2^+)$ with the global types of the Reidemeister moves, eight

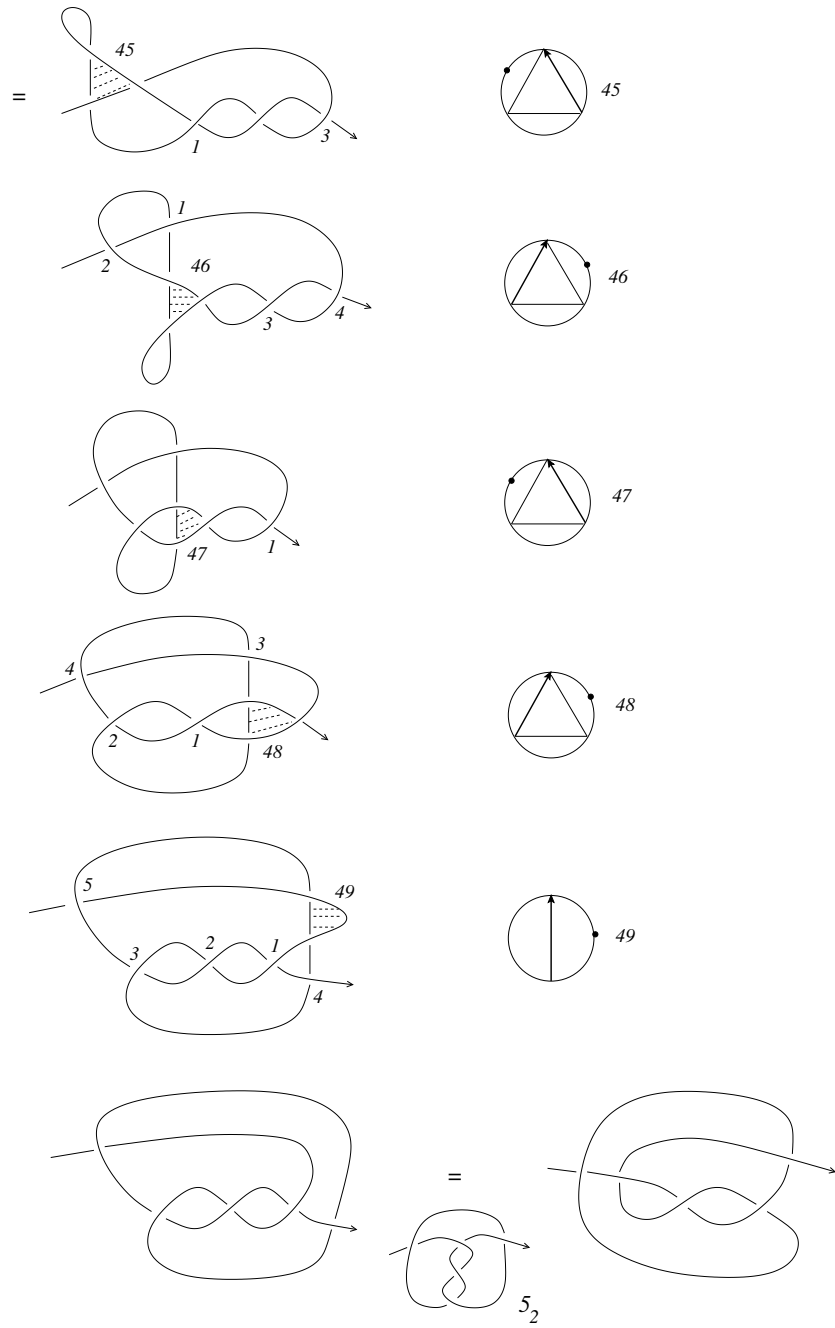


Figure 73: The loop $\hat{5}_2^+$ with the global types of the Reidemeister moves, nine

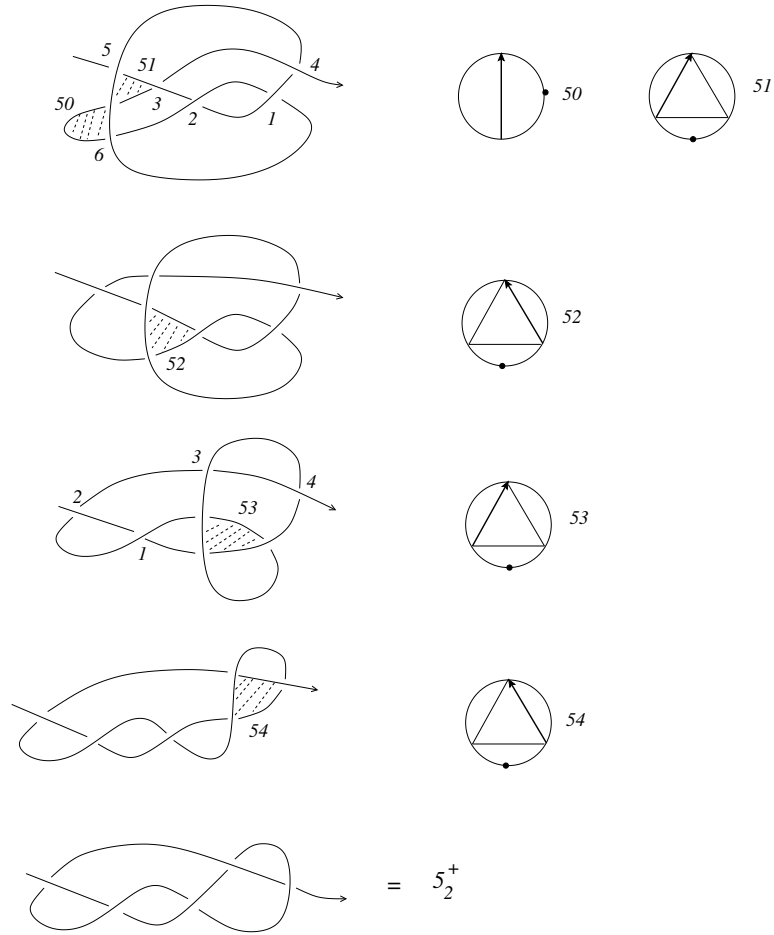


Figure 74: The loop $\hat{5}_2^+$ with the global types of the Reidemeister moves, ten

$$\begin{aligned}
I_2 &+ \left(\begin{array}{c} \text{Diagram 1} \\ =0 \end{array} - \begin{array}{c} \text{Diagram 2} \\ =0 \end{array} \right) - \begin{array}{c} \text{Diagram 3} \\ =0 \end{array} \\
I_3 &+ \begin{array}{c} \text{Diagram 4} \\ =0 \end{array} \quad I_4 - \left(\begin{array}{c} \text{Diagram 5} \\ =0 \end{array} - \begin{array}{c} \text{Diagram 6} \\ =0 \end{array} \right) \\
II_1 &+ \begin{array}{c} \text{Diagram 7} \\ =0 \end{array} \quad III_2 + \begin{array}{c} \text{Diagram 8} \\ =0 \end{array} \\
III_3 &+ (-1) \left(\begin{array}{c} \text{Diagram 9} \\ =0 \end{array} - \begin{array}{c} \text{Diagram 10} \\ =0 \end{array} \right) - \begin{array}{c} \text{Diagram 11} \\ =0 \end{array} \\
III_4 &- (-1) \left(\begin{array}{c} \text{Diagram 12} \\ =0 \end{array} - \begin{array}{c} \text{Diagram 13} \\ =0 \end{array} \right) + IV_1 + \begin{array}{c} \text{Diagram 14} \\ =0 \end{array} \\
&= \begin{array}{c} \text{Diagram 15} \\ K_2^{+-} \end{array} - \begin{array}{c} \text{Diagram 16} \\ K_2^{+-} \end{array} + \begin{array}{c} \text{Diagram 17} \\ K_2^{-+} \end{array} - \begin{array}{c} \text{Diagram 18} \\ K_2^{-+} \end{array}
\end{aligned}$$

Figure 75: Calculation of $R_2(hat(4_1))$

Proof. It is an easy matter to draw a loop for $\text{hat}(3_1)$ which realizes $c_H(3_1) = 4$. The representative of $\text{hat}(4_1)$ given in Fig. 55 realizes $\max(c(K_t)) = 7$, but it contains a bigon with vertices of different signs. However there are exactly two diagrams, namely 3 in Fig. 57 and 3 in Fig. 59 which have no bigons and which have exactly 6 crossings. We have to show that there is no other representative of $\text{hat}(4_1)$ where this number is less than 6. Each representative of $\text{hat}(4_1)$ contains a Reidemeister II move where two crossings vanish together from a branch which moves over the rest of the diagram and such that there are exactly 3 crossings on the vertical part of the moving branch. Moving this branch further backwards over the next crossing we obtain a diagram with no loops, no bigons with vertices of different signs and with at least 6 crossings (as in in Fig. 57). \square

It is possible that the embedded 1T-relation and the embedded 2T-relation (generalized in the evident way to bigons with oriented boundary by smoothing both double points with respect to the orientation) will turn out to be the only relations in K_d for $d > 2$. (The embedded 2T-relation does not occur in K_2 but it does already occur in $\hat{\beta}_2$.) This motivates the above definition of $c_H(K)$.

It follows now immediately from Definitions 2 and 26 and from the natural generalizations of the Definitions 3 and 4 that for each knot K and for each 1-cocycle invariant R_d of degree d with values in K_d (modulo the embedded 1T-relation and the embedded 2T-relation) we have $R_d(\text{hat}(K)) = 0$ for each $d > c_H(K)$.

Question 4 *Let K be a hyperbolic knot. Does there exist a 1-cocycle invariant R_d of degree $d = c_H(K)$ and such that $R_{c_H(K)}(\text{hat}(K)) \neq 0$?*

For the moment we have only non trivial 1-cocycle invariants up to degree 2. But if 1-cocycle invariants of higher degrees do exist and if the answer to the above question is affirmative then it would lead to a complete knot invariant (at least for hyperbolic knots) as explained at the end of the Introduction.

3.2 Closed braids

Let us start by recalling Hatcher's result.

Proposition 3 *The loops $\text{rot}(\hat{\beta})$ and $\text{hat}(\hat{\beta})$ represent linearly dependent homology classes in $H_1(M_{\hat{\beta}}; \mathbb{Q})$ if and only if $\hat{\beta}$ is isotopic to a torus knot in ∂V .*

Proof (Hatcher). The rotations give an action of $\mathbb{Z} \times \mathbb{Z}$, and one can look at the induced action on the fundamental group of the knot complement, with respect to a base point in the boundary torus ∂V of the solid torus. Call this fundamental group G . The action of $\mathbb{Z} \times \mathbb{Z}$ on G is conjugation by elements of the $\mathbb{Z} \times \mathbb{Z}$ subgroup of G represented by loops in the boundary torus. The action will be faithful (zero kernel) if the center of G is trivial. The only (irreducible) 3-manifolds whose fundamental groups have a nontrivial center are Seifert fibered manifolds defined by a circle action. The only such manifolds that embed in \mathbb{R}^3 and have two boundary components (as here) are the obvious ones that correspond to cable knots, that is, the complement of a knot in a solid torus that is isotopic to a nontrivial loop in the boundary torus. \square

There aren't any Reidemeister moves in $rot(\hat{\beta})$ and hence $R_1(rot(\hat{\beta})) = 0$. Consequently, the interesting loop is again $hat(\hat{\beta})$ and we represent it by a sequence of braid words. We use the standard notations for braid groups, but for shorter writing we denote σ_i by i and σ_i^{-1} by \bar{i} . A double point which comes from a crossing σ_i is denoted by t_i^+ and one which comes from a crossing σ_i^{-1} by t_i^- (which corresponds also to the usual notations besides the signs).

We consider a loop representing $hat(\hat{\beta})$ for $\beta = \sigma_1\sigma_2^{-1} \in B_3$. Each of the twenty two arrows corresponds to a Reidemeister move and we indicate the involved crossings by a bracket. (Remember that the braid words correspond to closed braids and hence they are well defined up to cyclic permutations.)

$$\begin{aligned} 1\bar{2} &\rightarrow (1\bar{1})1\bar{2} \rightarrow 1(2\bar{2})\bar{1}1\bar{2} \rightarrow 12(1\bar{1})\bar{2}1\bar{1}\bar{2} \rightarrow \bar{1}\bar{2}\bar{1}1(\bar{2}12)1 \rightarrow \bar{1}\bar{2}\bar{1}112(\bar{1}1) \rightarrow \\ &\bar{1}\bar{2}\bar{1}112(1\bar{1}) \rightarrow \bar{1}\bar{2}\bar{1}1(121)\bar{1} \rightarrow \bar{1}\bar{2}(\bar{1}1)212\bar{1} \rightarrow \bar{1}(\bar{2}2)12\bar{1} \rightarrow (\bar{1}1)2\bar{1} \rightarrow 2\bar{1} \rightarrow \\ &(1\bar{1})2\bar{1} \rightarrow 1(2\bar{2})\bar{1}2\bar{1} \rightarrow 12(1\bar{1})\bar{2}1\bar{2}\bar{1} \rightarrow \bar{1}\bar{2}\bar{1}2(\bar{1}1)21 \rightarrow \bar{1}\bar{2}\bar{1}2(1\bar{1})21 \rightarrow \bar{1}\bar{2}\bar{1}21(\bar{1}21) \rightarrow \\ &\bar{1}\bar{2}\bar{1}(212)1\bar{2} \rightarrow \bar{1}\bar{2}(\bar{1}1)211\bar{2} \rightarrow \bar{1}(\bar{2}2)11\bar{2} \rightarrow (\bar{1}1)1\bar{2} \rightarrow 1\bar{2} \end{aligned}$$

The weights of a Reidemeister move are invariant under all those isotopies where no branch moves over or under or between the branches of the Reidemeister move (compare Section 4). Consequently, we can simplify the braid words by these isotopies (in particular move 6 cancels out with move 11).

We show the relevant part of the Reidemeister moves together with the relevant part of the Gauss diagrams, the signs and the types in Fig. 76.

One easily calculates now (compare the Introduction):

$$\begin{aligned} R_1(hat(\hat{\beta})) &= -1t_1^-\bar{2}212 + t_1^+\bar{1}\bar{2}\bar{2}12 - 1t_2^+1\bar{1}\bar{1}\bar{2} + 2t_1^+2\bar{1}\bar{1}\bar{2} - t_1^-1\bar{2}1 + \bar{1}t_1^+2\bar{1} - \\ &t_2^-211\bar{2}\bar{1} + \bar{2}t_2^+11\bar{2}\bar{1} + \bar{2}t_1^+2\bar{2} - t_1^-21\bar{2} = 2[t_1^+2\bar{1}\bar{1} + t_1^+\bar{2}] - 2[t_1^-1\bar{2}1 + t_1^-21\bar{2}] \end{aligned}$$

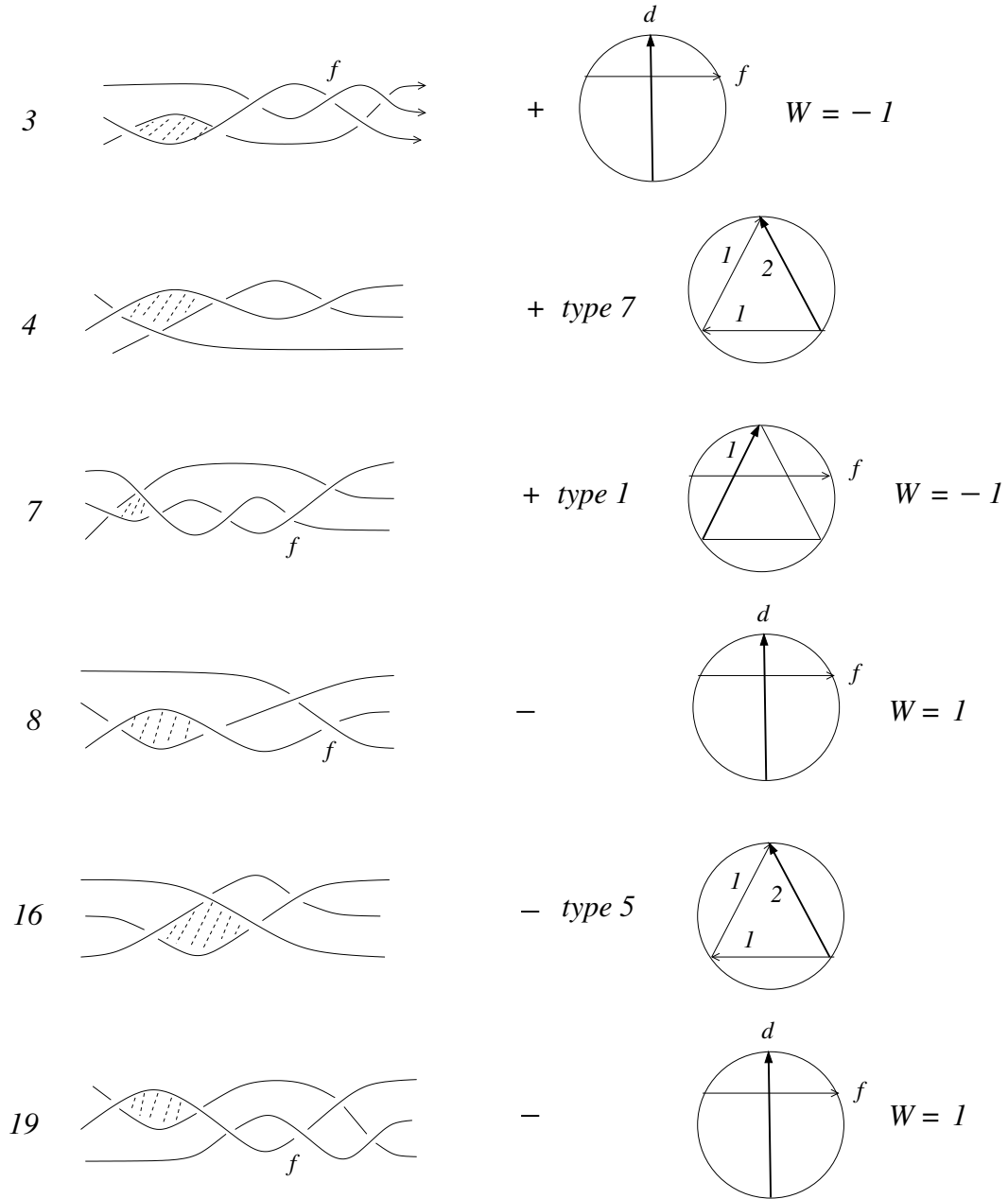


Figure 76: Relevant Reidemeister moves with signs, types and weights for $R_1(\text{hat}(\sigma_1 \hat{\sigma}_2^{-1}))$

Notice that the two singular knots in $\hat{\beta}_1^+$ have linking number -1 respectively 0 between the two components of the smoothing link and the two knots in $\hat{\beta}_1^-$ have linking number +1 respectively 0. So, there aren't possible any further simplifications.

The calculation of $R_2(\text{hat}(\hat{\beta}))$ is completely analogous, but remember the embedded 2T-relation in $\hat{\beta}_2^{+-}$ and in $\hat{\beta}_2^{-+}$ (compare the Introduction). The moves 1,3, 7, 8, 17, 19 contribute now to $R_2(\text{hat}(\hat{\beta}))$ too.

One calculates (but we left the verification to the reader) that

$$R_2(\text{hat}(\hat{\beta})) = [t_1^+ \bar{2}t_1^+ \bar{1} - t_1^+ \bar{1}\bar{2}\bar{2}t_1^+ 2] \oplus [t_1^+ 21t_1^- \bar{2}\bar{2}] \oplus [-t_1^- 12t_1^+ \bar{2}\bar{2}] \oplus [t_1^- 221t_1^- 2\bar{1}\bar{2} - t_1^- \bar{2}12t_1^- 1]$$

If we smooth in all six singular knots the two double points against the orientation then we obtain always a 2-component link which contains a trivial knot. However its linking number (up to sign) with the other component is always non trivial besides for $t_1^+ \bar{2}t_1^+ \bar{1}$ and $t_1^- \bar{2}12t_1^- 1$ (for the verifications one has to draw the singular closed braids). Consequently, the relation does not apply and moreover the two knots in $\hat{\beta}_2^{++}$ respectively $\hat{\beta}_2^{--}$ are not isotopic.

The HOMFLYPT skein module for closed 3-braids in the solid torus is generated by the standard closure of the permutation braids 1, σ_1 and $\sigma_1\sigma_2$.

An easy calculation from $R_1(\text{hat}(\hat{\beta}))$ by using the Kauffman-Vogel skein relations gives now

$$PR_1(\text{hat}(\hat{\beta})) = 2z^2\hat{1} - 4z\hat{\sigma}_1 - 2(A+B)z^2\hat{\sigma}_1 + 2(A+B)z\sigma_1\hat{\sigma}_2$$

The variable v does never occur for closed braids and hence up to normalization there is no difference between PR_1 and ΔR_1 (but notice that a difference would appear even for closed braids in the case of the Kauffman polynomial for singular links).

A standard calculation gives

$$\begin{aligned}\Delta_{\hat{1}\cup L}(u, t) &= (u-1)^2 \\ \Delta_{\hat{\sigma}_1\cup L}(u, t) &= u^2 + (t-1)u - t \\ \Delta_{\sigma_1\hat{\sigma}_2\cup L}(u, t) &= u^2 + tu + t^2\end{aligned}$$

and the substitution into $\Delta R_1(\text{hat}(\hat{\beta}))$ leads to the formula given in the Introduction.

For $\beta = \sigma_1\sigma_2\sigma_3^{-1}$ we represent $\text{hat}(\hat{\beta})$ by a loop of the form

$$\beta \rightarrow \Delta^2\Delta^{-2}\beta = \Delta^{-2}\beta\Delta^2 \rightarrow \Delta^{-2}\Delta^2\beta \rightarrow \beta$$

We call this a *combinatorial loop* $\text{hat}(\hat{\beta})$.

This loop is very long (it contains exactly 40 Reidemeister moves) and below we give only the ten Reidemeister II moves and the six Reidemeister III moves which have the right global type (compare Definition 21) in order to contribute a priori to R_1 . In order to calculate the weight $W(p)$ one has to draw each time the closed braid and the corresponding Gauss diagram.

- move 1: $-(\bar{3}3)32\bar{1}$, $W(p) = 0$
- move 2: $-(\bar{3}3)123\bar{2}3\bar{1}\bar{2}$, $W(p) = 0$
- move 3: $-(\bar{3}3)\bar{3}112\bar{1}$, $W(p) = 0$
- move 4: $-(\bar{3}3)2112\bar{3}\bar{1}\bar{2}$, $W(p) = 1$
- move 5: $+(\bar{3}3)\bar{2}\bar{1}322$, $W(p) = 0$
- move 6: $+(\bar{3}3)112\bar{1}\bar{3}$, $W(p) = -1$
- move 7: $+(\bar{3}3)\bar{2}\bar{3}122$, $W(p) = -1$
- move 8: $+(\bar{3}3)\bar{1}33\bar{2}12\bar{3}$, $W(p) = -1$
- move 9: $+(1\bar{1})\bar{1}32$, $W(p) = 0$
- move 10: $-(\bar{3}3)\bar{3}112\bar{1}$, $W(p) = 0$
- move 11: $+(\bar{3}23)\bar{3}\bar{2}\bar{3}123$, global type r, local type 7, $W(p) = -1$
- move 12: $-(212)\bar{2}\bar{1}\bar{1}3$, global type r, local type 1, $W(p) = 0$
- move 13: $+(121)\bar{3}\bar{2}$, global type r, local type 1, $W(p) = 0$
- move 14: $-(323)1\bar{3}\bar{2}\bar{1}$, global type r, local type 1, $W(p) = 0$
- move 15: $-(\bar{2}32)1\bar{2}1\bar{3}$, global type l, local type 5
- move 16: $+(232)32\bar{1}\bar{3}\bar{2}\bar{3}$, global type l, local type 1

We see that finally only seven Reidemeister moves contribute non trivially to R_1 . One easily calculates now

$$R_1(\text{hat}(\hat{\beta})) = -t_3^- 321123\bar{1}\bar{2} + \bar{3}t_3^+ 21123\bar{1}\bar{2} - t_3^- 12 + t_3^+ \bar{3}12\bar{3} - 3t_3^- \bar{2}\bar{3}122 + t_3^+ \bar{3}\bar{2}\bar{3}122 - t_3^- \bar{1}33\bar{2}12 + t_3^+ \bar{1}3\bar{2}12\bar{3} - 2t_3^+ \bar{3}\bar{2}\bar{3}12 + t_2^+ 3\bar{2}\bar{3}\bar{2}\bar{3}123 - t_2^- 321\bar{2}1\bar{3} + t_2^+ 3232\bar{1}\bar{3}\bar{2}\bar{3}$$

It simplifies to the expression given in Fig. 17 in the Introduction.

It follows that

$$PR_1(\text{hat}(\hat{\beta})) = -2[A2\bar{1}-B12]-A\bar{3}12\bar{3}-A1\bar{2}1\bar{3}-A\bar{2}\bar{3}\bar{2}1\bar{3}233+B321123\bar{1}\bar{2}+B\bar{2}\bar{3}1223+B332\bar{1}$$

The HOMFLYPT skein module for closed 4-braids in the solid torus is generated by the standard closure of the permutation braids 1, σ_1 , $\sigma_1\sigma_2$, $\sigma_1\sigma_3$ and $\sigma_1\sigma_2\sigma_3$.

One calculates

$$PR_1(\text{hat}(\hat{\beta})) = (-Az^2 + Bz^2)\hat{1} + (4Az - Az^3 - 4Bz + Bz^3)\hat{\sigma}_1 + (-5A - Az^2 + 5B - 4Bz^2)\sigma_1\hat{\sigma}_2 + (Az^2 - Bz^2)\sigma_1\hat{\sigma}_3 + (Az + 4Bz)\sigma_1\hat{\sigma}_2\sigma_3$$

A standard calculation gives

$$\begin{aligned}\Delta_{\hat{1}\cup L}(u, t) &= (u - 1)^3 \\ \Delta_{\hat{\sigma}_1\cup L}(u, t) &= (u - 1)(u^2 + (t - 1)u - t) \\ \Delta_{\sigma_1\hat{\sigma}_2\cup L}(u, t) &= u^3 + u^2(t - 1) + u(t - 1)t - t^2 \\ \Delta_{\sigma_1\hat{\sigma}_3\cup L}(u, t) &= u^3 + u^2(2t - 1) + u(t^2 - 2t) - t^2 \\ \Delta_{\sigma_1\hat{\sigma}_2\sigma_3\cup L}(u, t) &= u^3 + u^2t + ut^2 + t^3\end{aligned}$$

Substituting $A = B + z$, $z = t^{1/2} - t^{-1/2}$ and the above polynomials into $PR_1(\text{hat}(\hat{\beta}))$ leads finally to the invariant

$$\begin{aligned}\Delta R_1(\text{hat}(\hat{\beta}))(B, t, u) &= B[5(u^3 + u^2t + ut^2 + t^3) - 5(t^{1/2} - t^{-1/2})(u^3 + u^2(t - 1) + u(t - 1)t - t^2)] \\ &\quad - (u - 1)^3(t - 2 + t^{-1}) + (u - 1)(u^2 + u(t - 1) - t)(-t^{3/2} + 7t^{1/2} - 7t^{-1/2} + t^{-3/2}) \\ &\quad - (t + 3 + t^{-1})(u^3 + u^2(t - 1) + u(t - 1)t - t^2) + (u^3 + u^2(2t - 1) + u(t^2 - 2t) - t^2)(t - 2 + t^{-1}) \\ &\quad + (u^3 + u^2t + ut^2 + t^3)(t^{1/2} - t^{-1/2})\end{aligned}$$

Specializing now by $A + B = 1$ and $t = -1$ we obtain the polynomial $\Delta R_1(\text{hat}(\hat{\beta}))(u)$ from the Introduction and Mathematica (special thanks to Hitoshi) says that $|u_\beta|/\lambda_\beta = 1.00143\dots$

Unfortunately (for me) one needs now a computer program in order to calculate $\Delta R_1(\text{hat}(\hat{\beta}^{4m+1}))(u)$ for larger m .

Let us finish this section by showing that a natural generalization of the Entropy conjecture is true for periodic braids.

The global type of a Reidemeister II move is determined by the homological marking of the distinguished crossing d . We call a braid word for a periodic braid *general* if it is obtained from a positive braid word by applying an odd number of Reidemeister II moves of homological marking 1.

Remember that the entropy of a periodic braid is 0, see e.g. [13].

Proposition 4 *Let β be a general braid word which represents a periodic n -braid which closes to a knot. Then*

$$\lim_{m \rightarrow \infty} \log |u_{\beta^{mn+1}}| / (mn + 1) = 0.$$

Proof. The closed periodic braid can be represented as a (p, q) -torus knot in ∂V . In this case the loop $p \times \text{rot}(\hat{\beta})$ is evidently just equal to the loop $q \times \text{hat}(\hat{\beta})$. It follows that $R_1(\text{hat}(\hat{\beta})) = 0$ if $\hat{\beta}$ is represented by a positive braid word. In this case u_β is not well defined.

$$\begin{aligned}
& \text{Diagram 1} \longrightarrow \text{Diagram 2} = \text{Diagram 3} + \text{Diagram 4} \\
& + W (\text{Diagram 5} - \text{Diagram 6}) - (W - 1) (\text{Diagram 7} - \text{Diagram 8}) \\
& = \text{Diagram 9} - \text{Diagram 10}
\end{aligned}$$

Figure 77: $R_1 \neq 0$ on the meridian of a self-tangency in a flex of homological marking 1

For each generic loop γ in $M_{\hat{\beta}}$ we define the *linking number* $l(\gamma)$ with $\bar{\Sigma}_{self-flex,1}^{(2)}$ by one half of (the algebraic number of Reidemeister II moves of homological marking 1 and of local type $\sigma_i \sigma_i^{-1}$ minus the algebraic number of Reidemeister II moves of homological marking 1 and of local type $\sigma_j^{-1} \sigma_j$). These strata of codimension 1 form a 1-chain with boundary $\bar{\Sigma}_{self-flex,1}^{(2)}$.

Let β' be a braid word which is obtained from a positive braid word β by a Reidemeister II move of homological marking 1. One easily sees that $l(\text{hat}(\hat{\beta}')) = l(\text{hat}(\hat{\beta})) + 1$ or $l(\text{hat}(\hat{\beta}')) = l(\text{hat}(\hat{\beta})) - 1$. Let m be a meridian of $\Sigma_{self-flex,1}^{(2)}$ (compare Section 4.2). We show $R_1(m) \neq 0$ for one of the two local types of $\Sigma_{self-flex,1}^{(2)}$ in Fig. 77 (the other local type is analogous). Notice that the coefficient of $R_1(m)$ does not depend on the rest of the diagram. It follows that $R_1(\text{hat}(\hat{\beta}')) \neq 0$ and this is still the case for all other general braid words β' in our sense. Consequently, $\Delta R_1(\text{hat}(\hat{\beta}'))(u)$ is some non trivial polynomial of degree $n - 1$ and $u_{\beta'}$ is well defined (compare the Introduction). Because the coefficient of $R_1(m)$ is determined locally and adding rational multiples of a full twist to the braid doesn't change the roots of the polynomial, it follows that

$$\Delta R_1(\text{hat}((\hat{\beta}')^{mn+1}))(u) = (mn + 1) \Delta R_1(\text{hat}(\hat{\beta}'))(u) \text{ and consequently } u_{(\beta')^{mn+1}} = u_{\beta'}.$$

$$\lim_{m \rightarrow \infty} \log |u_{(\beta')^{mn+1}}| / (mn + 1) = 0.$$

□

4 Proofs

Our main results are based on very complicated combinatorics and the interested reader has certainly a hard time to check all the details. We apologize for this. However, we see the combinatorics in this paper as some discrete analysis: integrating a discrete differential 1-form over a discrete loop in the topological moduli space of a long knot. As already mentioned at the end of the Introduction, it would be very important to transform this discrete analysis into real analysis.

Nowadays, new invariants in knot theory come usually from some mathematical physics which is transformed into differential geometry (the perturbative approach) and representation theory (the non perturbative approach) and only at the very end into something which can be calculated in a combinatorial way from a knot diagram. Unfortunately, we have to start with this very end because it seems that in our case all the previous steps are missing for the moment (compare the questions at the end of the Introduction). However, this lack of understanding is partially compensated by the possibility to calculate the invariants in a combinatorial way.

The classical tetrahedron equation is a 3-dimensional generalization of the Yang-Baxter equation. It is a local equation which is fundamental for studying integrable models in $2+1$ -dimensional mathematical physics. This equation has many solutions and the first one was found by Zamolodchikov (see e.g. [30]). But it seems that the present paper is the very first one which considers the tetrahedron equation from a global point of view. The game is to find solutions of this equation which have enough symmetries in order to lead to a 1-cocycle in the knot space but which have still a lack of symmetry so that the 1-cocycle does not become exact. (In anterior work we had constructed lots of exact 1-cocycles, see e.g. [4], [16].)

4.1 Generalities and reductions by using singularity theory

We look at the local tetrahedron equation from the point of view of singularities of the projection of lines. We fix an orthogonal projection $pr : \mathbb{C} \times \mathbb{R} \rightarrow \mathbb{C}$. Consider four oriented straight lines which form a braid and such that the intersection of their projection into \mathbb{C} consists of a single point. We call this an *ordinary quadruple crossing*. After a generic perturbation of the four lines we will see now exactly six ordinary crossings. We assume that all six cross-

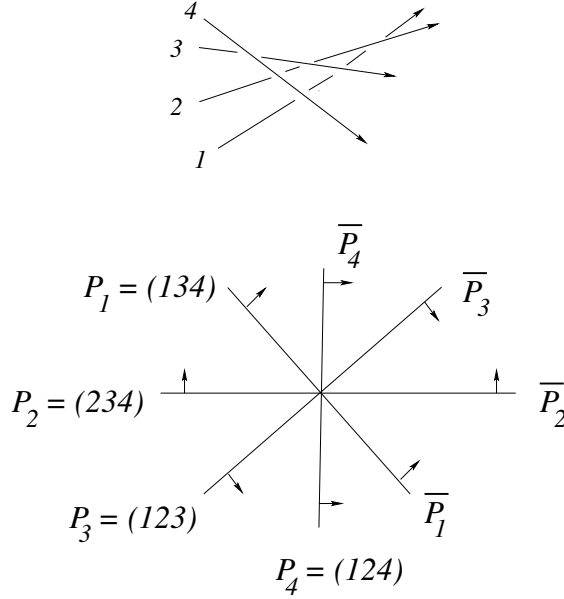


Figure 78: A non generic quadruple crossing

ings are positive and we call the corresponding quadruple crossing a *positive quadruple crossing*. Quadruple crossings form smooth strata of codimension 2 in the topological moduli space of lines in 3-space which is equipped with a fixed projection pr . Each generic point in such a stratum is adjacent to exactly eight smooth strata of codimension 1. Each of them corresponds to configurations of lines which have exactly one ordinary triple crossing besides the remaining ordinary crossings. We number the lines from 1 to 4 from the lowest to the highest (with respect to the projection pr). The eight strata of triple crossings glue pairwise together to form four smooth strata which intersect pairwise transversally in the stratum of the quadruple crossing (see e.g. [19]). The strata of triple crossings are determined by the names of the three lines which give the triple crossing. For shorter writing we give them names from P_1 to P_4 and \bar{P}_1 to \bar{P}_4 for the corresponding stratum on the other side of the quadruple crossing. We show the intersection of a normal 2-disc of the stratum of codimension 2 of a positive quadruple crossing with the strata of codimension 1 in Fig. 78. We give in the figure also the coorientation of the strata of codimension 1, compare Fig. 20. (We could interpret the six ordinary crossings as the edges of a tetrahedron and the four triple crossings likewise as the vertices's or the 2-faces of the tetrahedron.)

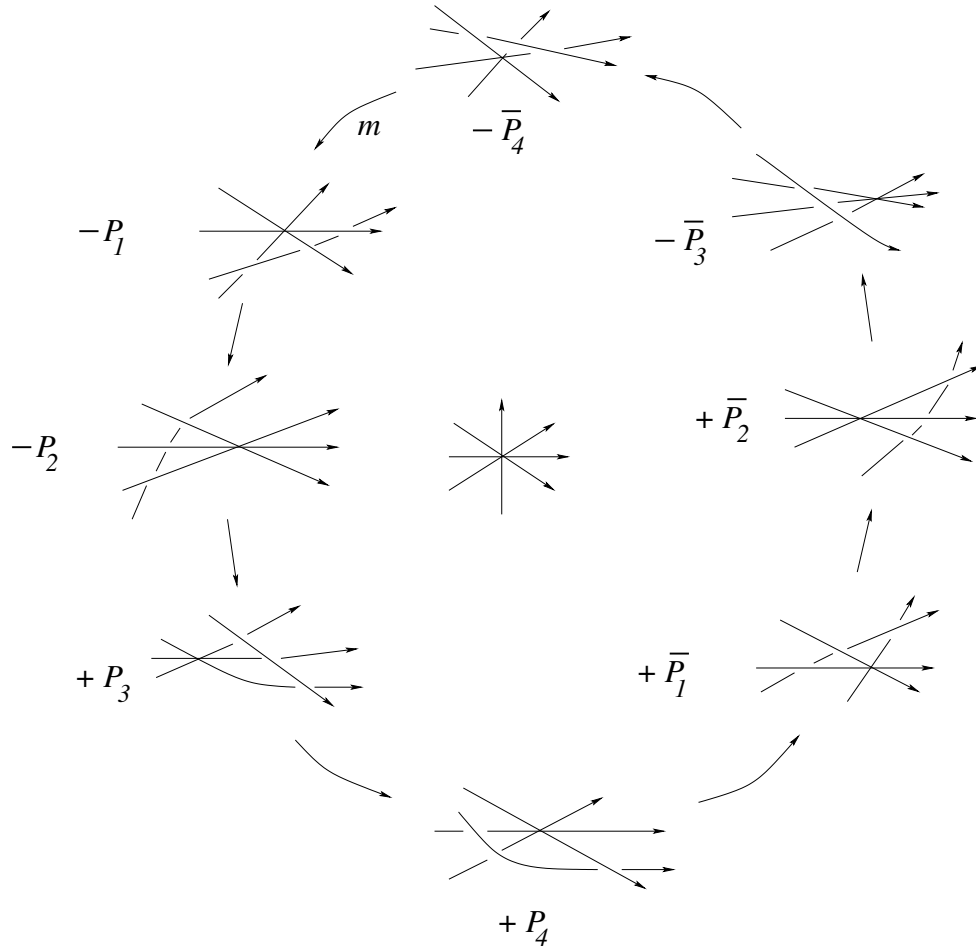


Figure 79: Unfolding of a positive quadruple crossing

Let us consider a small circle in the normal 2-disc and which goes once around the stratum of the quadruple crossing. We call it a *meridian* m of the quadruple crossing. Going along the meridian m we see ordinary diagrams of 4-braids and exactly eight diagrams with an ordinary triple crossing. We show this in Fig. 79. (For simplicity we have drawn the triple crossings as triple points, but the branches do never intersect.)

For the classical tetrahedron equation one associates to each stratum P_i some operator (or some R-matrix) which depends only on the names of the three lines and to each stratum \bar{P}_i the inverse operator. The tetrahedron equation says now that if we go along the meridian m then the product of

these operators is equal to the identity. Notice, that in the literature (see e.g. [30]) one considers planar configurations of lines. But this is of course equivalent to our situation because all crossings are positive and hence the lift of the lines into 3-space is determined by the planar picture. Moreover, each move of the lines in the plane which preserves the transversality lifts to an isotopy of the lines in 3-space.

However, the solutions of the classical tetrahedron equation are not well adapted in order to construct 1-cocycles for moduli spaces of knots. There is no natural way to give names to the three branches of a triple crossing in an arbitrary knot isotopy besides in the case of braids. But it is not hard to see that in the case of braids Markov moves would make big trouble (see e.g. [6] for the definition of Markov moves). As well known, a Markov move leads only to a normalization factor in the construction of 0-cocycles (see e.g. [48]). However, the place in the diagram and the moment in the isotopy of a Markov move become important in the construction of 1-cocycles (as already indicated by the lack of control over the Markov moves in Markov's theorem). To overcome this difficulty we search for a solution of the tetrahedron equation which does not use names of the branches.

The idea is to associate to a triple crossing p of a diagram of a string link K , a global element in K_1 or K_2 instead of a local operator.

Let us consider a diagram of a string link with a positive quadruple crossing *quad* and let p be e.g. the positive triple crossing associated to the adjacent stratum P_1 . We consider three cubes: $I_p^2 \times \mathbb{R} \subset I_{quad}^2 \times \mathbb{R} \subset \mathbb{C} \times \mathbb{R}$. Here I_p^2 is a small square which contains the triple point $pr(p)$ and I_{quad}^2 is a slightly bigger square which contains the quadruple point $pr(quad)$. We illustrate this in Fig. 80. Let us replace the triple crossing p in $I_p^2 \times I$ by some standard linear combination of embedded chord diagrams, say $L(p)$. Gluing to $L(p)$ the rest of the string link K outside of $I_p^2 \times I$ gives an element, say $K(p) \in K_1$. A triple crossing in an oriented isotopy corresponds to a Reidemeister move of type III.

Let m be the oriented meridian of the positive quadruple crossing. Our tetrahedron equation in K_1 is now

$$(1) \sum_{p \in m} \text{sign}(p) K(p) = 0$$

where the sum is over all eight triple crossings in m .

One sees immediately that this is still a local equation because it is sufficient to consider only the part of the embedded chord diagrams which is in $I_{quad}^2 \times \mathbb{R}$. This equation has an unique solution, which we call the *local*

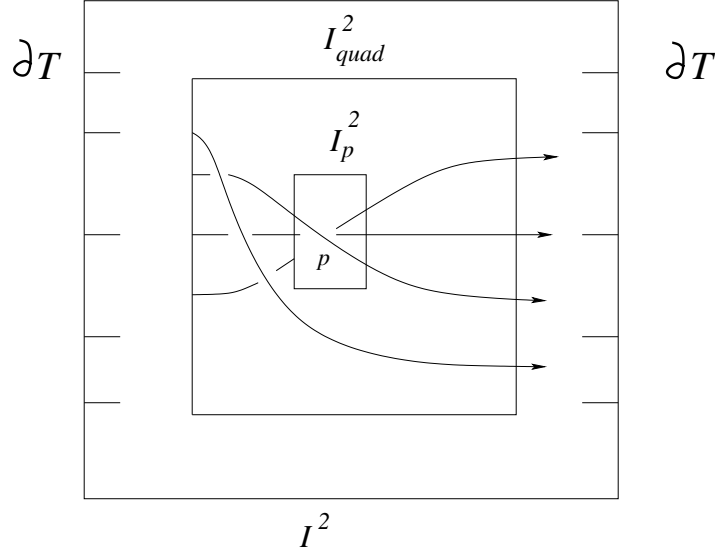


Figure 80: Increasing cubes

solution, compare Section 4.4.

We consider then integer valued *weights* $W(p)$ of the triple crossings which depend on the whole long knot (or string link) K and not only on the part of it in $I_{quad}^2 \times \mathbb{R}$. Moreover, they depend crucially on the point at infinity and they can not be defined for compact knots in S^3 . Therefore we have to consider *twenty four* different positive tetrahedron equations, corresponding to the six different abstract closures of the four lines in $I_{quad}^2 \times \mathbb{R}$ to a circle and to the four different choices of the point at infinity in each of the six cases. One easily sees that there are exactly *forty eight* local types of quadruple crossings (analog to the eight local types of triple crossings). Hence we are looking for non symmetric solutions (i.e. the contributions $sign(p)R_1(p)$ should be in general not invariant under change of orientation, mirror image, rotation by π around the imaginary axes $i\mathbb{R} \times 0 \subset \mathbb{C} \times \mathbb{R}$ and the compositions of these involutions) and which depend non trivially on the point at infinity. This leads to a system of $24 \times 48 = 1152$ equations in K_1 respectively K_2 ! It turns out that such solutions do exist and we call them *solutions of a global tetrahedron equation*.

In order to reduce the complexity of the problem we use singularity theory for projections pr of knots into the plan. The infinite dimensional spaces M_K has a natural *stratification with respect to* pr :

$$M_K = \Sigma^{(0)} \cup \Sigma^{(1)} \cup \Sigma^{(2)} \cup \Sigma^{(3)} \cup \Sigma^{(4)} \dots$$

Here, $\Sigma^{(i)}$ denotes the union of all strata of codimension i .

The strata of codimension 0 correspond to the usual generic *diagrams of knots*, i.e. all singularities in the projection are ordinary double points. So, our *discriminant* is the complement of $\Sigma^{(0)}$ in M_K . Notice that this discriminant of non-generic diagrams is very different from Vassiliev's discriminant of singular knots [50].

The three types of strata of codimension 1 correspond to the *Reidemeister moves*, i.e. non generic diagrams which have exactly one ordinary triple point, denoted by $\Sigma_{tri}^{(1)}$, or one ordinary self-tangency, denoted by $\Sigma_{tan}^{(1)}$, or one ordinary cusp, denoted by $\Sigma_{cusp}^{(1)}$, in the projection pr . As already mentioned we call the triple point together with the under-over information (i.e. its embedded resolution) a *triple crossing*.

Proposition 5 *There are exactly six types of strata of codimension 2. They correspond to non generic diagrams which have exactly either*

- (1) *one ordinary quadruple point, denoted by $\Sigma_{quad}^{(2)}$*
- (2) *one ordinary self-tangency with a transverse branch passing through the tangent point, denoted by $\Sigma_{trans-self}^{(2)}$*
- (3) *one ordinary self-tangency in an ordinary flex ($x = y^3$), denoted by $\Sigma_{self-flex}^{(2)}$*
- (4) *two singularities of codimension 1 in disjoint small discs (this corresponds to the transverse intersection of two strata from $\Sigma^{(1)}$, i.e. two simultaneous Reidemeister moves at different places of the diagram)*
- (5) *one ordinary cusp ($x^2 = y^3$) with a transverse branch passing through the cusp, denoted by $\Sigma_{trans-cusp}^{(2)}$*
- (6) *one degenerate cusp, locally given by $x^2 = y^5$, denoted by $\Sigma_{cusp-deg}^{(2)}$*

We show these strata in Fig. 81.

For a proof as well as for all other necessary preparations from singularity theory see [19] and references therein (in particular the singularity theory of Thom and Mather).

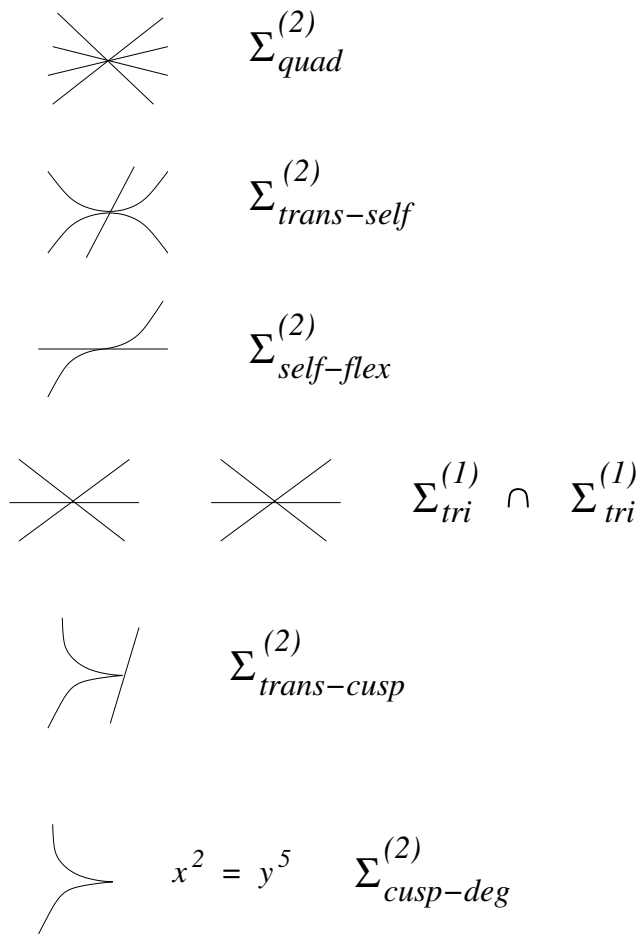


Figure 81: The strata of codimension 2 of the discriminant

The list above of singularities of codimension two can be seen as an analogue for one parameter families of diagrams of the Reidemeister theorem (which gives the list of singularities of codimension one).

A generic arc s in M_K intersects $\Sigma_{tri}^{(1)}$, $\Sigma_{tan}^{(1)}$ and $\Sigma_{cusp}^{(1)}$ transversally in a finite number of points and it does not intersect at all strata of higher codimension. To each intersection point with $\Sigma_{tri}^{(1)}$ and $\Sigma_{tan}^{(1)}$ we associate an element in K_1 (or K_2). We sum up with signs the contributions over all intersection points in s and obtain an element $R_1(s) \in K_1$ (respectively $R_2(s) \in K_2$).

We use now the strata from $\Sigma^{(2)}$ to show the invariance of $R_1(s)$ under all generic homotopies of s in M_K which fix the endpoints of s . A homotopy is *generic* if it intersects $\Sigma^{(1)}$ transversally besides for a finite number of points in s where s has an ordinary tangency with $\Sigma^{(1)}$, it intersects $\Sigma^{(2)}$ transversally in a finite number of points and it doesn't intersect at all $\Sigma^{(i)}$ for $i > 2$. The contributions to $R_1(s)$ come from discrete points in s and hence they survive under generic Morse modifications of s . It follows that if $R_1(s)$ is invariant under generic homotopies of s then it is a 1-cocycle for M_K .

We see immediately that $R_1(s)$ is invariant by passing through a tangency of s with $\Sigma^{(1)}$. Indeed, the two intersection points have identical contributions but they enter with different signs and cancel out. In order to show the invariance under generic homotopies we have to study now normal 2-discs for the strata in $\Sigma^{(2)} \subset M_K$. For each type of stratum in $\Sigma^{(2)}$ we have to show that $R_1(m) = 0$ for the boundary m of the corresponding normal 2-disc. We call m a *meridian*. $\Sigma_{quad}^{(2)}$ is by far the hardest case which leads to the tetrahedron equation (Section 4.4).

Different local types of triple crossings come together in points of $\Sigma_{trans-self}^{(2)}$, but one easily sees that the global type of the triple crossings is always preserved. We make now a graph Γ for each global type of a triple crossing in the following way: the vertices's correspond to the different local types of triple crossings. We connect two vertices's by an edge if and only if the corresponding strata of triple crossings are adjacent to a stratum of $\Sigma_{trans-self}^{(2)}$. One easily sees that the resulting graph is the 1-skeleton of the 3-dimensional cube I^3 (compare Section 4.5). In particular, it is connected. (Studying the normal discs to $\Sigma_{trans-self}^{(2)}$ in M_K one shows that if a 0-cochain is invariant under passing all $\Sigma_{tan}^{(1)}$ and just one local type of a stratum $\Sigma_{tri}^{(1)}$ then it is invariant under passing all remaining local types of triple crossings because Γ

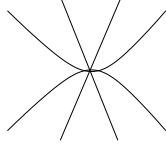


Figure 82: A quadruple crossing with two tangential branches

is connected.) The edges of the graph $\Gamma = skl_1(I^3)$ correspond to the types of strata in $\Sigma_{trans-self}^{(2)}$. The solution of the positive tetrahedron equation tells us what is the contribution to R_1 (or R_2) of a positive triple crossing (i.e. all three involved crossings are positive). The meridians of the strata from $\Sigma_{trans-self}^{(2)}$ give equations which allow us to determine the contributions of all other types of triple crossings as well as the contributions of self-tangencies. However, a global phenomenon occurs: each loop in Γ could give an additional equation. Evidently, it suffices to consider the loops which are the boundaries of the 2-faces from $skl_2(I^3)$. We call all the equations which come from the meridians of $\Sigma_{trans-self}^{(2)}$ and from the loops in $\Gamma = skl_1(I^3)$ the *cube equations* (Section 4.5). (Notice that a loop in Γ is more general than a loop in M_K . For a loop in Γ we come back to the same local type of a triple crossing but not necessarily to the same whole diagram of K .)

We need only the following strata from $\Sigma^{(3)}$ in order to simplify the proof of the invariance of R_1 (or R_2) in generic homotopies which pass through strata from $\Sigma^{(2)}$:

- (1) one degenerate quadruple crossing where exactly two branches have an ordinary self-tangency in the quadruple point, denoted by $\Sigma_{trans-trans-self}^{(3)}$ (see Fig. 82).
- (2) one self-tangency in an ordinary flex with a transverse branch passing through the tangent point, denoted by $\Sigma_{trans-self-flex}^{(3)}$ (see Fig. 83).
- (3) the transverse intersection of a stratum from $\Sigma^{(1)}$ with a stratum of $\Sigma_{trans-self}^{(2)}$

Again, for each fixed global type of a quadruple crossing we form a graph with the local types of quadruple crossings as vertices's and the adjacent strata of $\Sigma_{trans-trans-self}^{(3)}$ as edges. One easily sees that the resulting graph Γ has exactly 48 vertices's and that it is again connected. Luckily, we don't

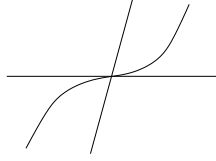


Figure 83: A self-tangency in a flex

need to study the unfolding of $\Sigma_{trans-trans-self}^{(3)}$ in much detail. It is clear that each meridional 2-sphere for $\Sigma_{trans-trans-self}^{(3)}$ intersects $\Sigma^{(2)}$ transversally in a finite number of points, namely exactly in two strata from $\Sigma_{quad}^{(2)}$ and in lots of strata from $\Sigma_{trans-self}^{(2)}$ and from $\Sigma^{(1)} \cap \Sigma^{(1)}$ and there are no other intersections with strata of codimension 2. If we know now that $R_1(m) = 0$ for the meridian m of one of the quadruple crossings, that $R_1(m) = 0$ for all meridians of $\Sigma_{trans-self}^{(2)}$ (i.e. R_1 satisfies the cube equations) and for all meridians of $\Sigma^{(1)} \cap \Sigma^{(1)}$ (i.e. R_1 is invariant under passing simultaneous Reidemeister moves at different places in the diagram) then $R_1(m) = 0$ for the other quadruple crossing too (the same is of course also true for R_2). It follows that for each of the fixed 24 global types (see Fig. 84, where in each case we have four possibilities for the point at infinity) the 48 tetrahedron equations reduce to a single one, which is called the *positive global tetrahedron equation*. There is no further reduction possible because we are searching for non symmetric solutions and which depend non trivially from the point at infinity!

In the cube equations there are also two local types of edges, corresponding to the two different local types of a Reidemeister II move with given orientations, compare Fig. 85. We reduce them to a single type of the edge by using the strata from $\Sigma_{trans-self-flex}^{(3)}$. The meridional 2-sphere for $\Sigma_{trans-self-flex}^{(3)}$ intersects $\Sigma^{(2)}$ transversally in exactly two strata from $\Sigma_{trans-self}^{(2)}$, which correspond to the two different types of the edge, and in lots of strata from $\Sigma_{self-flex}^{(2)}$ and from $\Sigma^{(1)} \cap \Sigma^{(1)}$. Hence, again the invariance under passing one of the two local types of strata from $\Sigma_{trans-self}^{(2)}$ together with the invariance under passing all strata from $\Sigma_{self-flex}^{(2)}$ and $\Sigma^{(1)} \cap \Sigma^{(1)}$ guaranties the invariance under passing the other local type of $\Sigma_{trans-self}^{(2)}$ too.

The unfolding (i.e. the intersection of a normal disc with the stratification

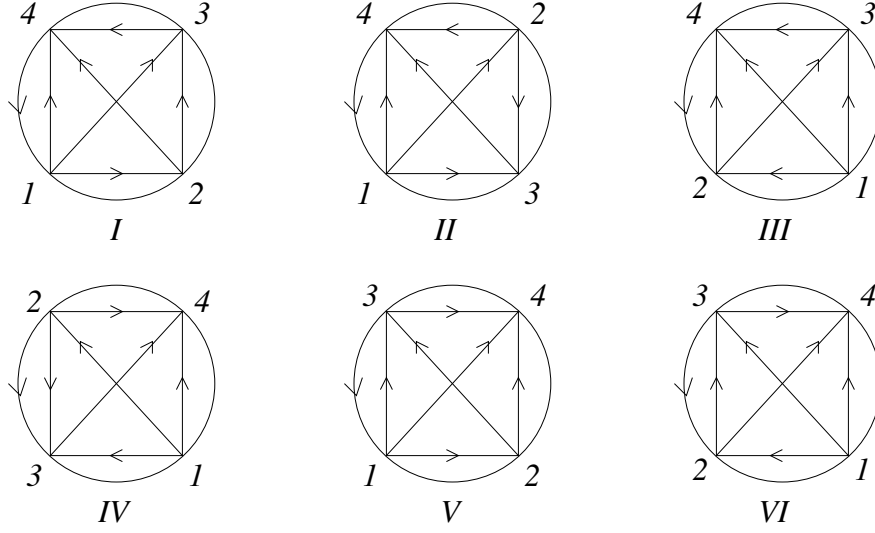


Figure 84: Global types of quadruple crossings

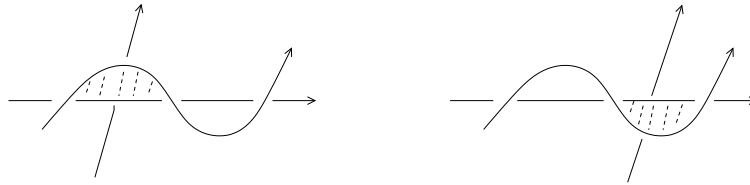


Figure 85: Two different local types of an edge 1-7 in the cube equations and which come together in $\Sigma_{trans-self-flex}^{(3)}$

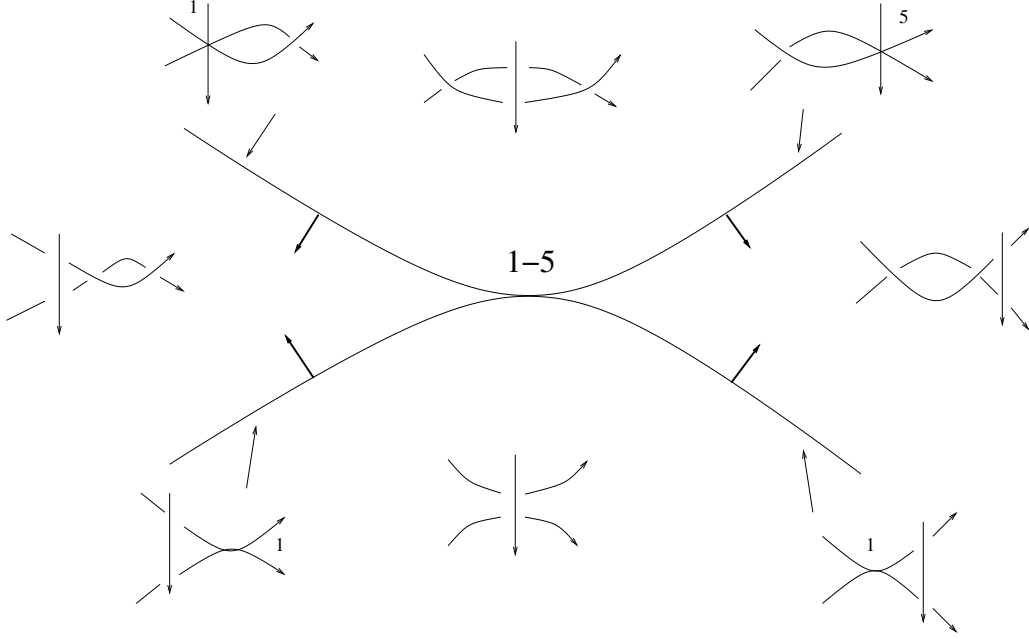


Figure 86: The unfolding of a self-tangency with a transverse branch

of M_K) of e.g. the edge $1 - 5$ of Γ is shown in Fig. 86 (compare [19]). The intersection of a meridional 2-sphere for $\Sigma^{(1)} \cap \Sigma_{trans-self}^{(2)}$ with $\Sigma^{(2)}$ consists evidently of the transverse intersections of the stratum $\Sigma^{(1)}$ with all the strata of codimension 1 in the unfolding of $\Sigma_{trans-self}^{(2)}$. It follows again that it is sufficient to prove the invariance under passing $\Sigma^{(1)} \cap \Sigma^{(1)}$ only for positive triple crossings (i.e. of local type 1) and only for one of the two local types of self-tangencies with a given orientation.

We show now the invariance of R_1 and R_2 under homotopies which pass through the strata from Proposition 5 in the following Subsections: 4.2: (3) and (6), 4.3: (4), 4.4: (1), 4.5: (2), 4.6: (5). Notice that in the case of closed braids the strata of the types (5) and (6) can not occur.

4.2 Reidemeister II moves in a cusp and in a flex

As a warm-up we consider first the less important strata. All weights and contributions were defined in Section 2.

Let's start with $\Sigma_{cusp-deg}^{(2)}$. A meridian for one type is shown in Fig. 87. There is a single Reidemeister II move p which could a priori contribute if it

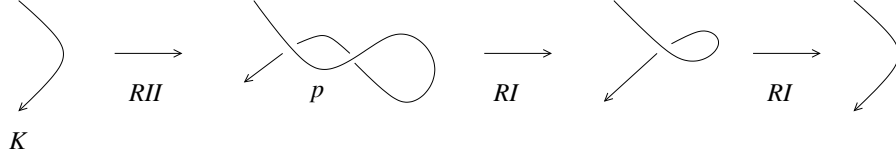


Figure 87: A meridian for a degenerated cusp

$$+ v_2(K) (\text{figure-eight with crossing labeled } + - \text{figure-eight with crossing labeled } -) = 0$$

Figure 88: R_1 on the meridian of a degenerated cusp

has the right global type. It follows easily from the Polyak-Viro formula, see [42], that in this case $W_2(p) = v_2(K)$. The contribution $R_1(p)$ is shown in Fig. 88 and we see that it vanishes because of the embedded 1T-relation.

The generalized embedded 1T-relation applies to the distinguished crossings d of p and hence the contribution of $R_2(p)$ is 0 too.

The considerations for all other types of $\Sigma_{cusp-deg}^{(2)}$ are completely analogous.

We show the unfolding and a meridian for one type of $\Sigma_{self-flex}^{(2)}$ in Fig. 89. There are exactly two Reidemeister II moves, p_1 and p_2 . The third crossings, which are not in the Reidemeister moves, are never f-crossings in the case of long knots. If one is a r-crossing for one of the two moves then the other is a r-crossing for the other move with exactly the same f-crossing. Consequently, $W_2(p_1) = W_2(p_2)$. We show the calculation of $R_1(m)$ in Fig. 90. The calculations of $R_2(m) = 0$ and for all the other types of $\Sigma_{self-flex}^{(2)}$ are completely analogous.

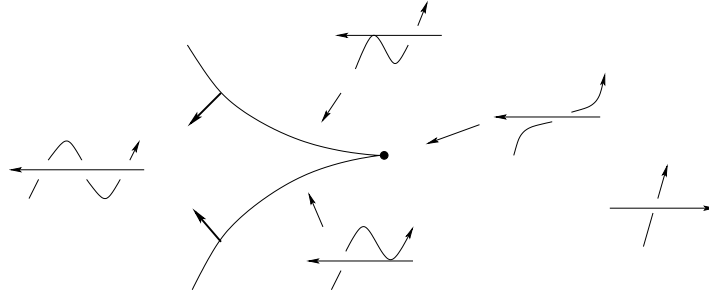


Figure 89: The unfolding for the self-tangency in a flex

$$\begin{aligned}
& + W_2 (p_1) \quad (\text{diagram with } + \text{ crossing} - \text{diagram with } - \text{ crossing}) \\
& - W_2 (p_2) \quad (\text{diagram with } + \text{ crossing} - \text{diagram with } - \text{ crossing}) = 0
\end{aligned}$$

Figure 90: R_1 vanishes on the meridian of a self-tangency in a flex

$$\begin{aligned}
& + (\text{diagram with } + \text{ crossing} - \text{diagram with } + \text{ crossing}) \\
& - (\text{diagram with } - \text{ crossing} - \text{diagram with } + \text{ crossing}) = 0
\end{aligned}$$

Figure 91: R_2 vanishes on the meridian of a self-tangency in a flex

But we see immediately that in general $R_1(m) \neq 0$ for the meridian of $\Sigma_{self-flex}^{(2)}$ in the case of closed braids because the third crossing in the picture could contribute to $W(p)$ for exactly one of the two Reidemeister II moves (compare Section 3.2). Hence R_1 is only a 1-cocycle in the complement of $\bar{\Sigma}_{self-flex}^{(2)}$.

In the case of R_2 for closed braids the third crossings contribute always simultaneously to both Reidemeister II moves (because of our symmetrization of the f-crossings). We show $R_2(m)$ in Fig. 91 and we see that it vanishes because of the embedded 2T-relation (remember that we do not allow the move for singular knots which was shown in Fig. 1). The remaining part of $R_2(m)$ for f-crossings far away in the diagram from the Reidemeister II move vanishes evidently.

4.3 Simultaneous Reidemeister moves

An example of a meridian of $\Sigma^{(1)} \cap \Sigma^{(1)}$ is shown in Fig. 92. It is clear that e.g. the f-crossings for p_1 do not change when the meridian m crosses the discriminant at p_2 . Hence the linear weight $W_1(p_1)$ (compare Definition 11) is the same for both intersections of m with the stratum of the discriminant

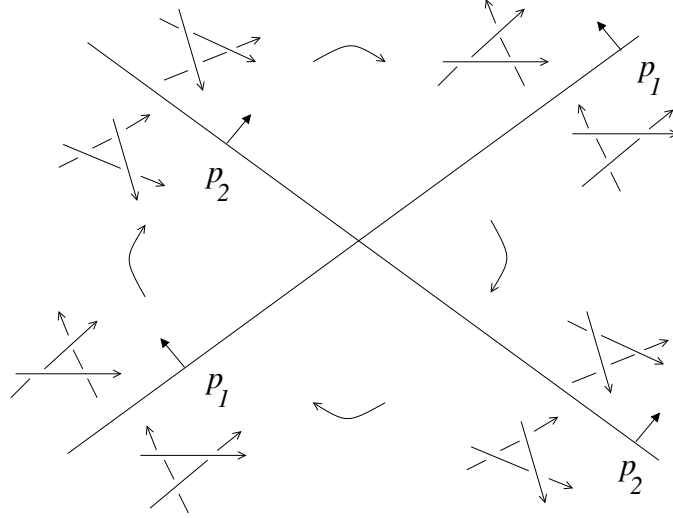


Figure 92: Meridian of two simultaneous Reidemeister III moves

which corresponds to p_1 and the contributions to R_1 as well as to R_2 cancel out because the singular knots on both sides of the stratum p_1 of the discriminant are isotopic.

Let's consider the quadratic weight $W_2(p)$ (compare Definition 10).

Lemma 1 *$W_2(p)$ is an isotopy invariant for each Reidemeister move of type I, II or III, i.e. $W_2(p)$ is invariant under any isotopy of the rest of the diagram outside of $I_p^2 \times \mathbb{R}$.*

The lemma implies that $W_2(p)$ doesn't change under a homotopy of an arc which passes through $\Sigma^{(1)} \cap \Sigma^{(1)}$, and hence the contributions to R_1 cancel out as shown in Fig. 93.

Proof. It is obvious that $W_2(p)$ is invariant under Reidemeister moves of type I and II. The latter comes from the fact that both new crossings are simultaneously crossings of type f or r and that they have different writhe. As was explained in Section 4.1 the graph Γ implies now that it is sufficient to prove the invariance of $W_2(p)$ only under positive Reidemeister moves of type III. There are two global types and for each of them there are three possibilities for the point at infinity. We give names 1, 2, 3 to the crossings and a, b, c to the points at infinity and we show the six cases in Fig. 94 and Fig. 95. Evidently, we have only to consider the mutual position of the three

$$\begin{aligned}
& W_2(p_1) \left(\begin{array}{c} \text{Diagram 1} \\ d(p_1) \end{array} - \begin{array}{c} \text{Diagram 2} \end{array}, \begin{array}{c} \text{Diagram 3} \\ p_2 \end{array} \right) \\
& + W_2(p_2) \left(\begin{array}{c} \text{Diagram 4} \\ d(p_2) \end{array} - \begin{array}{c} \text{Diagram 5} \end{array}, \begin{array}{c} \text{Diagram 6} \\ p_1 \end{array} \right) \\
& - W_2(p_1) \left(\begin{array}{c} \text{Diagram 7} \\ d(p_1) \end{array} - \begin{array}{c} \text{Diagram 8} \end{array}, \begin{array}{c} \text{Diagram 9} \\ p_2 \end{array} \right) \\
& - W_2(p_2) \left(\begin{array}{c} \text{Diagram 10} \\ d(p_2) \end{array} - \begin{array}{c} \text{Diagram 11} \end{array}, \begin{array}{c} \text{Diagram 12} \\ p_1 \end{array} \right) \\
& = 0
\end{aligned}$$

Figure 93: Calculation of R_1 on a meridian of two simultaneous Reidemeister III moves

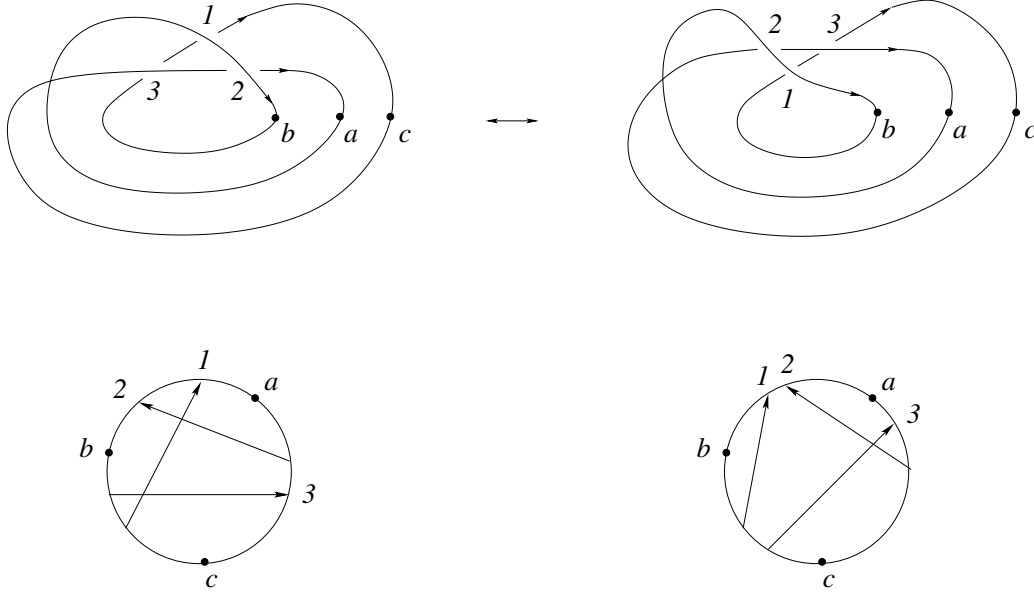


Figure 94: R_{III} of type r

crossings in the pictures because the contributions with all other crossings do not change.

r_a : there is only 3 which could be a f-crossing but it does not contribute with another crossing in the picture to $W_2(p)$.

r_b : no r-crossing at all.

r_c : only 2 could be a f-crossing. In that case it contributes on the left side exactly with the r-crossing 1 and on the right side exactly with the r-crossing 3.

l_a : no f-crossing at all.

l_b : 1 and 2 could be f-crossings but non of them contributes with the crossing 3 to $W_2(p)$.

l_c : 1 and 3 could be f-crossings. But the foots of 1 and 3 are arbitrary close. Consequently, they can be f-crossings only simultaneously! In that case 3 contributes with 2 on the left side and 1 with 2 on the right side.

Consequently, we have proven that $W_2(p)$ is invariant.

□

Lemma 2 *Let m be a meridian of $\Sigma^{(1)} \cap \Sigma^{(1)}$. Then $R_2(m) = 0$.*

Proof. Each Reidemeister move of type II or III appears twice and with

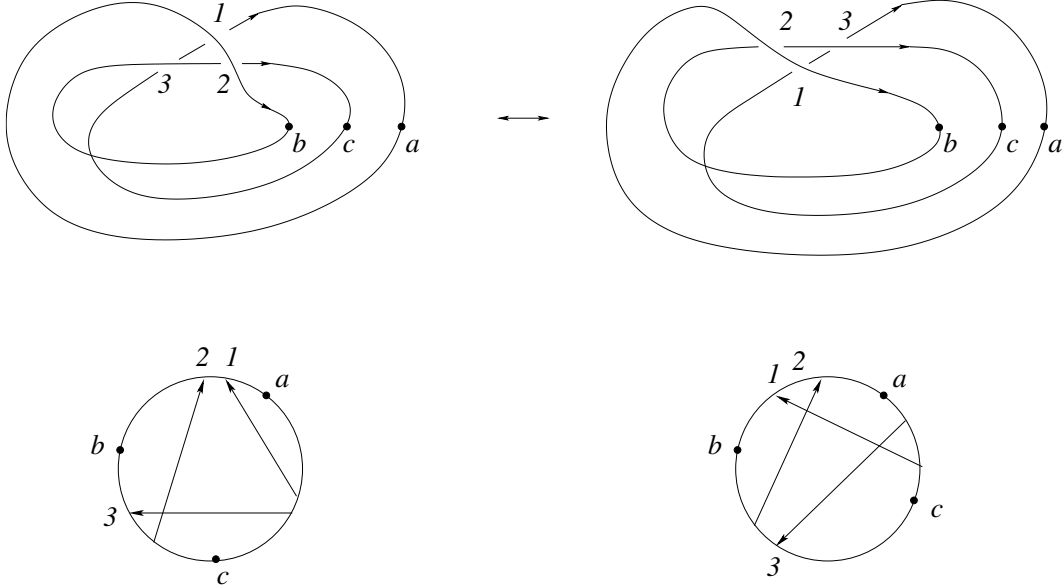


Figure 95: R_{III} of type l

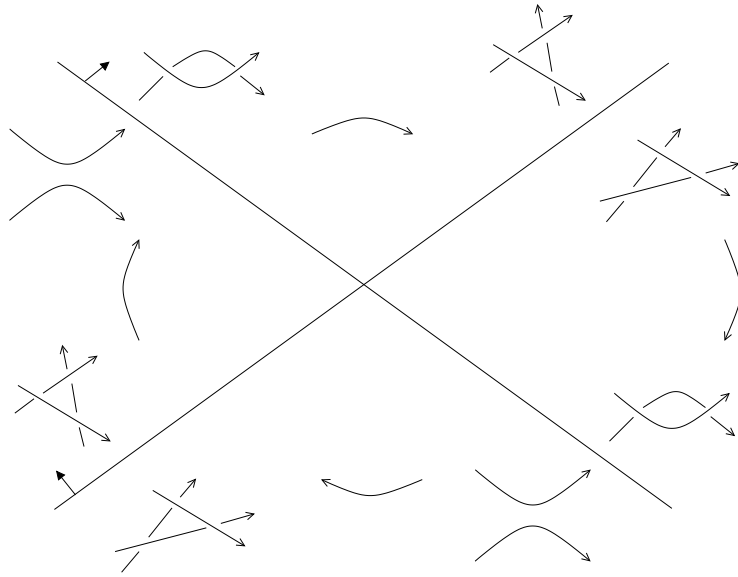
different signs in m . Consequently, all those contributions cancel out where two of the three crossings of the Reidemeister move become singular. So we have only to consider the contributions with simultaneously one singular crossing in p_1 and one in p_2 . It follows directly from the symmetrizing definition of R_2 that the distinguished crossing $d(p_1)$ is a f-crossing for p_2 if and only if $d(p_2)$ is a f-crossing for p_1 . We show an example of the calculation of $R_2(m)$ in Fig. 96, where one of the strata of $\Sigma^{(1)}$ corresponds to a Reidemeister II move. The example from Fig. 92, where both strata correspond to Reidemeister III moves, is shown in Fig. 97. The triple crossings are of local type 1 here. It follows now from the cube equations (see Section 4.5) that automatically $R_2(m) = 0$ too for all other local types of triple crossings. \square

The case of $R_1(m)$ and $R_2(m)$ for closed braids is completely analogue (and even simpler, because there is no quadratic weight W_2) and is left to the reader.

4.4 Tetrahedron equation

This subsection contains the heart of this paper.

As explained in Section 4.1 it suffices to consider global positive quadruple



$$+ \left(\begin{array}{c} \text{crossing} \\ + \end{array} - \begin{array}{c} \text{crossing} \\ - \end{array}, - \begin{array}{c} \text{crossing} \\ \text{crossing} \end{array} \right)$$

$$- \left(- \begin{array}{c} \text{crossing} \\ \text{crossing} \end{array} - \begin{array}{c} \text{crossing} \\ \text{crossing} \end{array}, \begin{array}{c} \text{crossing} \\ + \end{array} \right)$$

$$+ \left(- \begin{array}{c} \text{crossing} \\ \text{crossing} \end{array} - \begin{array}{c} \text{crossing} \\ \text{crossing} \end{array}, \begin{array}{c} \text{crossing} \\ - \end{array} \right)$$

$$- \left(\begin{array}{c} \text{crossing} \\ + \end{array} - \begin{array}{c} \text{crossing} \\ - \end{array}, \begin{array}{c} \text{crossing} \\ \text{crossing} \end{array} \right)$$

$$= 0$$

Figure 96: R_2 on a meridian of a Reidemeister II move together with a Reidemeister III move

$$\begin{aligned}
& + \left(\begin{array}{c} \text{Diagram 1} \\ p_1 \end{array} - \begin{array}{c} \text{Diagram 2} \end{array}, \begin{array}{c} \text{Diagram 3} \\ p_2 \end{array} \right) \\
& + \left(\begin{array}{c} \text{Diagram 4} \\ p_2 \end{array} - \begin{array}{c} \text{Diagram 5} \end{array}, \begin{array}{c} \text{Diagram 6} \\ p_1 \end{array} \right) \\
& - \left(\begin{array}{c} \text{Diagram 7} \\ p_1 \end{array} - \begin{array}{c} \text{Diagram 8} \end{array}, \begin{array}{c} \text{Diagram 9} \\ p_2 \end{array} \right) \\
& - \left(\begin{array}{c} \text{Diagram 10} \\ p_2 \end{array} - \begin{array}{c} \text{Diagram 11} \end{array}, \begin{array}{c} \text{Diagram 12} \\ p_1 \end{array} \right) \\
& = 0
\end{aligned}$$

Figure 97: R_2 on the meridian of two simultaneous Reidemeister III moves

crossings with a fixed point at infinity. The following lemma is of crucial importance.

Lemma 3 *The f -crossings of the eight adjacent strata of triple crossings (compare Fig. 79) have the following properties:*

- *the f -crossings in P_2 are identical with those in \bar{P}_2 (we naturally identify crossings in an isotopy outside Reidemeister moves of type I and II)*
- *the f -crossings in P_1, \bar{P}_1, P_4 and \bar{P}_4 are all identical*
- *the f -crossings in P_3 are either identical with those in \bar{P}_3 or there is exactly one new f -crossing in \bar{P}_3 with respect to P_3 . In the latter case the new crossing is always exactly the crossing hm in P_1 and \bar{P}_1*
- *the new f -crossing in \bar{P}_3 appears if and only if P_1 (and hence also \bar{P}_1) is of one of the two global types r_a or l_c .*
- *the distinguished crossing d in P_3 and \bar{P}_3 is always the crossing ml in P_1 and \bar{P}_1*

Proof. We have checked the assertions of the lemma in all twenty four cases (denoted by the global type of the quadruple crossing together with the point at infinity) using Fig. 98-109. Notice that the crossing hm in P_1 and \bar{P}_1 is always the crossing 34 and that d is of type 0 if ∞ is on the right side of it in the figures. The distinguished crossing d in P_3 is always the crossing 13 which is always the crossing ml in P_1 too.

We consider just some examples. In particular we show that it is necessary to add the "degenerate" configuration in Fig. 23 and we left the rest of the verification to the reader.

The f -crossings are:

case I_1 . non at all

case I_2 . non at all

case I_3 . In P_1, \bar{P}_1 : 34 (both are the degenerate case). In P_4, \bar{P}_4 : 34 (the third configuration and the first configuration in Fig. 23). In P_2, \bar{P}_2 : 34. In P_3 : non. In \bar{P}_3 : 34.

case I_4 . In $P_1, \bar{P}_1, P_4, \bar{P}_4$: 34, 24, 23. In P_2, \bar{P}_2 : non. In P_3 : 23, 24. In \bar{P}_3 : 23, 24, 34.

case VI_3 : In P_2 : 12, 13, 14. In \bar{P}_2 : 12, 13, 14 (12 shows that the fourth configuration in Fig. 23 is necessary too).

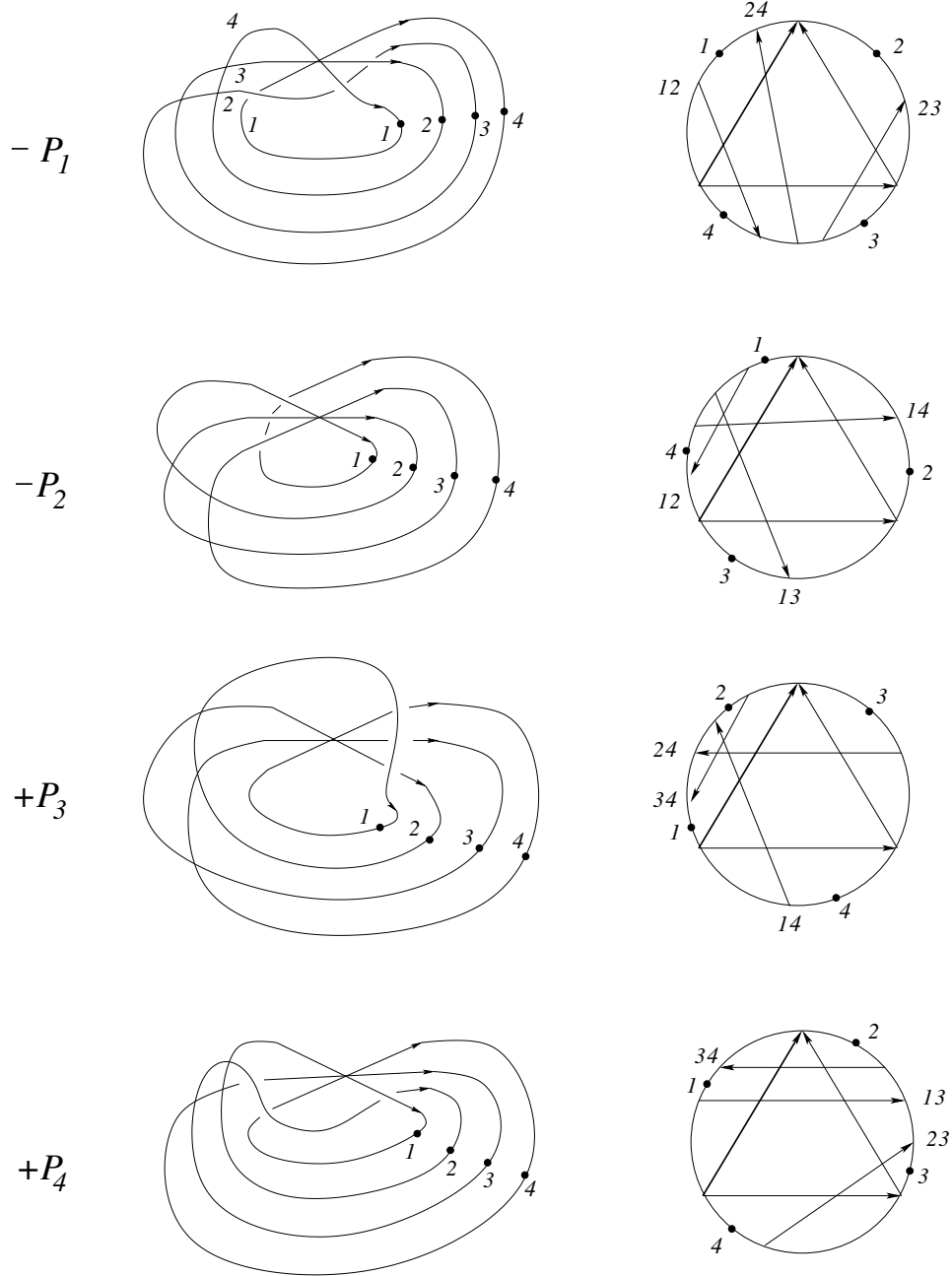


Figure 98: first half of the meridian for global type I

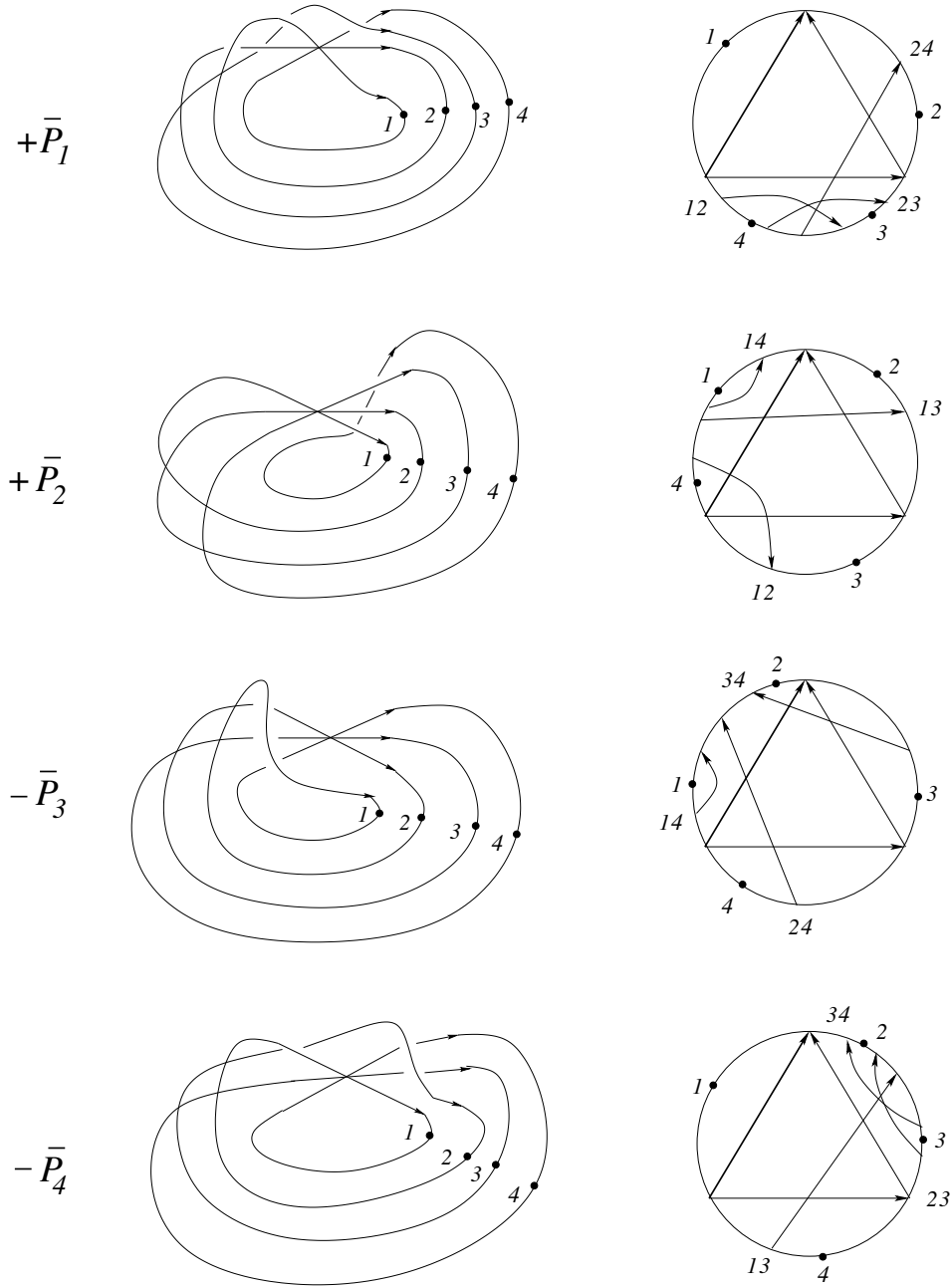


Figure 99: second half of the meridian for global type I

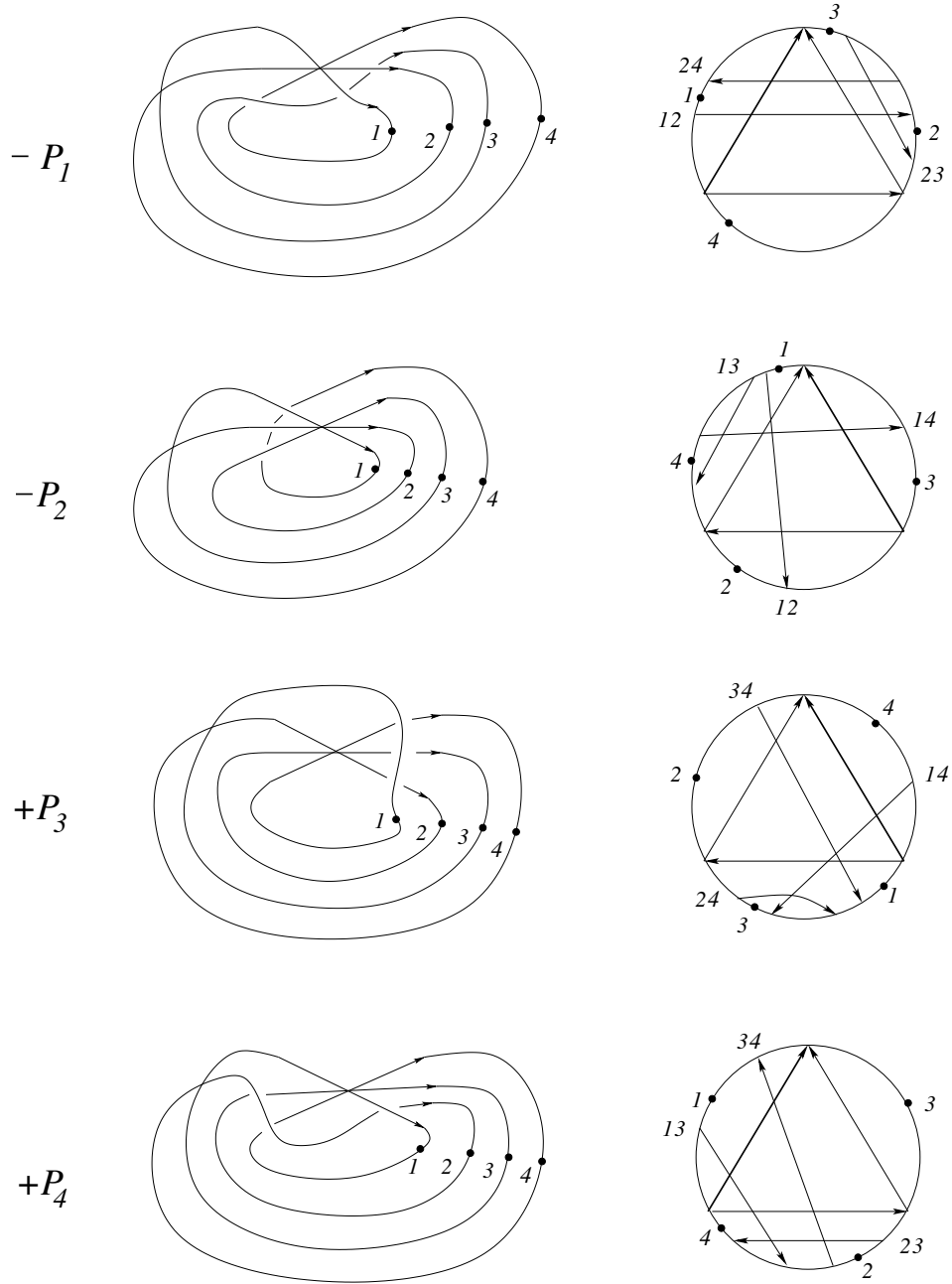


Figure 100: first half of the meridian for global type II

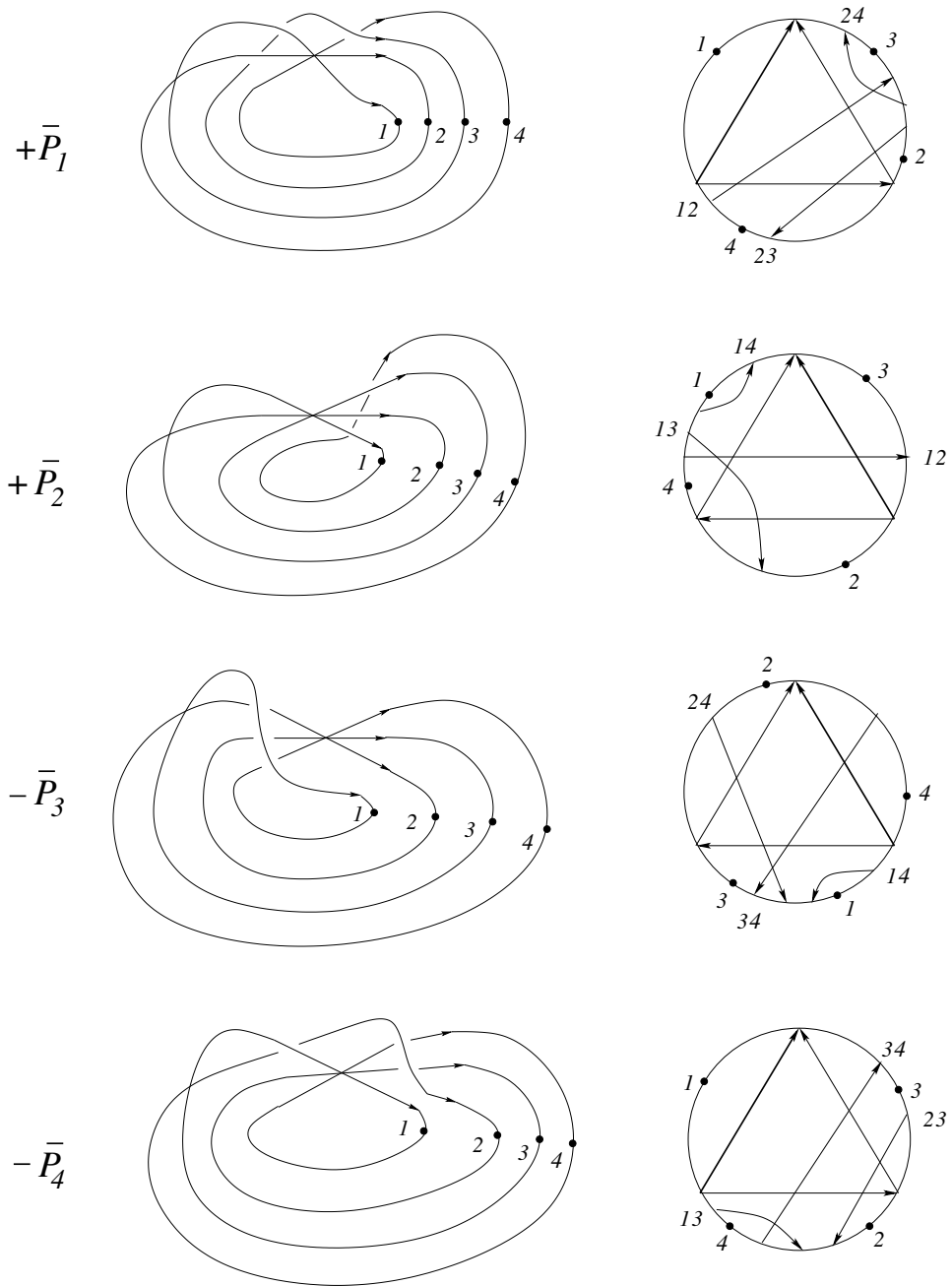


Figure 101: second half of the meridian for global type II

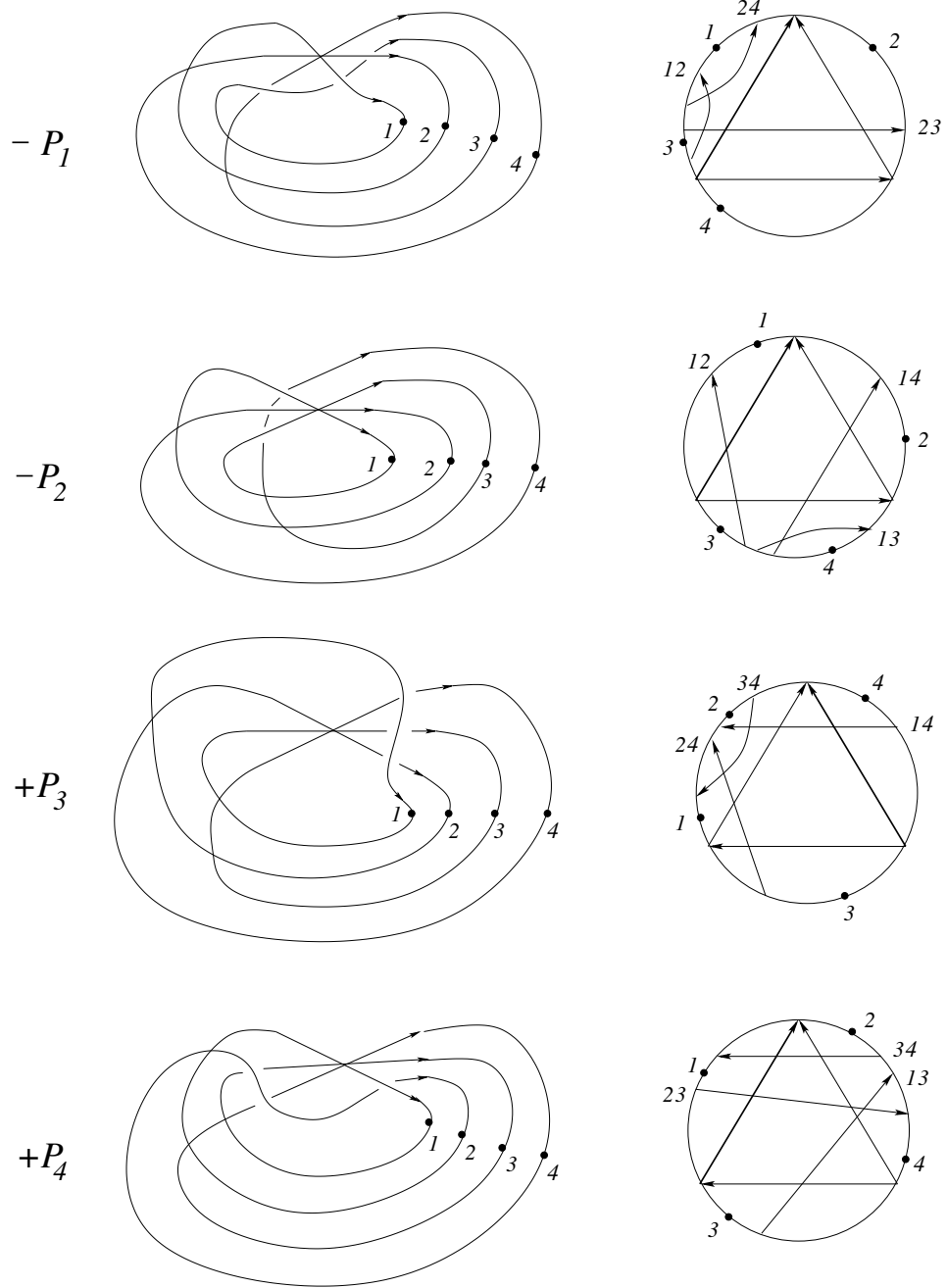


Figure 102: first half of the meridian for global type III

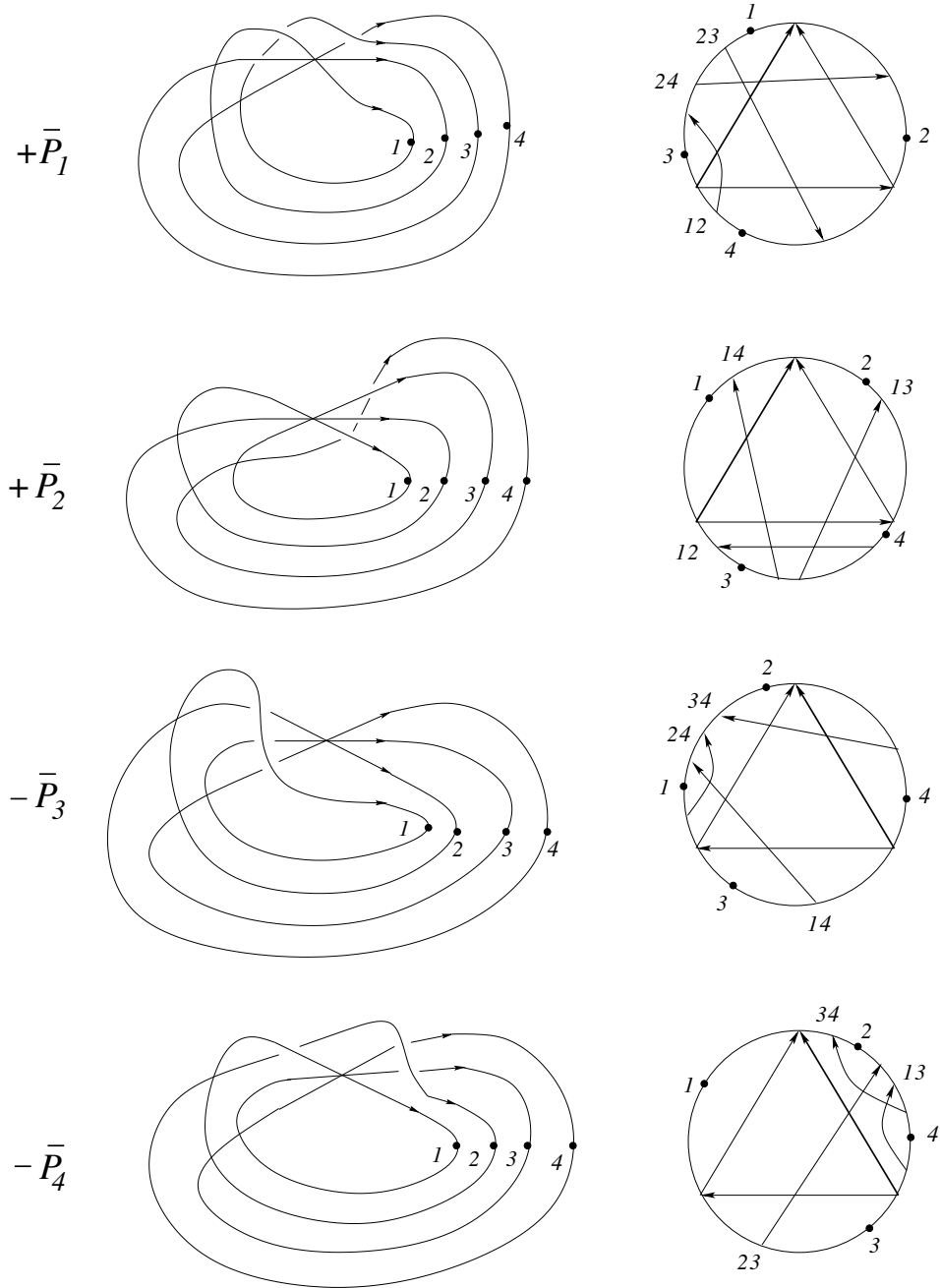


Figure 103: second half of the meridian for global type III

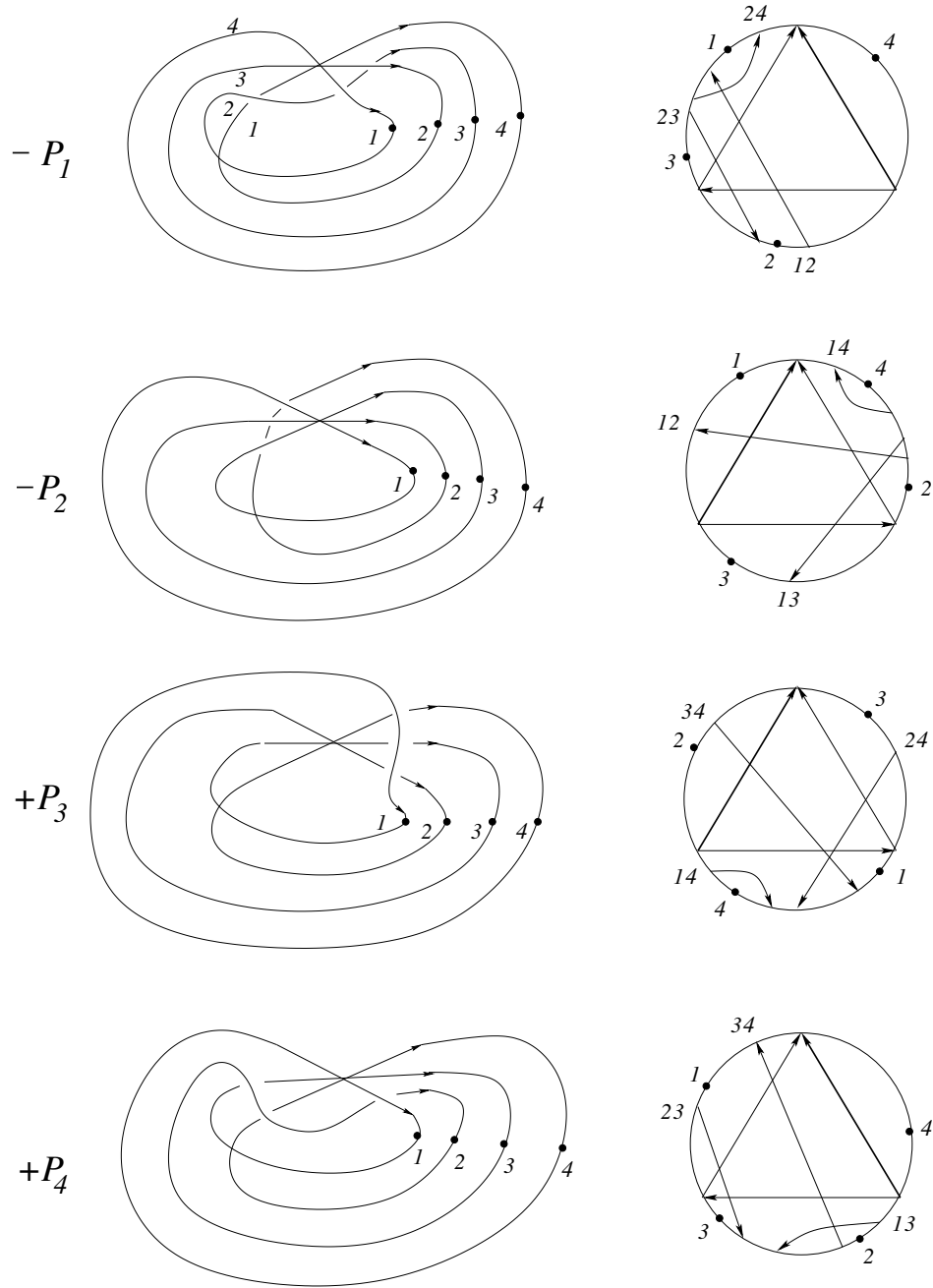


Figure 104: first half of the meridian for global type IV

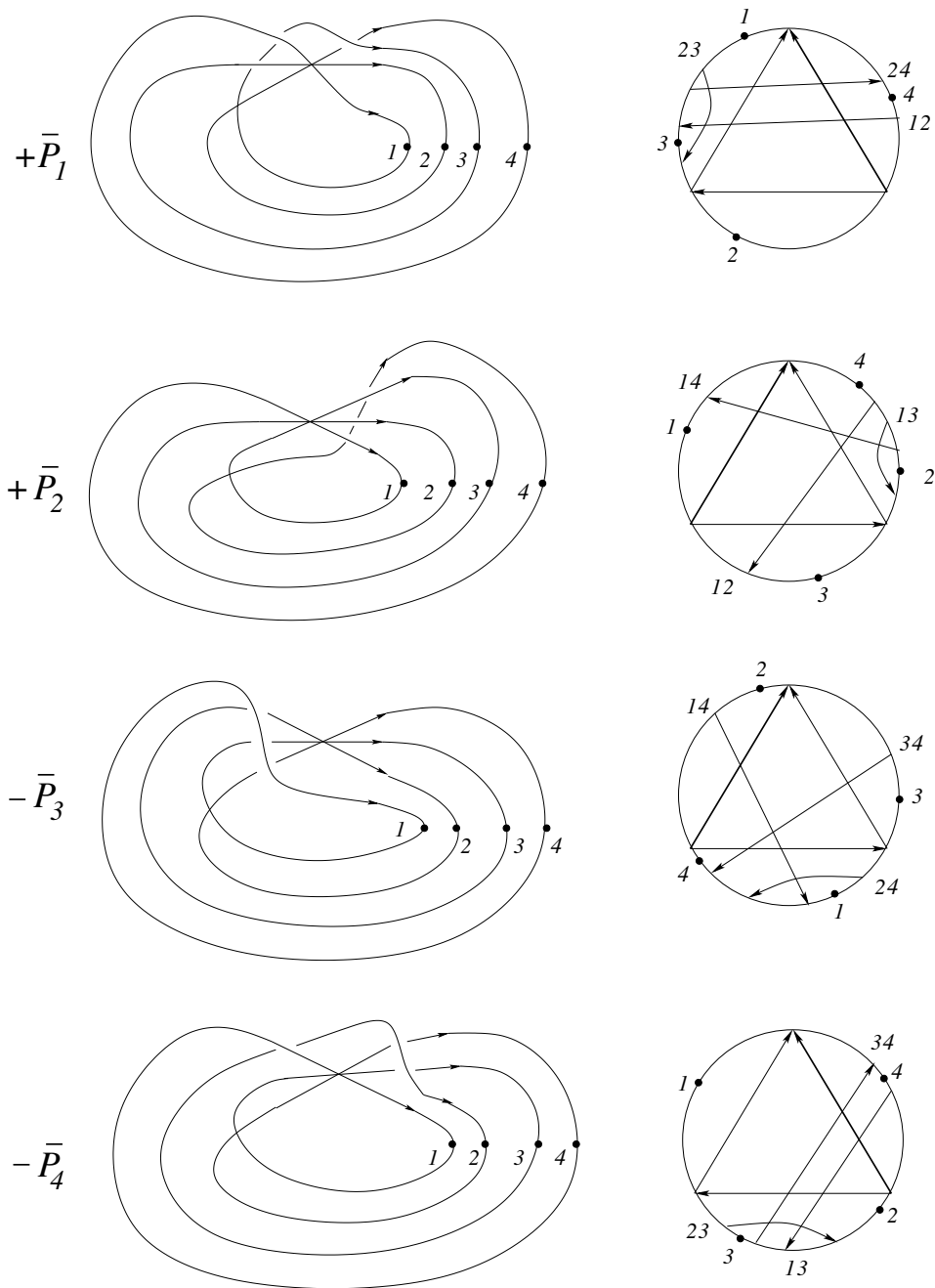


Figure 105: second half of the meridian for global type IV

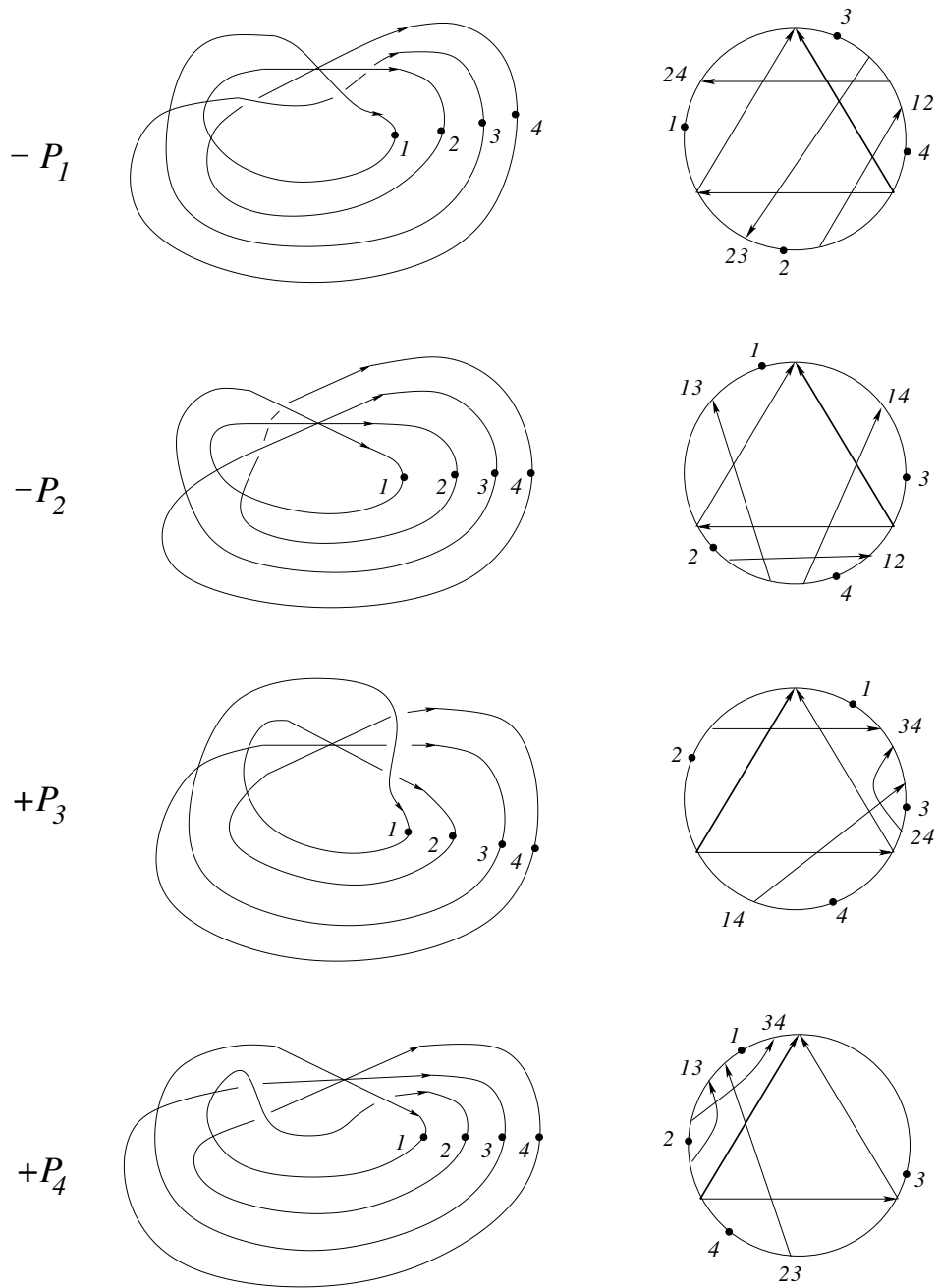


Figure 106: first half of the meridian for global type V

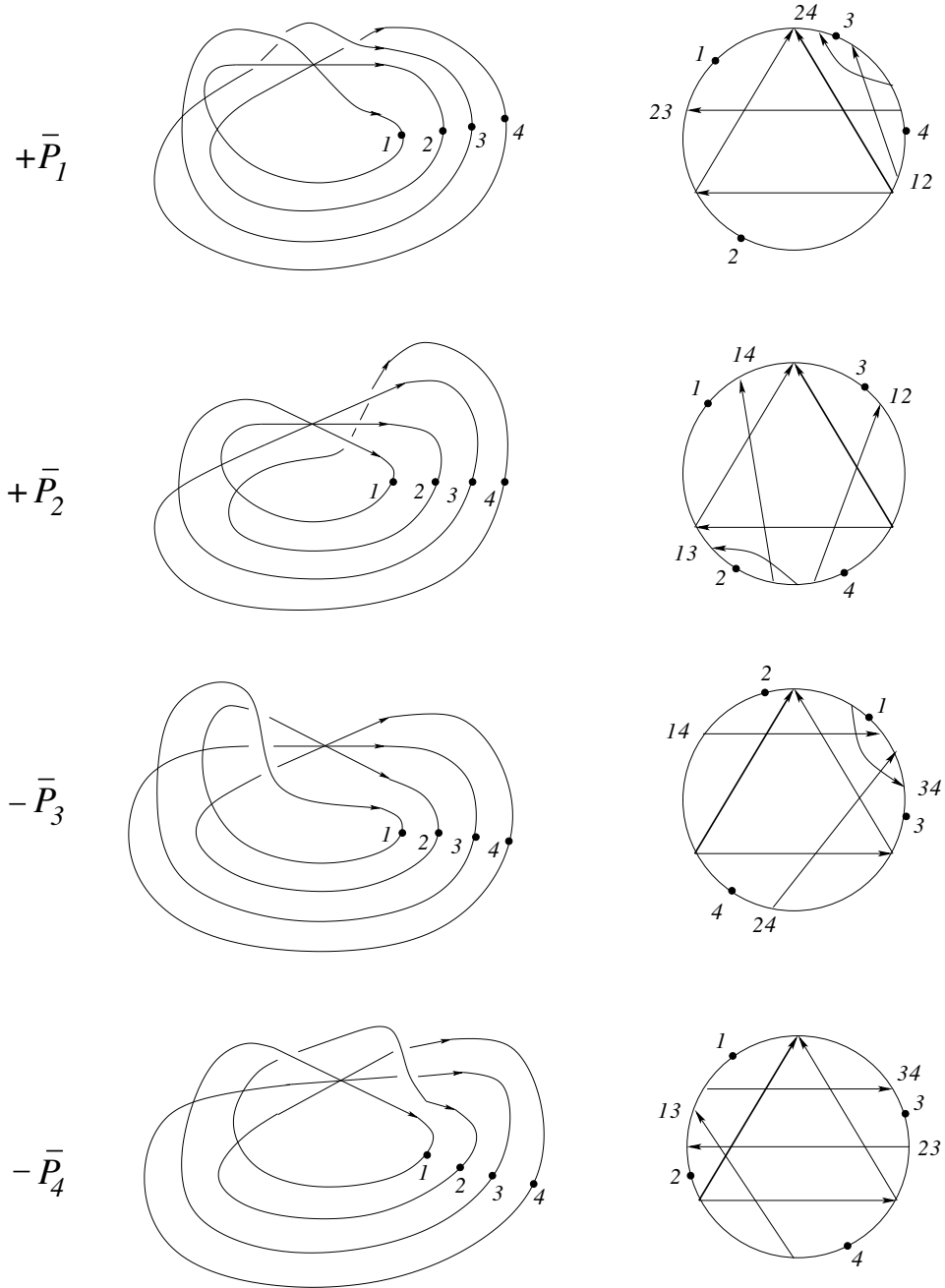


Figure 107: second half of the meridian for global type V

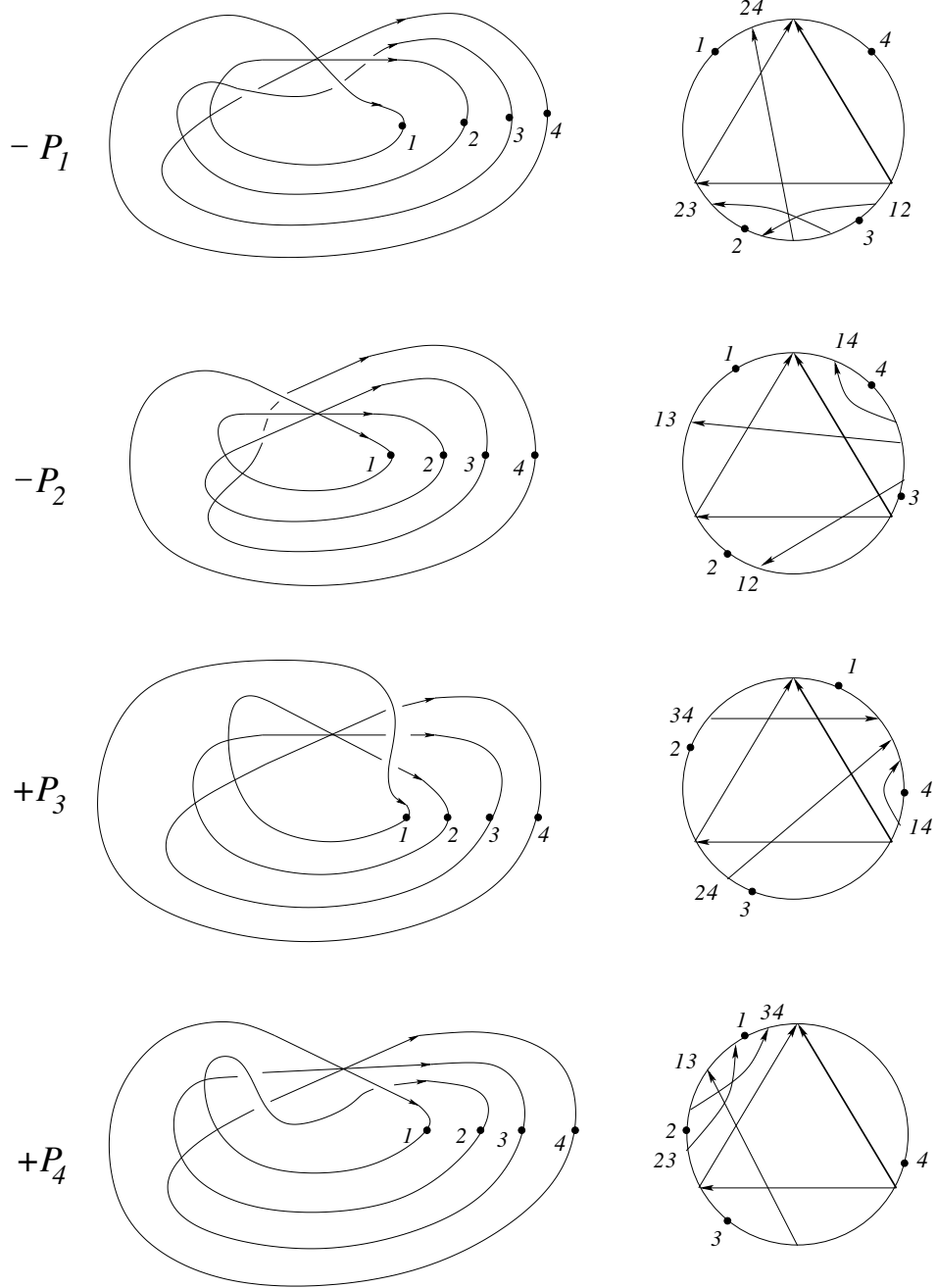


Figure 108: first half of the meridian for global type VI

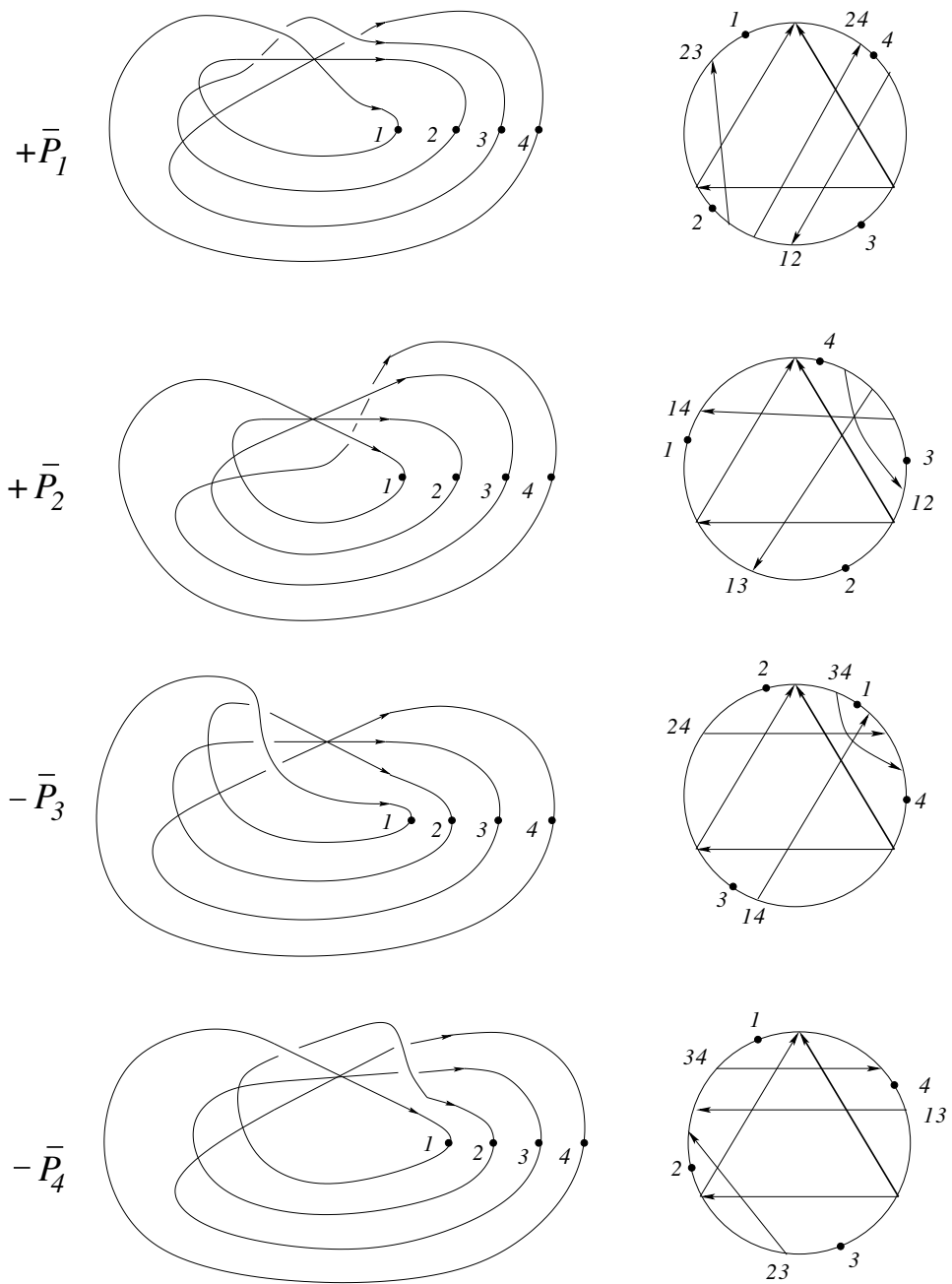


Figure 109: second half of the meridian for global type VI

case VI_1 : In P_3 : non. In \bar{P}_3 : 34 (shows that the global type l_c is necessary too). \square

It turns out that Lemma 3 could be used to define already a solution of the global tetrahedron equation (compare [18], Proposition 2). However, this solution is not controllable under moving cusps, compare Section 4.6. This forces us to go one step further and to introduce quadratic weights.

Let us consider now the quadratic weight $W_2(p)$.

Let us denote by $W_2(p, f)$ the contribution of a given f-crossing f to $W_2(p)$.

In the case that the f-crossings in P_3 and \bar{P}_3 are not the same we get now

$$W_2(\bar{P}_3) = W_2(P_3) + W_2(p, f)$$

where f is the new f-crossing in \bar{P}_3 . But luckily the new f-crossing f is always just the crossing hm in P_1 (compare the previous lemma). This has lead us to the definition of $W_1(p)$.

The linear weight $W_1(p)$ is defined with respect to the single f-crossing hm (normally we should denote it by $W_1(p, hm)$). Notice that we do not multiply by the writhe $w(hm)$. For the positive tetrahedron equation this wouldn't make any difference. But we will see later that this is forced by the cube equations.

The following lemma is a "quadratic refinement" of the previous lemma.

Lemma 4 (1) $W_2(P_1) = W_2(\bar{P}_1) = W_2(P_4) = W_2(\bar{P}_4)$

(2) $W_2(P_2) = W_2(\bar{P}_2)$

(3) Let P_i for some $i \in \{1, 2\}$ be of one of the global types r_a or l_c . Then $W_1(P_i) = W_1(\bar{P}_i)$.

(4) If the f-crossings in P_3 and \bar{P}_3 coincide then $W_2(P_3) = W_2(\bar{P}_3)$

(5) Let f be the new f-crossing in \bar{P}_3 with respect to P_3 and let $f = hm$ be the corresponding crossing in P_1 . Then $W_2(\bar{P}_3) - W_2(P_3) = W_2(\bar{P}_3, f)$ and $W_2(\bar{P}_3, f) = W_1(P_1) = W_1(\bar{P}_1)$.

(6) Let P_i for some $i \in \{3, 4\}$ be of one of the global types r_a or l_c . Then either simultaneously $W_1(P_3) = W_1(\bar{P}_3)$ and $W_1(P_4) = W_1(\bar{P}_4)$ or simultaneously $W_1(P_3) = W_1(\bar{P}_3) + 1$ and $W_1(P_4) = W_1(\bar{P}_4) + 1$.

Proof. The proof is by inspection of all f-crossings, all r-crossings and all hm-crossings in all twenty four cases in the figures. We give it below in details. (Those strata which can never contribute are dropped.) It shows in

particular that it is necessary to add the degenerate configurations in Fig. 25 and Fig. 27.

I_1 : nothing at all

I_2 : $W_2(P_1) = W_2(\bar{P}_1) = W_2(P_4) = W_2(\bar{P}_4) = 0$. $W_2(P_2) = W_2(\bar{P}_2) = 0$.

I_3 : $W_2(P_1) = W_2(\bar{P}_1) = W_2(P_4) = W_2(\bar{P}_4) = 2$. $W_2(P_2) = W_2(\bar{P}_2) = 2$. $W_1(P_1) = W_1(\bar{P}_1) = 2$. $W_1(P_2) = W_1(\bar{P}_2) = 2$. $W_2(P_3) = 0$ and $W_2(\bar{P}_3) = W_2(\bar{P}_3, f) = 2$.

I_4 : $W_2(P_1) = W_2(\bar{P}_1) = W_2(P_4) = W_2(\bar{P}_4) = 4$. $W_1(P_1) = W_1(\bar{P}_1) = 1$. $W_1(P_3) = W_1(\bar{P}_3) = 1$. $W_1(P_4) = W_1(\bar{P}_4) = 2$. $W_2(\bar{P}_3) - W_2(P_3) = W_2(\bar{P}_3, f) = 1$.

II_1 : $W_1(P_2) = W_1(\bar{P}_2) = 0$.

II_2 : $W_2(P_1) = W_2(\bar{P}_1) = W_2(P_4) = W_2(\bar{P}_4) = 2$. $W_1(P_3) = 1$ and $W_1(\bar{P}_3) = 0$. $W_1(P_4) = 1$ and $W_1(\bar{P}_4) = 2$.

II_3 : $W_2(P_1) = W_2(\bar{P}_1) = W_2(P_4) = W_2(\bar{P}_4) = 0$. $W_2(P_2) = W_2(\bar{P}_2) = 0$.

II_4 : $W_2(P_1) = W_2(\bar{P}_1) = W_2(P_4) = W_2(\bar{P}_4) = 3$. $W_1(P_1) = W_1(\bar{P}_1) = 2$. $W_1(P_2) = W_1(\bar{P}_2) = 2$. $W_2(\bar{P}_3) - W_2(P_3) = W_2(\bar{P}_3, f) = 2$. $W_1(P_4) = W_1(\bar{P}_4) = 1$.

III_1 : $W_1(P_3) = W_1(\bar{P}_3) = W_1(P_4) = W_1(\bar{P}_4) = 0$.

III_2 : $W_2(P_1) = W_2(\bar{P}_1) = W_2(P_4) = W_2(\bar{P}_4) = 0$. $W_2(P_2) = W_2(\bar{P}_2) = 0$. $W_1(P_3) = W_1(\bar{P}_3) = 0$.

III_3 : $W_2(P_2) = W_2(\bar{P}_2) = 3$. $W_1(P_2) = W_1(\bar{P}_2) = 1$.

III_4 : $W_2(P_1) = W_2(\bar{P}_1) = W_2(P_4) = W_2(\bar{P}_4) = 2$. $W_1(P_1) = W_1(\bar{P}_1) = 2$. $W_2(P_2) = W_2(\bar{P}_2) = 2$. $W_1(P_2) = W_1(\bar{P}_2) = 2$. $W_2(\bar{P}_3) - W_2(P_3) = W_2(\bar{P}_3, f) = 2$.

IV_1 : $W_1(P_1) = W_1(\bar{P}_1) = 0$. $W_2(\bar{P}_3) - W_2(P_3) = W_2(\bar{P}_3, f) = 0$. $W_1(P_3) = W_1(\bar{P}_3) = 1$. $W_1(P_4) = W_1(\bar{P}_4) = 0$.

IV_2 : $W_2(P_2) = W_2(\bar{P}_2) = 3$.

IV_3 : $W_1(P_1) = W_1(\bar{P}_1) = 1$. $W_1(P_2) = W_1(\bar{P}_2) = 1$. $W_2(P_2) = W_2(\bar{P}_2) = 2$. $W_2(\bar{P}_3) - W_2(P_3) = W_2(\bar{P}_3, f) = 1$.

IV_4 : $W_2(P_1) = W_2(\bar{P}_1) = W_2(P_4) = W_2(\bar{P}_4) = 0$. $W_2(P_2) = W_2(\bar{P}_2) = 0$. $W_1(P_3) = W_1(\bar{P}_3) = 1$. $W_2(P_3) = W_2(\bar{P}_3) = 1$.

$$\begin{aligned}
R_1(\gamma) = & \sum_{\substack{p \text{ of type} \\ r_a \text{ and } l_c}} \text{sign}(p) W_1(p) \quad \begin{array}{c} \nearrow \\ \text{---} \bullet \text{---} \searrow \\ + \end{array} \\
& + \sum_{\substack{d(p) \\ \text{of type } 0}} \text{sign}(p) W_2(p) \left(\begin{array}{c} \nearrow \\ \text{---} \bullet \text{---} \searrow \\ \nearrow \end{array} - \begin{array}{c} \nearrow \\ \text{---} \bullet \text{---} \searrow \\ \nwarrow \end{array} \right)
\end{aligned}$$

Figure 110: The 1-cochain $R_1(\gamma)$ on positive triple crossings

V_1 : $W_1(P_1) = W_1(\bar{P}_1) = 0$. $W_1(P_2) = W_1(\bar{P}_2) = 0$. $W_2(\bar{P}_3) - W_2(P_3) = W_2(\bar{P}_3, f) = 0$.

V_2 : nothing at all

V_3 : $W_2(P_1) = W_2(\bar{P}_1) = W_2(P_4) = W_2(\bar{P}_4) = 0$. $W_2(P_2) = W_2(\bar{P}_2) = 0$. $W_2(P_3) = W_2(\bar{P}_3) = 0$.

V_4 : $W_2(P_1) = W_2(\bar{P}_1) = W_2(P_4) = W_2(\bar{P}_4) = 4$. $W_2(P_3) = W_2(\bar{P}_3) = 4$. $W_2(P_4) = W_2(\bar{P}_4) = 4$. $W_1(P_3) = 3$. $W_1(\bar{P}_3) = 2$. $W_1(P_4) = 1$. $W_1(\bar{P}_4) = 2$.

VI_1 : $W_1(P_1) = W_1(\bar{P}_1) = 0$. $W_1(P_2) = W_1(\bar{P}_2) = 0$. $W_1(P_4) = W_1(\bar{P}_4) = 0$. $W_2(\bar{P}_3) - W_2(P_3) = W_2(\bar{P}_3, f) = 0$.

VI_2 : $W_1(P_3) = 1$. $W_1(\bar{P}_3) = 0$. $W_1(P_4) = 0$. $W_1(\bar{P}_4) = 1$.

VI_3 : $W_2(P_2) = W_2(\bar{P}_2) = 4$.

VI_4 : $W_2(P_1) = W_2(\bar{P}_1) = W_2(P_4) = W_2(\bar{P}_4) = 0$. $W_2(P_2) = W_2(\bar{P}_2) = 0$. $W_2(P_3) = W_2(\bar{P}_3) = 0$.

□

Let γ be an oriented generic arc in M_K which intersects $\Sigma^{(1)}$ only in positive triple crossings.

Definition 27 The evaluation of the 1-cochain R_1 on γ is defined in Fig. 110 where the first sum is over all triple crossings of the global types r_a and l_c . The second sum is over all triple crossings p which have a distinguished crossing d of type 0.

$$\begin{aligned}
& - \left(\begin{array}{c} \text{Diagram 1} \\ 1 \end{array} - \begin{array}{c} \text{Diagram 2} \\ 2 \end{array} \right) \\
& + \left(\begin{array}{c} \text{Diagram 3} \\ 3 \end{array} - \begin{array}{c} \text{Diagram 2} \\ 2 \end{array} \right) \\
& + \left(\begin{array}{c} \text{Diagram 4} \\ 4 \end{array} - \begin{array}{c} \text{Diagram 3} \\ 3 \end{array} \right) \\
& - \left(\begin{array}{c} \text{Diagram 4} \\ 4 \end{array} - \begin{array}{c} \text{Diagram 1} \\ 1 \end{array} \right) \\
& = 0
\end{aligned}$$

Figure 111: The standard solution without weights

Proposition 6 *Let m be the meridian for a positive quadruple crossing. Then $R_1(m) = 0$.*

Proof. The distinguished crossing d is the same for P_1 , \bar{P}_1 , P_4 and \bar{P}_4 and which share the same W_2 as follows from (1) in Lemma 4. We calculate their contribution to the second sum for R_1 in Fig. 111, which turns out to be 0.

Making the distinguished crossing d singular in P_2 and \bar{P}_2 leads to isotopic singular knots. The same is true for P_3 and \bar{P}_3 . It follows now from (2) in Lemma 4 that the contributions of P_2 and \bar{P}_2 to the second sum in R_1 cancel out. The same is true for P_3 and \bar{P}_3 if they share the same f-crossings, as follows from (4) in Lemma 4.

The double point in the first sum of R_1 corresponds to the crossing ml and hence the corresponding singular knots in P_i and \bar{P}_i are always isotopic

$$\begin{aligned}
& -W_I \left(\text{diagram 1} \right) + W_I \left(\text{diagram 2} \right) \\
& -W_I \left(\text{diagram 3} - \text{diagram 4} \right) \\
& = 0
\end{aligned}$$

Figure 112: The remaining part of R_1 for the meridian of a positive quadruple crossing from (5) in Lemma 4

$$+ \left(\text{diagram 5} - \text{diagram 6} \right) = 0$$

Figure 113: Cancellation from (6) in Lemma 4

for $i \in \{2, 3, 4\}$. It follows now from (3) in Lemma 4 that the contributions of P_2 and \bar{P}_2 to the first sum in R_1 cancel always out.

It follows from Lemma 3 that P_1 and \bar{P}_1 do not contribute to the first sum if P_3 and \bar{P}_3 share the same f-crossings, because P_1 and \bar{P}_1 have not the right global type. If there is a new f-crossing in \bar{P}_3 then it follows from (5) in Lemma 4 that the contributions of P_1 , \bar{P}_1 , P_3 and \bar{P}_3 to $R_1(m)$ cancel out as shown in Fig. 112 (remember that according to Lemma 3 the distinguished crossing d in P_3 and \bar{P}_3 is always the crossing ml in P_1 and \bar{P}_1).

It follows from (6) in Lemma 4 that we can have only simultaneously $W_1(P_3) = W_1(\bar{P}_3) + 1$ and $W_1(\bar{P}_4) = W_1(P_4) + 1$. But the crossing ml in P_3 and P_4 is for both strata the crossing 12 and hence the contributions of P_3 , \bar{P}_3 , P_4 and \bar{P}_4 cancel out as shown in Fig. 113. \square

Remark 7 *There are of course "dual" solutions R_1 by using the second formula of Polyak-Viro for $v_2(K)$ (see Fig. 114) and by using symmetries as the orientation change and the rotation by π around the imaginary axes $i\mathbb{R} \times 0 \subset \mathbb{C} \times \mathbb{R}$ for the definition of the weights W_1 and W_2 .*

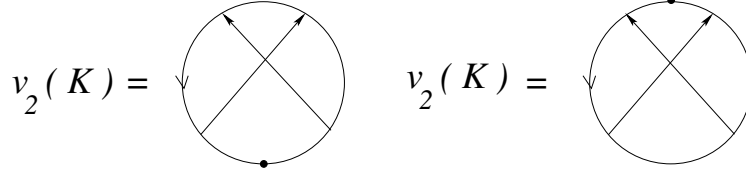


Figure 114: Polyak-Viro formula for the Vassiliev invariant v_2

Remark 8 *Let us summarize the combinatorial structure of R_1 which leads to $R_1(m) = 0$ for the meridian m of a positive quadruple crossing.*

(1) *The strata $P_1, \bar{P}_1, P_4, \bar{P}_4$ share the same distinguished crossing d and their contributions with d singular cancel out.*

(2) *All contributions of P_2 and \bar{P}_2 cancel out.*

(3) *The strata P_3 and \bar{P}_3 contribute non trivially with d singular if and only if P_1 and \bar{P}_1 are of global type r_a or l_c and in this case the contributions of P_3 and \bar{P}_3 with d singular cancel out with those of P_1 and \bar{P}_1 with ml singular.*

(4) *The contributions of P_3 and \bar{P}_3 with ml singular cancel always out with those from P_4 and \bar{P}_4 with ml singular too.*

Question 5 *Can one define 1-cocycle invariants of degree one by using weights of degrees higher than two (this is not the same as 1-cocycle invariants of higher degree)?*

Let us consider now $R_2(m)$ for a positive quadruple crossing (compare Definition 16 but only for positive triple crossings and without self-tangencies).

The d-crossings are symmetrized and they always intersect the f-crossings, compare Definition 15. We do not need any longer the r-crossings and the weight is replaced by making each individual couple of a d-crossing and a f-crossing simultaneously singular.

Proposition 7 *Let m be the meridian for a positive quadruple crossing. Then $R_2(m) = 0$.*

Proof. It follows immediately from (1) in Remark 8 that if a f-crossing does not belong to the six crossings involved in the quadruple crossing then its contributions to $R_2(m)$ cancel out. Hence we have only to consider the six crossings from the quadruple crossing. The calculation is very extensive. We

$$\begin{aligned}
I_3: & - \text{diagram 1} - \text{diagram 2} + \text{diagram 3} \\
& + \text{diagram 4} - (\text{diagram 5} - \text{diagram 6}) = 0
\end{aligned}$$

Figure 115: $R_2(m) = 0$ for I_3

give it in all details only for quadruple crossings of global type I by using the figures Fig. 98 and Fig. 99. All the other cases are similar and are left to the reader.

We go along the meridian m from P_1 up to \bar{P}_4 . For the convenience of the reader we indicate by a number the couples of singular knots which cancel out together.

I_1 : no contributions at all.

I_2 : no contributions at all.

The case I_3 is shown in Fig. 115.

The case I_4 is shown in Fig. 116.

Notice that the combinatorial structure of $R_2(m) = 0$ is rather difficult. For example, the five contributions of \bar{P}_4 in case I_4 cancel out with two contribution from P_1 , two contributions from \bar{P}_1 and one contribution of \bar{P}_2 . \square

Let us consider now the case of closed n -braids in the solid torus for $n > 3$ (there isn't any tetrahedron equation for $n < 4$).

We consider R_1 from Definitions 21 and 22, but we need here only positive triple crossings and no self-tangencies.

Proposition 8 *Let m be the meridian for a positive quadruple crossing. Then $R_1(m) = 0$.*

Proof. The combinatorial structure of $R_1(m) = 0$ is exactly the same as described in Remark 8, but the proof is much simpler. We use again Fig. 98-109. The global type I is shown in Fig. 84. Each of the four arcs in the circle represents a positive homology class in the solid torus. Therefore only

$$\begin{aligned}
I_4: & - \left(\text{diagram 1} - \text{diagram 2} \right) \\
& - \text{diagram 3} + \text{diagram 4} \\
& + \left(\text{diagram 5} - \text{diagram 2} \right) + \text{diagram 6} \\
& + \left(\text{diagram 7} - \text{diagram 5} \right) \\
& + \left(\text{diagram 8} - \text{diagram 6} \right) \\
& + \text{diagram 9} + \left(\text{diagram 10} - \text{diagram 8} \right) \\
& - \text{diagram 4} - \left(\text{diagram 7} - \text{diagram 1} \right) \\
& - \left(\text{diagram 9} - \text{diagram 3} \right) - \text{diagram 10} = 0
\end{aligned}$$

Figure 116: $R_2(m) = 0$ for I_4

the crossing 14 can have the homological marking 1 and it is a d-crossing. It follows immediately from (1) in Remark 8 that if a f-crossing does not belong to the six crossings involved in the quadruple crossing then its contributions to $R_1(m)$ cancel out. There aren't any other f-crossings and there is no triple crossing of global type l which contributes to R_1 . Hence $R_1(m) = 0$. The global type II is shown in Fig. 84 too. Only the crossings 14 and 23 can have marking 1. The crossing 23 is not a d-crossing and it can not be a f-crossing for 14 (under a small perturbation the corresponding two arrows will never intersect). There are no triple crossings of type l which could contribute to R_1 . It follows that $R_1(m) = 0$. The global type III is shown in Fig. 84. Only the crossings 24 and 12 can have marking 1 and only 24 is a d-crossing, namely for $-P_2$ and \bar{P}_2 . If 24 and 12 have both marking 1 then 14 has marking 2 and P_4 and \bar{P}_4 are of the global type l which contributes to R_1 . We see from the Gauss diagram of P_2 that 12 is not a f-crossing (the corresponding arrow intersects the d-crossing 24 in the wrong direction) and hence the contributions cancel out as in (2) of Remark 7. Consequently, only P_4 and $-\bar{P}_4$ contribute to $R_1(m)$ with ml as double point. But ml for P_4 and $-\bar{P}_4$ corresponds to the crossing 12 which is under all other branches. Consequently, the contributions of P_4 and $-\bar{P}_4$ cancel out and $R_1(m) = 0$. The global type IV is shown in Fig. 84. Only the crossings 13 and 24 can have marking 1. The crossing 13 is a d-crossing for P_3 and $-\bar{P}_3$ and the crossing 24 is a d-crossing for $-P_2$ and \bar{P}_2 . Again, the two crossings with marking 1 can never intersect. But for P_2 the fourth branch moves just under the triple crossing and for P_3 just over the triple crossing and hence the contributions cancel out for each of them and $R_1(m) = 0$. The global type V is shown in Fig. 84. Only the crossings 13 and 34 can have marking 1 and in this case the crossing 14 has marking 2 and $-P_1$ and \bar{P}_1 are of the global type l which contributes. The crossing 13 is a d-crossing for P_3 and $-\bar{P}_3$ and the crossing 34 is a f-crossing only for P_3 . We show the calculation of $R_1(m) = 0$ in Fig. 117.

The global type VI is shown in Fig. 84. Only the crossings 12, 23 and 34 can have marking 1. But non of them is a d-crossing. Again, $-P_2$ and \bar{P}_2 as well as P_3 and $-\bar{P}_3$ can be of the type l which contributes. But for the same reason as in the case IV their contributions cancel out and $R_1(m) = 0$. \square

Let us consider now R_2 for closed n-braids (compare the Definitions 23 and 24).

Proposition 9 *Let m be the meridian for a positive quadruple crossing.*

$$\begin{aligned}
& - \text{diagram} \\
& + \left(\text{diagram} - \text{diagram} \right) \\
& + \text{diagram} = 0
\end{aligned}$$

Figure 117: $R_1(m) = 0$ for the global type V

Then $R_2(m) = 0$.

Proof. The proof is much simpler as in the case of long knots. We use the informations contained in the proof of the previous proposition.

Global type I: $R_2(m) = 0$ follows again from (1) in Remark 8.

Global type II: exactly the same argument.

Global type III: the crossing 12 is now a f-crossing for $-P_2$ (because of the symmetrization) and P_4 and $-\bar{P}_4$ contribute because of their global type. The calculation of $R_1(m) = 0$ is shown in Fig. 118.

Global type IV: same argument as for the type II.

Global type V: the crossing 34 is a f-crossing for P_3 and $-P_1$ and \bar{P}_1 are of the global type l which contributes. The calculation of $R_2(m) = 0$ is shown in Fig. 118 too.

Global type VI: $R_2(m) = 0$ for exactly the same reason as for $R_1(m) = 0$.

□

Notice that we haven't used here the embedded 2T-relation.

4.5 Cube equations

We have to consider now all other local types of triple crossings together with the self-tangencies. We know already the singularizations for the local type 1 from the solution of the tetrahedron equation and we will determine the singularizations of all other local types from the cube equations. The

$$\begin{aligned}
& - \left(\begin{array}{c} \text{Diagram 1} \\ \text{Diagram 2} \end{array} - \begin{array}{c} \text{Diagram 3} \\ \text{Diagram 4} \end{array} \right) \\
& + \begin{array}{c} \text{Diagram 5} \\ \text{Diagram 6} \end{array} - \begin{array}{c} \text{Diagram 7} \\ \text{Diagram 8} \end{array} = 0
\end{aligned}$$

global type III

$$\begin{aligned}
& - \begin{array}{c} \text{Diagram 9} \\ \text{Diagram 10} \end{array} \\
& + \left(\begin{array}{c} \text{Diagram 11} \\ \text{Diagram 12} \end{array} - \begin{array}{c} \text{Diagram 13} \\ \text{Diagram 14} \end{array} \right) \\
& + \begin{array}{c} \text{Diagram 15} \\ \text{Diagram 16} \end{array} = 0
\end{aligned}$$

global type V

Figure 118: $R_2(m) = 0$ for the global types III and V

local types of triple crossings were shown in Fig. 20. The diagrams which correspond to the edges of the graph Γ (compare Section 4.1) are shown in Fig. 119. The projection of a triple crossing p into the plan separates the plan near p into three couples of a region and its dual. The regions correspond exactly to the three edges adjacent to the vertex corresponding to the local type of the triple crossing (we can forget about the three dual regions because of $\Sigma_{trans-self-flex}^{(3)}$ as explained in Section 4.1). We show the corresponding graph Γ now in Fig. 120. The unfolding of e.g. the edge $1 - 5$ is shown in Fig. 86 (compare [19]).

Observation 1 *The diagrams corresponding to the two vertices's of an edge differ just by the two crossings of the self-tangency which replace each other in the triangle as shown in Fig. 121. Consequently, the two vertices of an edge have always the same global type and always different local types and the two crossings which are interchanged can only be simultaneously f-crossings. Moreover, the two self-tangencies in the unfolding (of an edge) can contribute non trivially to R_1 if they have different weight $W_2(p)$ or if their singularizations are not isotopic. The latter happens exactly for the edges "1-6", "3-5", "4-7" and "2-8" (where the third branch passes between the two branches of the self-tangency).*

It follows that we have to solve the cube equations for the graph Γ exactly six times: one solution for each global type of triple crossings.

Proposition 10 *Let m be a meridian of $\Sigma_{trans-self}^{(2)}$ or a loop in Γ . Then $R_1(m) = 0$ for the singularizations given in Definition 12.*

Proof. First of all we observe that the two vertices of an edge (i.e. triple crossings) share the same f-crossings. The f-crossings could only change if the foot of a f-crossing slides over the head of the crossing d . But this is not the case as it was shown in Fig. 121. Indeed, the foot of the crossing which changes in the triangle can not coincide with the head of d because the latter coincides always with the head of another crossing.

It suffices of course to consider only the four crossings involved in an edge because the position of the triple crossings and the self-tangencies with respect to all other crossings do not change.

We start with the solutions for triple crossings of global type l . In the figures we show the Gauss diagrams of the two triple crossings together with

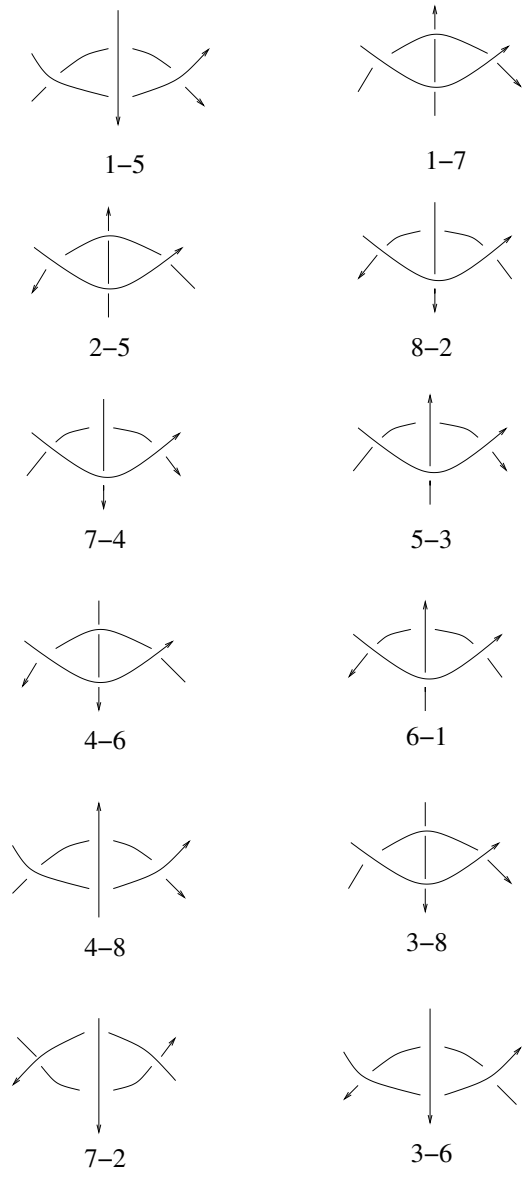


Figure 119: The twelve edges of the graph Γ

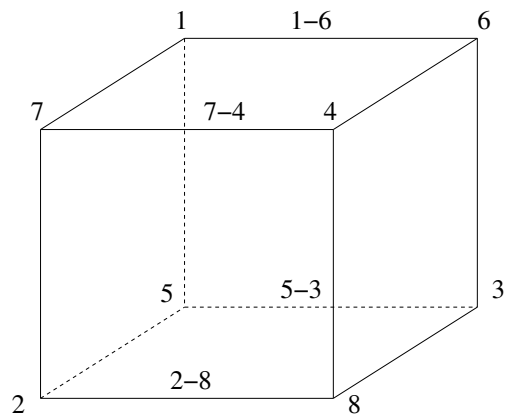


Figure 120: The graph Γ

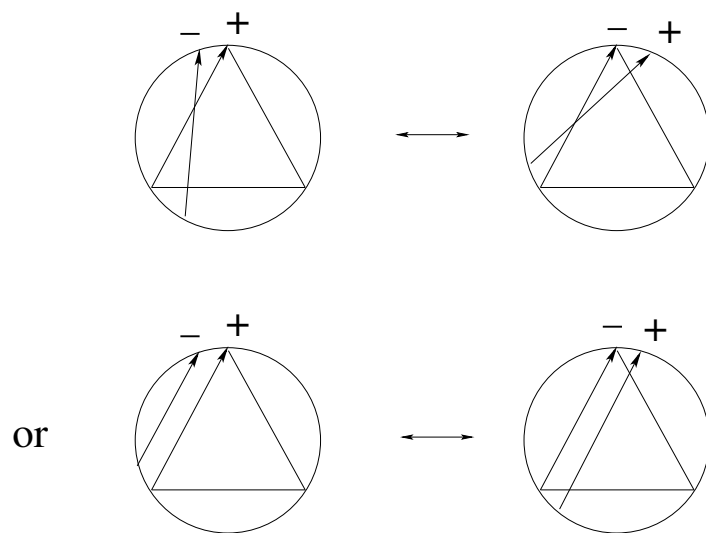


Figure 121: two crossings replace each other for an edge of Γ

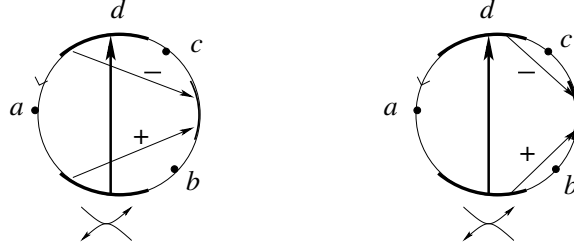


Figure 122: The two self-tangencies for the edge $l7 - 2$

the points at infinity and the Gauss diagram of just one of the two self-tangencies. The Gauss diagram of the second self-tangency is derived from the first one in the following way: the two arrows slide over the arrow d but their mutual position does not change. We show an example in Fig. 122. Notice that in the thick part of the circle there aren't any other heads or foots of arrows.

To each figure of an edge corresponds a second figure. In the first line on the left we have the singularization with linear weight $W_1(p)$ which is already known, i.e. which corresponds with the singularization at ml . (Of course we draw only the case when the triple crossing contributes, i.e. global type r_a or l_c and we drop $W_1(p)$ in the figures.) This determines the new singularization on the right. We put the singularizations in rectangles for better visualizing them. In the second line we give the corresponding singularizations with quadratic weight $W_2(p)$ (i.e. which correspond to the singularization at d , but we drop the common factor $W_2(p)$).

For the global type l the fourth arrow which is not in the triangle is always almost identical with an arrow of the triangle. Consequently, in the case l_c it can not be a r-crossing with respect to hm . In the case l_b it could be a r-crossing with respect to some f-crossing. But the almost identical arrow in the triangle would be a r-crossing for the same f-crossing too. Their contributions cancel out, because they have different writhe.

The mutual position of the two arrows for a self-tangency does not change. Only the position with respect to the distinguished crossing d changes. It remains to consider the edges "1-5", "4-8", "2-7" and "3-6" for l_c , where one of the two self-tangencies has a new f-crossing with respect to the other self-tangency. But one sees immediately from the figures that this new f-crossing is exactly the crossing hm in the triple crossings. In this case, exactly one of the self-tangencies contributes with the factor $W_1(p)$ and enters the

equation for the singularization at the crossing ml of the triple crossings. Hence sometimes the self-tangencies contribute non trivially to the first line (when $W_2(p)$ changes) and sometimes they contribute non trivially to the second line (when the third branch passes between the branches of the self-tangency).

We proceed then in exactly the same way for the global type r . But notice the difference which comes from the fact that we have broken the symmetry: the global type r_a contributes both with linear weight $W_1(p)$ as well as with quadratic weight $W_2(p)$. Exactly the same arguments as previously apply in the case r_b too. In the case r_c there are no contributions at all. The differences appear in the case r_a . Here sometimes the fourth crossing, which is not in the triangle, is a r-crossing exactly for one of the two triple crossings.

We examine the figures (don't forget the degenerate configurations):

- edge "1-7": type 1 and type 7 share the same W_1 and W_2
- edge "3-8": type 3 and type 8 share the same W_1 and W_2
- edge "4-6": same W_1 but $W_2 + 1$ for type 4 and $W_2 - 1$ for type 6
- edge "5-2": same W_1 but $W_2 + 1$ for type 5 and $W_2 - 1$ for type 2
- edge "1-5": $W_1 - 1$ and $W_2 - 1$ for type 1 with respect to type 5
- edge "7-4": $W_1 - 1$ and $W_2 + 1$ for type 4 with respect to type 7
- edge "5-3": $W_1 + 1$ and $W_2 + 1$ for type 5 with respect to type 3
- edge "4-8": $W_1 - 1$ and $W_2 + 1$ for type 4 with respect to type 8
- edge "7-2": $W_1 + 1$ and $W_2 - 1$ for type 2 with respect to type 7
- edge "3-6": $W_1 - 1$ and $W_2 - 1$ for type 6 with respect to type 3
- edge "8-2": $W_1 - 1$ and $W_2 + 1$ for type 8 with respect to type 2
- edge "1-6": $W_1 + 1$ and $W_2 + 1$ for type 1 with respect to type 6

This forces the constant correction terms for the weights given in Definition 12.

For the self-tangencies "8-2" as well as in "1-6" we have the same W_2 as in type 8 respectively type 1. In the self-tangencies "7-4" and "5-3" we have W_2 is the same as in type 7 respectively type 3.

After establishing the singularizations for all eight local types of triple crossings we have to verify that the solution is consistent for the loops in Γ . We have to do this for the boundary of the three different types of 2-faces "1-7-2-5", "1-6-4-7" and "7-4-8-2" of the cube, i.e. we have just to check that the remaining fourth edge leads to the same result. The remaining 2-faces, which are parallel to these three, are completely analogous. A part of the proof is in the figures Fig. 123-125. The remaining cases are quit similar and we leave them to the reader.

□

Notice that we haven't used here at all the embedded 1T-relation.

We have to solve now the cube equations for R_2 , compare Definition 16.

Proposition 11 *Let m be a meridian of $\Sigma_{trans-self}^{(2)}$ or a loop in Γ . Then $R_2(m) = 0$ in K_2 .*

Proof. If a f-crossing is not amongst the four involved crossings of the edge then the singularization is exactly the same as for R_1 besides that the f-crossing becomes now singular too.

Notice that the crossing ml becomes singular exactly for the global types r_a and l_a . The crossing hm is a f-crossing exactly in these two cases too. We can use again the same figures with the Gauss diagrams of the edges in order to establish the singularizations for these global types. We give just some examples in Fig. 126 and Fig. 127, but we left the rest of the verification to the reader. □

Let us consider now the case of closed n-braids, which is in fact much easier.

Proposition 12 *Let m be a meridian of $\Sigma_{trans-self}^{(2)}$ or a loop in Γ . Then $R_1(m) = 0$ in $\hat{\beta}_1$ for the singularizations given in Definition 21.*

Proof. First of all we observe that the local types 2 and 6, as well as self-tangencies with different tangent direction, do not occur for closed braids. Indeed, all tangencies of the projection of the closed braid into \mathbb{C}^* are positive transverse to the levels of the function $arg(z)$. Consequently, the cube equations degenerate to the *hexagon equation*, namely the equator $1 - 7 - 4 - 8 - 3 - 5 - 1$ with respect to the poles 2 and 6 of the cube.

Let's start with the global types r . Only the distinguished crossing d can have marking 1. The proof is now exactly the same as in the case of long knots for all those f-crossings which are not amongst the four involved crossings of the edge. Hence it suffices to consider the four involved crossings. The self-tangencies do not contribute and there can be a f-crossing amongst the four involved crossings only if d is a crossing from the self-tangencies. This happens exactly for the edges $7 - 4$ and $3 - 5$, for which we use the corresponding figures from the case of long knots. This leads to the correction term -1 in $W(d)$ exactly for the local types 3, 4 and 8 (which corresponds

$$\begin{array}{c} \text{Diagram 1} \\ \text{+} \end{array} = \begin{array}{c} \text{Diagram 2} \\ \text{+} \end{array}$$

$$\begin{array}{c} \text{Diagram 3} \\ \text{+} \end{array} - \begin{array}{c} \text{Diagram 4} \\ \text{+} \end{array} = \begin{array}{c} \text{Diagram 5} \\ \text{+} \end{array} - \begin{array}{c} \text{Diagram 6} \\ \text{+} \end{array}$$

11-7

$$- \begin{array}{c} \text{Diagram 7} \\ \text{+} \end{array} + (\begin{array}{c} \text{Diagram 8} \\ \text{+} \end{array} - \begin{array}{c} \text{Diagram 9} \\ \text{+} \end{array}) = - \begin{array}{c} \text{Diagram 10} \\ \text{+} \end{array}$$

$$- (\begin{array}{c} \text{Diagram 11} \\ \text{+} \end{array} - \begin{array}{c} \text{Diagram 12} \\ \text{+} \end{array}) = (\begin{array}{c} \text{Diagram 13} \\ \text{+} \end{array} - \begin{array}{c} \text{Diagram 14} \\ \text{+} \end{array})$$

11-5

$$- \begin{array}{c} \text{Diagram 15} \\ \text{+} \end{array} = - \begin{array}{c} \text{Diagram 16} \\ \text{+} \end{array}$$

$$- (\begin{array}{c} \text{Diagram 17} \\ \text{+} \end{array} - \begin{array}{c} \text{Diagram 18} \\ \text{+} \end{array}) + (\begin{array}{c} \text{Diagram 19} \\ \text{+} \end{array} - \begin{array}{c} \text{Diagram 20} \\ \text{-} \end{array})$$

$$= - (- \begin{array}{c} \text{Diagram 21} \\ \text{-} \end{array} + \begin{array}{c} \text{Diagram 22} \\ \text{-} \end{array}) + (\begin{array}{c} \text{Diagram 23} \\ \text{+} \end{array} - \begin{array}{c} \text{Diagram 24} \\ \text{-} \end{array})$$

11-6

Figure 123: Singularizations for $l1 - 7$, $l1 - 5$ and $l1 - 6$

$$\begin{aligned}
& - \left(\text{diagram with box and } + \right) = + (-1) \left(\text{diagram with } + \right) - \left(\text{diagram with } - \right) \\
& - \left(- \left(\text{diagram with box and } + \right) + \left(\text{diagram with box and } + \right) \right) = - \left(\text{diagram with box and } + \right) - \left(\text{diagram with box and } + \right) \\
& \hspace{10em} l7-2 \\
& + \left(\text{diagram with box and } + \right) = + \left(\text{diagram with box and } + \right) \\
& + \left(\text{diagram with box and } + \right) - \left(\text{diagram with box and } + \right) + \left(\text{diagram with } + \right) - \left(\text{diagram with } - \right) \\
& = + \left(\text{diagram with box and } - \right) - \left(\text{diagram with box and } - \right) + \left(\text{diagram with } + \right) - \left(\text{diagram with } - \right) \\
& \hspace{10em} l7-4
\end{aligned}$$

Figure 124: Singularizations for $l7 - 2$ and $l7 - 4$

$$\begin{aligned}
& + \begin{array}{|c|} \hline \text{Diagram 1} \\ \hline \end{array} = + \begin{array}{|c|} \hline \text{Diagram 2} \\ \hline \end{array} \\
& + (\begin{array}{|c|} \hline \text{Diagram 3} \\ \hline \end{array} - \begin{array}{|c|} \hline \text{Diagram 4} \\ \hline \end{array}) = (\begin{array}{|c|} \hline \text{Diagram 5} \\ \hline \end{array} - \begin{array}{|c|} \hline \text{Diagram 6} \\ \hline \end{array}) \\
& \quad \quad \quad r1-7 \\
& - \begin{array}{|c|} \hline \text{Diagram 7} \\ \hline \end{array} + (- \begin{array}{|c|} \hline \text{Diagram 8} \\ \hline \end{array} - \begin{array}{|c|} \hline \text{Diagram 9} \\ \hline \end{array}) = - \begin{array}{|c|} \hline \text{Diagram 10} \\ \hline \end{array} \\
& - (\begin{array}{|c|} \hline \text{Diagram 11} \\ \hline \end{array} - \begin{array}{|c|} \hline \text{Diagram 12} \\ \hline \end{array}) = - (\begin{array}{|c|} \hline \text{Diagram 13} \\ \hline \end{array} - \begin{array}{|c|} \hline \text{Diagram 14} \\ \hline \end{array}) \\
& \quad \quad \quad r1-5 \\
& - \begin{array}{|c|} \hline \text{Diagram 15} \\ \hline \end{array} = - \begin{array}{|c|} \hline \text{Diagram 16} \\ \hline \end{array} \\
& - (\begin{array}{|c|} \hline \text{Diagram 17} \\ \hline \end{array} - \begin{array}{|c|} \hline \text{Diagram 18} \\ \hline \end{array}) + (\begin{array}{|c|} \hline \text{Diagram 19} \\ \hline \end{array} - \begin{array}{|c|} \hline \text{Diagram 20} \\ \hline \end{array}) \\
& = - (\begin{array}{|c|} \hline \text{Diagram 21} \\ \hline \end{array} - \begin{array}{|c|} \hline \text{Diagram 22} \\ \hline \end{array}) + (\begin{array}{|c|} \hline \text{Diagram 23} \\ \hline \end{array} - \begin{array}{|c|} \hline \text{Diagram 24} \\ \hline \end{array}) \\
& \quad \quad \quad r1-6
\end{aligned}$$

Figure 125: Singularizations for $r1 - 7$, $r1 - 5$ and $r1 - 6$

$$\begin{aligned}
& + (-1) \begin{array}{c} \text{Diagram 1} \\ \text{Diagram 2} \end{array} + (-1) \left(\begin{array}{c} \text{Diagram 3} \\ \text{Diagram 4} \end{array} - \begin{array}{c} \text{Diagram 5} \end{array} \right) \\
& + \left(\begin{array}{c} \text{Diagram 6} \\ \text{Diagram 7} \end{array} - \begin{array}{c} \text{Diagram 8} \end{array} \right) = + (-1) \begin{array}{c} \text{Diagram 9} \\ \text{Diagram 10} \end{array} \\
& \qquad \qquad \qquad 2l1-7 \\
& - (-1) \begin{array}{c} \text{Diagram 11} \\ \text{Diagram 12} \end{array} = - (-1) \begin{array}{c} \text{Diagram 13} \\ \text{Diagram 14} \end{array} \\
& \qquad \qquad \qquad 2l1-5 \\
& - (-1) \begin{array}{c} \text{Diagram 15} \\ \text{Diagram 16} \end{array} = - (-1) \begin{array}{c} \text{Diagram 17} \\ \text{Diagram 18} \end{array} \\
& + \left(\begin{array}{c} \text{Diagram 19} \\ \text{Diagram 20} \end{array} - \begin{array}{c} \text{Diagram 21} \\ \text{Diagram 22} \end{array} \right) \\
& \qquad \qquad \qquad 2l1-6 \\
& + (-1) \begin{array}{c} \text{Diagram 23} \\ \text{Diagram 24} \end{array} = + (-1) \begin{array}{c} \text{Diagram 25} \\ \text{Diagram 26} \end{array} \\
& - \left(\begin{array}{c} \text{Diagram 27} \\ \text{Diagram 28} \end{array} - \begin{array}{c} \text{Diagram 29} \\ \text{Diagram 30} \end{array} \right) \\
& \qquad \qquad \qquad 2l7-4
\end{aligned}$$

Figure 126: $R_2(m) = 0$ for l_a1-7 , l_a1-5 , l_a1-6 and l_a7-4

$$\begin{aligned}
& + \begin{array}{c} \text{crossing with 3 positive signs} \end{array} = + \begin{array}{c} \text{crossing with 1 negative and 1 positive sign} \end{array} \\
& + \left(\begin{array}{c} \text{crossing with 2 positive and 1 negative sign} \end{array} - \begin{array}{c} \text{crossing with 1 negative and 1 positive sign} \end{array} \right) \\
& + \left(\begin{array}{c} \text{crossing with 2 positive and 1 negative sign} \end{array} - \begin{array}{c} \text{crossing with 1 positive and 1 negative sign} \end{array} \right)
\end{aligned}$$

Figure 127: $R_2(m) = 0$ for $r_a 1 - 7$

exactly to the local types for which the distinguished crossing d is a negative crossing and which form a half of the hexagon). We show the calculations of $R_1(m) = 0$ for the edges $7 - 4$ and $3 - 5$ in Fig. 128. For all other local types the singularization is exactly the same as for R_1 in the case of long knots (but notice the sign change, which comes from our sign change for the local type 1 in the case of closed braids).

For the global types l there can be contributions from the involved four crossings only if at least two of the three crossings of the triple crossing have marking 1. But this is exactly the only global type for which the crossing ml becomes singular. The self-tangencies could contribute now if the crossing hm or ml is a crossing of the self-tangency. We use again the corresponding figures from the case of long knots and we show the calculations of $R_1(m) = 0$ in Fig. 129-130

□

This finishes the proof of Theorem 3.

Proposition 13 *Let m be a meridian of $\Sigma_{trans-self}^{(2)}$ or a loop in Γ . Then $R_2(m) = 0$ in $\hat{\beta}_2$ for the singularizations given in Definition 24.*

Proof. Let's start with the global type r . If the distinguished crossing is of marking 1 and it is not a crossing from the self-tangency then it is the only crossing of marking 1 amongst the four involved crossings. In this case the singularization is exactly the same as in the case of long knots. The distinguished crossing d is a crossing of the self-tangency exactly for the edges $7 - 4$ and $3 - 5$. Using again the corresponding figures from the case

$$\begin{aligned}
& + W(p) \left(\begin{array}{c} \text{Diagram 1} \\ \text{Diagram 2} \end{array} \right) \\
& + W(p) \left(\begin{array}{c} \text{Diagram 3} \\ \text{Diagram 4} \end{array} \right) \\
& = + (W(p) + 1) \left(\begin{array}{c} \text{Diagram 5} \\ \text{Diagram 6} \end{array} \right) \\
& + W(p) \left(\begin{array}{c} \text{Diagram 7} \\ \text{Diagram 8} \end{array} \right) \\
& \quad \text{br7-4} \\
& - W(p) \left(\begin{array}{c} \text{Diagram 9} \\ \text{Diagram 10} \end{array} \right) \\
& + W(p) \left(\begin{array}{c} \text{Diagram 11} \\ \text{Diagram 12} \end{array} \right) \\
& = - (W(p) + 1) \left(\begin{array}{c} \text{Diagram 13} \\ \text{Diagram 14} \end{array} \right) \\
& + W(p) \left(\begin{array}{c} \text{Diagram 15} \\ \text{Diagram 16} \end{array} \right) \\
& \quad \text{br5-3}
\end{aligned}$$

Figure 128: $R_1(m) = 0$ for $r7 - 4$ (respectively $r5 - 3$) in the braid case if $W(p)$ for the local type 4 (respectively 3) is corrected by -1

$$\begin{array}{c}
+ \quad \text{[Diagram: A braid with two strands crossing. The left strand has a dot with a '+' sign below it. The right strand has a dot with a '+' sign below it. The strands are labeled with arrows.] } = + \quad \text{[Diagram: A braid with two strands crossing. The left strand has a dot with a '+' sign below it. The right strand has a dot with a '+' sign below it. The strands are labeled with arrows.] } \\
bl1-7
\end{array}$$

$$\begin{array}{c}
+ \quad \text{[Diagram: A braid with two strands crossing. The left strand has a dot with a '+' sign below it. The right strand has a dot with a '+' sign below it. The strands are labeled with arrows.] } = + \quad \text{[Diagram: A braid with two strands crossing. The left strand has a dot with a '+' sign below it. The right strand has a dot with a '+' sign below it. The strands are labeled with arrows.] } \\
bl7-4
\end{array}$$

$$\begin{array}{c}
+ \quad \text{[Diagram: A braid with two strands crossing. The left strand has a dot with a '+' sign below it. The right strand has a dot with a '+' sign below it. The strands are labeled with arrows.] } = + \quad \text{[Diagram: A braid with two strands crossing. The left strand has a dot with a '+' sign below it. The right strand has a dot with a '+' sign below it. The strands are labeled with arrows.] } \\
\end{array}$$

$$\begin{array}{c}
+ (-1) (\quad \text{[Diagram: A braid with two strands crossing. The left strand has a dot with a '-' sign below it. The right strand has a dot with a '-' sign below it. The strands are labeled with arrows.] } - \quad \text{[Diagram: A braid with two strands crossing. The left strand has a dot with a '+' sign below it. The right strand has a dot with a '+' sign below it. The strands are labeled with arrows.] }) \\
bl4-8
\end{array}$$

$$\begin{array}{c}
- \quad \text{[Diagram: A braid with two strands crossing. The left strand has a dot with a '-' sign below it. The right strand has a dot with a '-' sign below it. The strands are labeled with arrows.] } = - \quad \text{[Diagram: A braid with two strands crossing. The left strand has a dot with a '-' sign below it. The right strand has a dot with a '-' sign below it. The strands are labeled with arrows.] } \\
bl3-8
\end{array}$$

Figure 129: $R_1(m) = 0$ for $l1 - 7$, $l7 - 4$, $l4 - 8$, $l3 - 8$ in the braid case

$bl5-3$

$bl1-5$

Figure 130: $R_1(m) = 0$ for $l5 - 3$, $l1 - 5$ in the braid case

of long knots we show the calculation of $R_2(m)$ in Fig. 131. In both cases a new relation occurs, but $R_2(m) = 0$ by the applications of the embedded 2T-relation, compare Definition 5.

For the global types l again there can be contributions only if at least two of the three crossings of the triple crossing have marking 1. But this is exactly the only global type for which the crossings ml and hm become singular. The self-tangencies could contribute now if the crossing hm or ml is a crossing of the self-tangency. We use again the corresponding figures from the case of long knots and we show the calculation of $R_2(m) = 0$ in Fig. 132-133. Notice that we do not need the embedded 2T-relation for the global type l but only for the global type r .

□

This finishes the proof of Theorem 4.

4.6 Moving cusps

Lemma 5 *The value of the 1-cocycles R_1 and R_2 on a meridian of $\Sigma^{(1)} \cap \Sigma_{cusp}^{(1)}$ is zero.*

Proof. The new crossing from $\Sigma_{cusp}^{(1)}$ could be a f-crossing in R_1 for the Reidemeister move in $\Sigma^{(1)}$. However, it is an isolated crossing and in particu-

$$\begin{aligned}
& + (-1) (\text{diagram 1} - \text{diagram 2}) \\
& = + (\text{diagram 3} - \text{diagram 4}) \\
& \qquad \qquad \qquad r7-4 \\
& - (-1) (\text{diagram 5} - \text{diagram 6}) \\
& = - (\text{diagram 7} - \text{diagram 8}) \\
& \qquad \qquad \qquad r5-3
\end{aligned}$$

Figure 131: $R_2(m)$ for $r7-4$ (respectively $r5-3$) in the braid case vanishes because of the embedded $2T$ -relation

$$+ \begin{array}{c} \nearrow \\ \text{+} \\ \text{+} \end{array} + \left(\begin{array}{c} \nearrow \\ \text{+} \\ \text{-} \end{array} - \begin{array}{c} \nearrow \\ \text{+} \\ \text{+} \\ \text{-} \end{array} \right)$$

$$= + \begin{array}{c} \nearrow \\ \text{+} \\ \text{-} \end{array}$$

l1-7

$$+ \begin{array}{c} \nearrow \\ \text{+} \\ \text{-} \end{array} = \begin{array}{c} \nearrow \\ \text{+} \\ \text{-} \end{array}$$

l7-4

$$+ \begin{array}{c} \nearrow \\ \text{+} \\ \text{-} \end{array} = + \begin{array}{c} \nearrow \\ \text{-} \\ \text{-} \end{array}$$

$$+ (-1) \left(\begin{array}{c} \nearrow \\ \text{-} \\ \text{-} \end{array} - \begin{array}{c} \nearrow \\ \text{+} \\ \text{-} \end{array} \right)$$

l4-8

Figure 132: $R_2(m)$ for $l1-7$, $l7-4$, $l4-8$ in the braid case

$$\begin{aligned}
& - \left(\text{Diagram 1} \right) + (-1) \left(\text{Diagram 2} - \text{Diagram 3} \right) \\
& = - \left(\text{Diagram 4} \right)
\end{aligned}$$

$l3-8$

$$\text{Diagram 5} = - \text{Diagram 6}$$

$l5-3$

$$\begin{aligned}
& - \left(\text{Diagram 7} \right) = - \left(\text{Diagram 8} \right) \\
& + \left(\text{Diagram 9} - \text{Diagram 10} \right)
\end{aligned}$$

$l1-5$

Figure 133: $R_2(m)$ for $l3-8$, $l5-3$, $l1-5$ in the braid case

lar it has no r-crossings at all. If it is a f-crossing for R_2 then its contribution is annihilated by the generalized embedded 1T-relation.

□

We have to deal now with the irreducible strata of codimension two which contain a diagram with a cusp. Notice that the local types 2 and 6 can evidently not occur as triple crossings. There are exactly sixteen possible local types. We list them in Fig. 134...Fig. 137, where we move the branch from the right to the left. For each local type we have exactly two global types, corresponding to the position of the point at infinity. We give in the figure also the Gauss diagrams of the triple crossing and of one of the self-tangencies. Notice that in each Gauss diagram of a triple crossing one of the three arcs is empty besides just one head or foot of an arrow. Let us denote each stratum of $\Sigma_{trans-cusp}^{(2)}$ simply by the global type of the corresponding triple crossing.

First of all we show that it is necessary to use the quadratic weight W_2 for the construction of R_1 . Indeed, assume that we replace W_2 by a linear weight W (which is just the sum of the writhes of the f-crossings) as indicated in Lemma 3. This implies that we have to replace W_2 by W for the self-tangencies too and that we have to replace the linear weight W_1 for the types r_a and l_c by the constant weight 1. We show the meridian of a stratum $\Sigma_{r_a}^{(2)}$ of local type 1 in Fig. 138. The calculation of $R_1(m)$ with linear weight is shown in Fig. 139. We have no control over the resulting singular knot because it depends on the place of the cusp in the knot diagram. This forces us indeed to use the quadratic weight in the definition of R_1 .

Lemma 6 *If $R_1(m) = 0$ for $\Sigma_{trans-cusp}^{(2)}$ with one orientation of the moving branch then it is also 0 for the other orientation of the moving branch.*

Proof. It suffices to notice that the contributions of the two Reidemeister II moves shown in Fig. 140 obviously cancel out.

□

Proposition 14 *Let m be a meridian of $\Sigma_{trans-cusp}^{(2)}$. Then $R_1(m) = 0$ for $\Sigma_{l_c}^{(2)}$ because of the embedded 1T-relation. $R_1(m) = 0$ for all other strata of $\Sigma_{trans-cusp}^{(2)}$ without using the embedded 1T-relation.*

Proof.

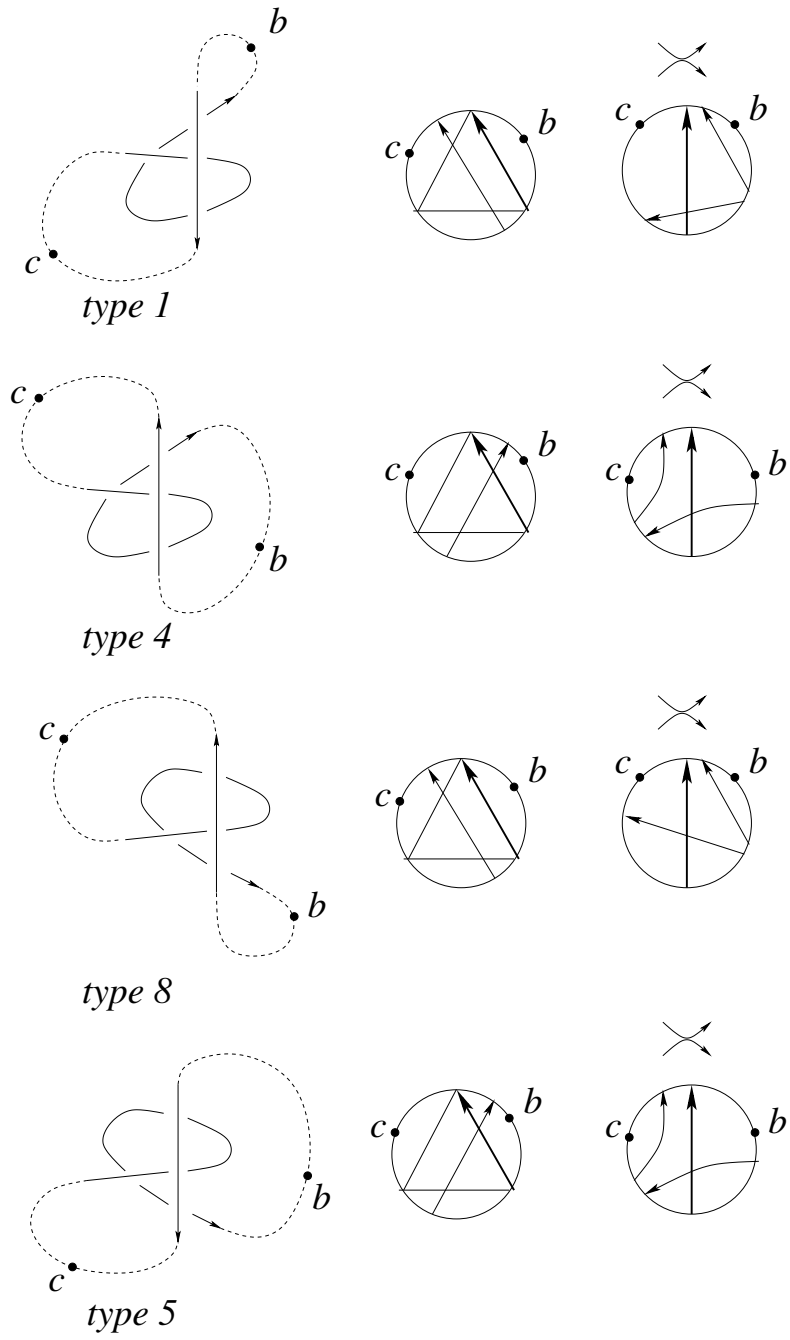


Figure 134: the strata $\Sigma_{l_c}^{(2)}$ and $\Sigma_{l_b}^{(2)}$

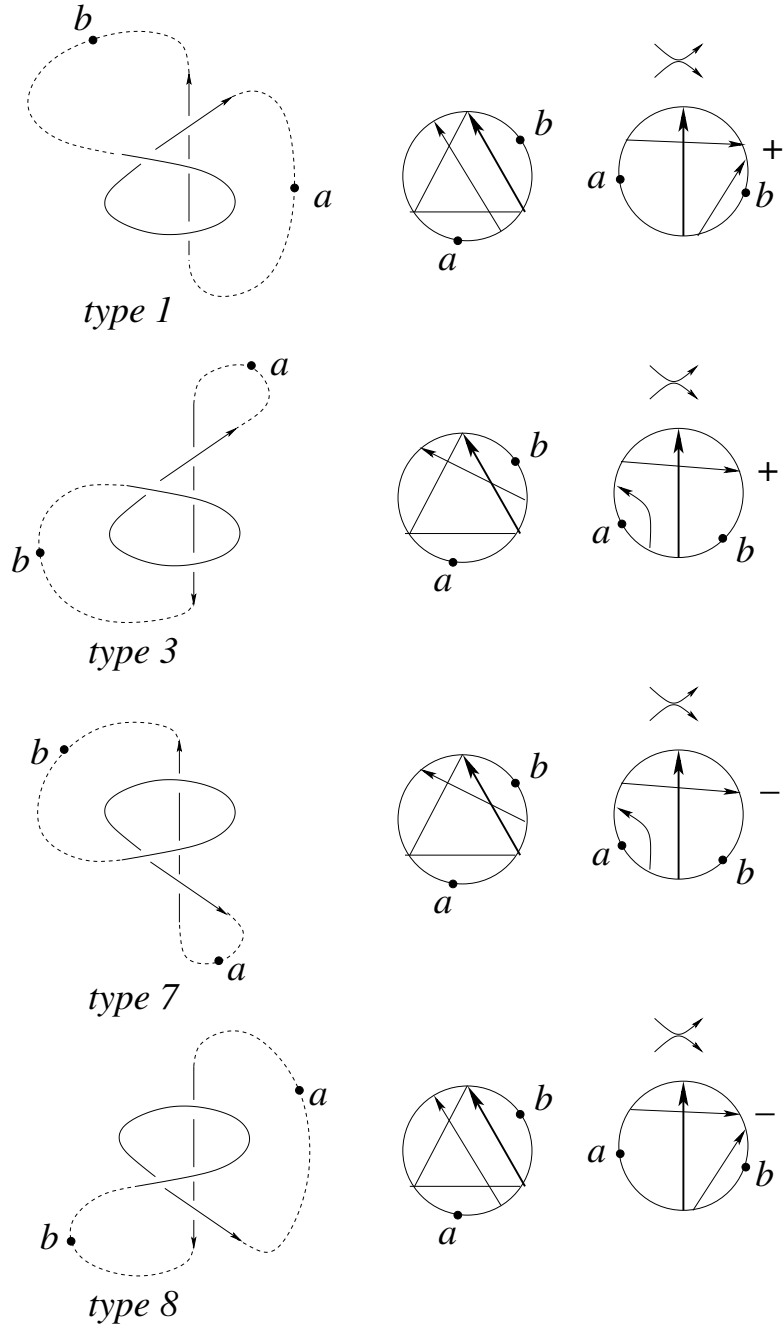


Figure 135: the strata $\Sigma_{l_a}^{(2)}$ and $\Sigma_{l_b}^{(2)}$

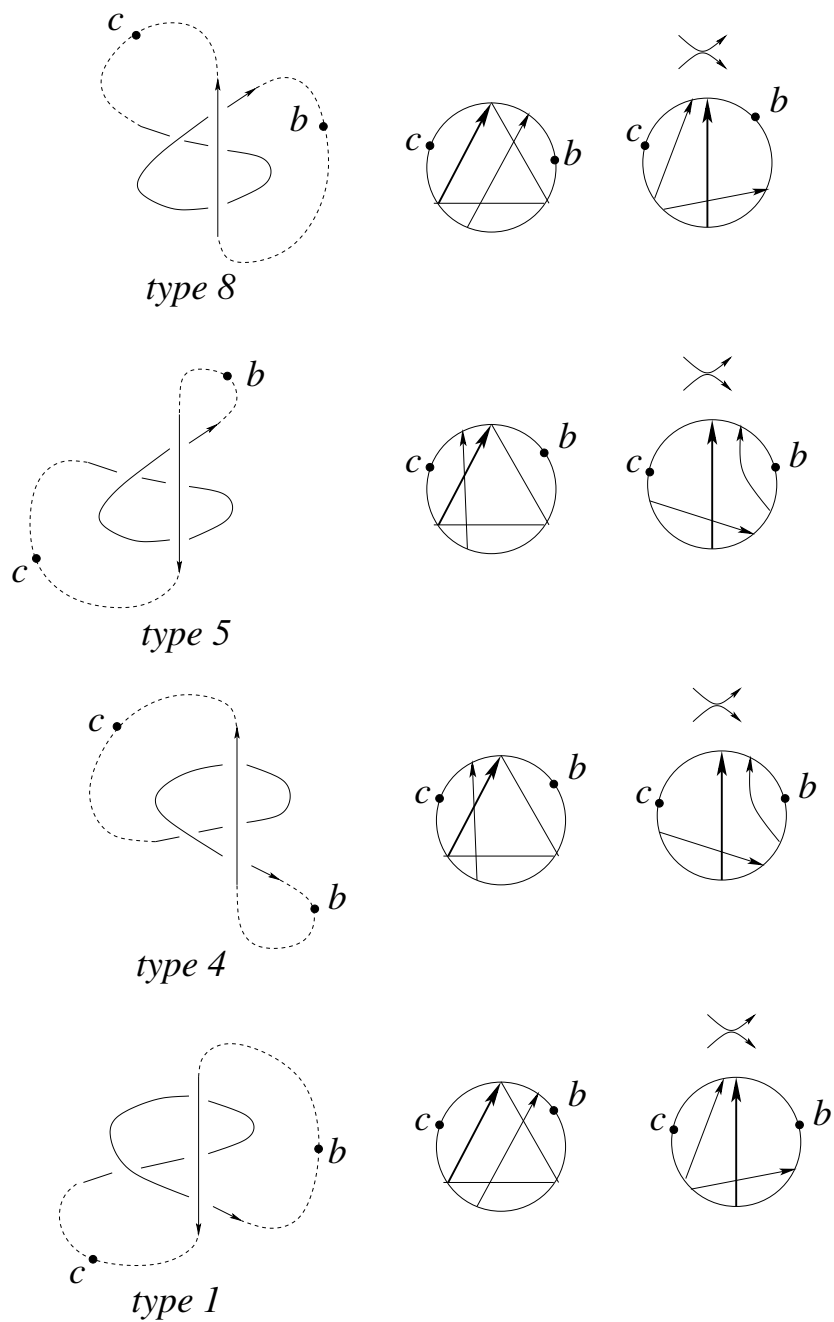


Figure 136: the strata $\Sigma_{r_b}^{(2)}$ and $\Sigma_{r_c}^{(2)}$

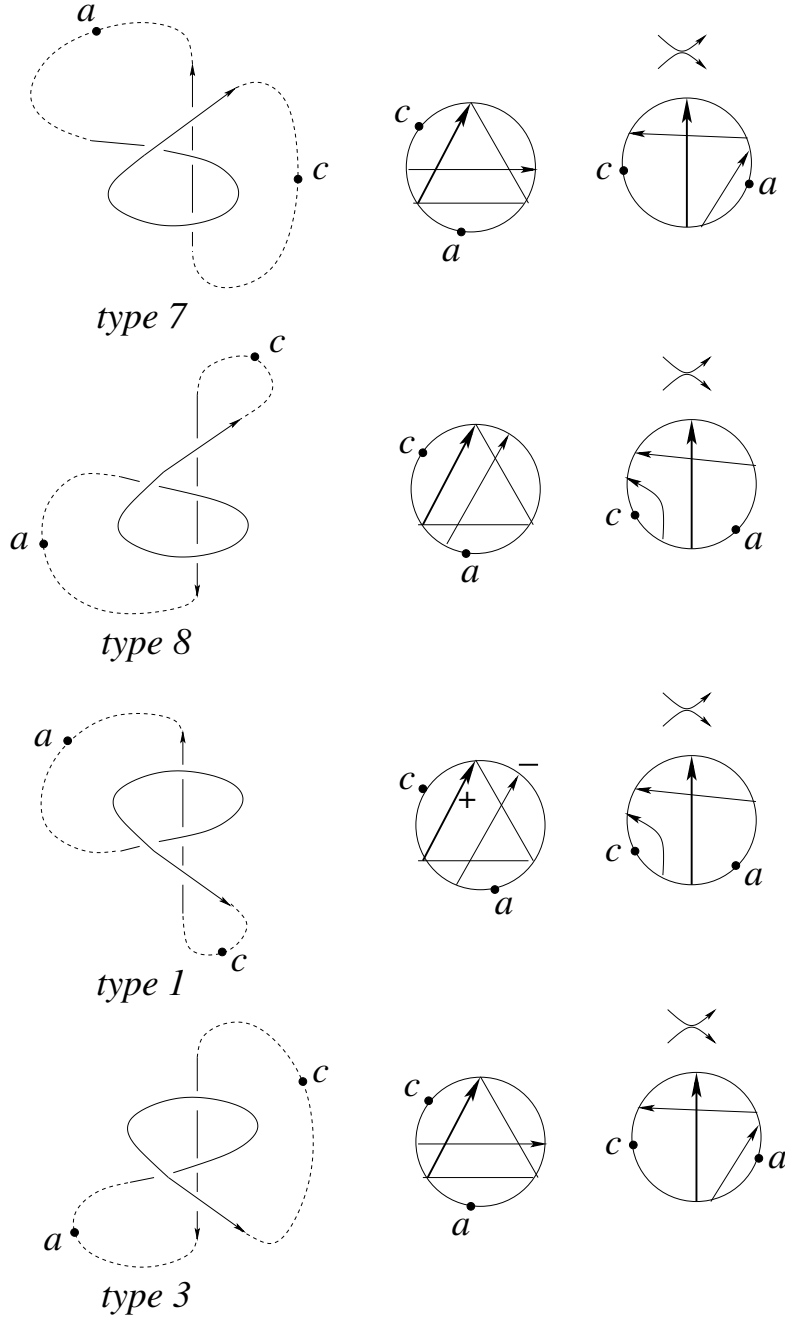


Figure 137: the strata $\Sigma_{r_a}^{(2)}$ and $\Sigma_{r_c}^{(2)}$

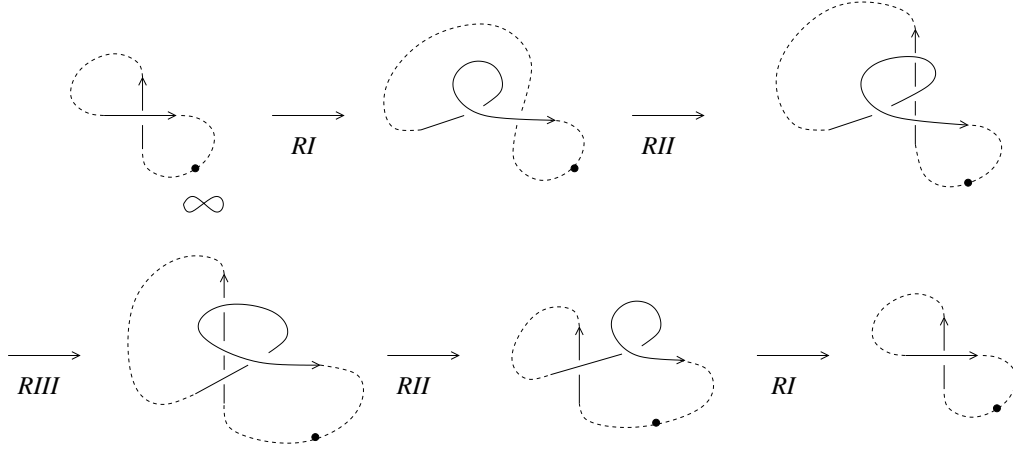


Figure 138: The meridian of a stratum $\Sigma_{r_a}^{(2)}$ of local type 1

$$\begin{aligned}
& + W(p) \left(\begin{array}{c} \uparrow \\ \text{Diagram 1} \\ \downarrow \end{array} - \begin{array}{c} \uparrow \\ \text{Diagram 2} \\ \downarrow \end{array} \right) \\
& - \begin{array}{c} \uparrow \\ \text{Diagram 3} \\ \downarrow \end{array} - W(p) \left(\begin{array}{c} \uparrow \\ \text{Diagram 4} \\ \downarrow \end{array} - \begin{array}{c} \uparrow \\ \text{Diagram 5} \\ \downarrow \end{array} \right) \\
& - W(p) \left(\begin{array}{c} \uparrow \\ \text{Diagram 6} \\ \downarrow \end{array} - \begin{array}{c} \uparrow \\ \text{Diagram 7} \\ \downarrow \end{array} \right) \\
& = - \begin{array}{c} \uparrow \\ \text{Diagram 8} \\ \downarrow \end{array} = - \begin{array}{c} \uparrow \\ \text{Diagram 9} \\ \downarrow \end{array}
\end{aligned}$$

Figure 139: Calculation of $R_1(m)$ with linear weight on the meridian of $\Sigma_{r_a}^{(2)}$

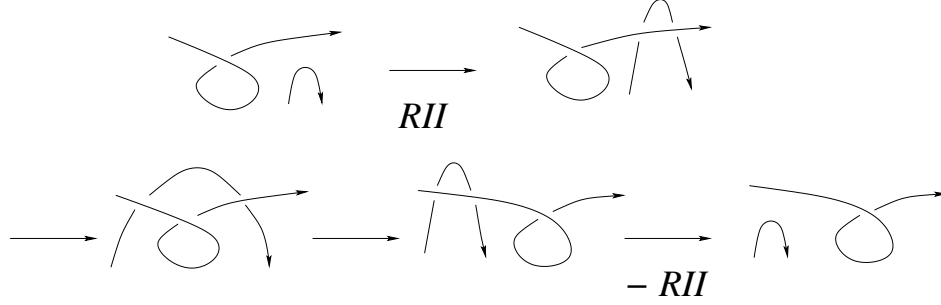


Figure 140: two Reidemeister *II* moves with canceling contributions

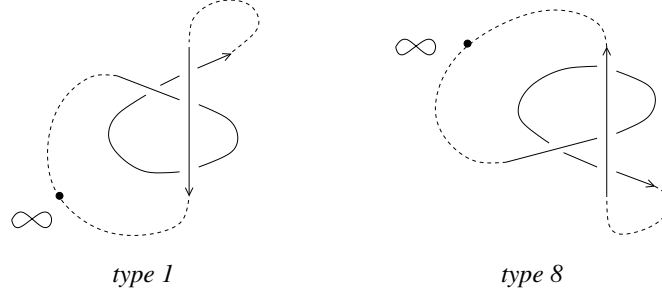


Figure 141: The strata $\Sigma_{l_c}^{(2)}$ of type 1 and 8

For the type $\Sigma_{l_c}^{(2)}$ only the triple crossing contributes to $R_1(m)$, namely by $W_1(p)$ times the knot with the double point in ml . It follows now from Lemma 6 that it is sufficient to consider the local types 1 and 8. We show them in Fig. 141. But ml is just the new crossing created from the cusp and the embedded 1T-relation applies.

We show that $R_1(m) = 0$ for $\Sigma_{l_b}^{(2)}$ (respectively $\Sigma_{r_a}^{(2)}$) of type 1 in Fig. 142. All other cases are completely analogous and are left to the reader.

□

This finishes the proof of Theorem 1.

Proposition 15 *Let m be a meridian of $\Sigma_{trans-cusp}^{(2)}$. Then $R_2(m) = 0$.*

Proof.

Notice that the new crossing from the cusp is never the distinguished crossing d for the triple crossing. One easily sees from Fig. 134...Fig. 137 that there is never a f-crossing amongst the four involved crossings besides for the degenerate cases l_a and r_a . Consequently, the proof of Proposition

$$\begin{aligned}
& +W_2 \left(\begin{array}{c} \uparrow \\ \diagup \quad \diagdown \\ \bullet + \\ \downarrow \end{array} - \begin{array}{c} \uparrow \\ \diagup \quad \diagdown \\ \bullet - \\ \downarrow \end{array} \right) \\
& -W_2 \left(\begin{array}{c} \uparrow \\ \diagup \quad \diagdown \\ \bullet + \\ \downarrow \end{array} - \begin{array}{c} \uparrow \\ \diagup \quad \diagdown \\ \bullet + \\ \downarrow \end{array} \right) \\
& -W_2 \left(\begin{array}{c} \uparrow \\ \diagup \quad \diagdown \\ \bullet + \\ \downarrow \end{array} - \begin{array}{c} \uparrow \\ \diagup \quad \diagdown \\ \bullet - \\ \downarrow \end{array} \right) = 0 \\
& \qquad \qquad \qquad \Sigma_{l_b}^{(2)}
\end{aligned}$$

$$\begin{aligned}
& +W_2 \left(\begin{array}{c} \uparrow \\ \diagup \quad \diagdown \\ \bullet + \\ \downarrow \end{array} - \begin{array}{c} \uparrow \\ \diagup \quad \diagdown \\ \bullet - \\ \downarrow \end{array} \right) \\
& -W_2 \left(\begin{array}{c} \uparrow \\ \diagup \quad \diagdown \\ \bullet + \\ \downarrow \end{array} - \begin{array}{c} \uparrow \\ \diagup \quad \diagdown \\ \bullet + \\ \downarrow \end{array} \right) \\
& -W_2 \left(\begin{array}{c} \uparrow \\ \diagup \quad \diagdown \\ \bullet + \\ \downarrow \end{array} - \begin{array}{c} \uparrow \\ \diagup \quad \diagdown \\ \bullet - \\ \downarrow \end{array} \right) = 0 \\
& \qquad \qquad \qquad \Sigma_{r_a}^{(2)}
\end{aligned}$$

Figure 142: $R_1(m) = 0$ for $\Sigma_{l_b}^{(2)}$ and $\Sigma_{r_a}^{(2)}$

$$\begin{aligned}
& + \left(\begin{array}{c} \text{Diagram 1} \end{array} - \begin{array}{c} \text{Diagram 2} \end{array} \right) \\
& + \left(\begin{array}{c} \text{Diagram 3} \end{array} - \begin{array}{c} \text{Diagram 4} \end{array} \right) \\
& - \left(\begin{array}{c} \text{Diagram 5} \end{array} - \begin{array}{c} \text{Diagram 6} \end{array} \right) = 0
\end{aligned}$$

Figure 143: $R_2(m) = 0$ for $\Sigma_{l_b}^{(2)}$ and $\Sigma_{l_c}^{(2)}$ of local type 1

$$\begin{aligned}
& - \left(- \begin{array}{c} \text{Diagram 1} \end{array} \right) = 0 \qquad - \begin{array}{c} \text{Diagram 2} \end{array} = 0 \\
& \qquad \qquad \Sigma_{l_a}^{(2)} \qquad \qquad \Sigma_{r_a}^{(2)}
\end{aligned}$$

Figure 144: $R_2(m) = 0$ for $\Sigma_{l_a}^{(2)}$ and $\Sigma_{r_a}^{(2)}$ of local type 1

14 still applies besides for the new case $\Sigma_{l_c}^{(2)}$ with d as singular crossing. The distinguished crossings for the two self-tangencies are always the same, namely the crossing hm for the triple crossing. However, the self-tangencies and the triple crossing have exactly the same f-crossings because hm and d of the triple crossing have the same head and the arc which connects their foot in the circle is empty. We show the calculation for l_b and l_c of local type 1 in Fig. 143. The f-crossings are all the same and far away (and therefore they are not drawn in the figure). The calculation of $R_2(m) = 0$ for $\Sigma_{l_a}^{(2)}$ (respectively $\Sigma_{r_a}^{(2)}$) of type 1 is shown in Fig. 144. All other cases are completely analogous and are left to the reader.

Notice that we need here the generalized embedded 1T-relation.

□

This finishes the proof of Theorem 2.

References

- [1] Alvarez M., Labastida J.: Vassiliev invariants for torus knots, *J. Knot Theory Ramif.* 5 (1996), 779-803
- [2] Band G., Boyland P.: The Burau estimate for the entropy of a braid, *arXiv: math/0612716v2*
- [3] Bar-Natan D. : On the Vassiliev knot invariants, *Topology* 34 (1995) 423-472
- [4] Bar-Natan D. (with Jana Archibald, Karene Chu, Thomas Fiedler): Some HOMFLYPT one parameter knot theory computations, www.toronto.edu/drorbn/misc/
- [5] Bar-Natan D., Thang T. Q. Le, Thurston D.: Two applications of elementary knot theory to Lie algebras and Vassiliev invariants, *Geometry & Topology* 7 (2003) 1-31
- [6] Birman J. : Braids , Links and Mapping class groups, *Annals of Mathematics Studies* 82 , Princeton University Press (1974)
- [7] Birman J., Gebhardt V., González-Meneses J.: Conjugacy in Garside groups III: Periodic braids, *J. of Algebra* 316 (2007) 746-776
- [8] Budney R., Conant J., Scannell K., Sinha D.: New perspectives on self-linking, *Advances in Math.* 191 (2005) 78-113
- [9] Budney R., Cohen F. : On the homology of the space of knots, *Geometry & Topology* 13 (2009) 99-139
- [10] Budney R. : Topology of spaces of knots in dimension 3, *Proceedings London Math. Soc.* 101 (2010) 477-496
- [11] Burde G., Zieschang H. : Knots, *de Gruyter Studies in Mathematics* 5, Berlin (1985)

- [12] Costantino F., Guéritaud F., van der Veen R. : On the volume conjecture for polyhedra, arXiv:1403.2347
- [13] Fathi A., Laudenbach F., Poenaru V.: Travaux de Thurston sur les surfaces, Asterisque 66-67, SMF Paris (1979)
- [14] Fiedler T. : Gauss Diagram Invariants for Knots and Links, Mathematics and Its Applications 532 , Kluwer Academic Publishers (2001)
- [15] Fiedler T. : Isotopy invariants for closed braids and almost closed braids via loops in stratified spaces, arXiv: math.GT/0606443
- [16] Fiedler T. : Knot polynomials via one parameter knot theory, arXiv: math/0612115
- [17] Fiedler T. : The Jones and Alexander polynomials for singular links, J. Knot Theory Ramif. 19 (2010) 859-866
- [18] Fiedler T. : Quantum one-cocycles for knots, arXiv: 1304.0970v2 (177 pp)
- [19] Fiedler T., Kurlin V. : A one-parameter approach to knot theory, J. Math. Soc. Japan 62 (2010) 167-211
- [20] Fuji H., Gukov S., Sulkowski P., (appendix by Awata H.) : Volume conjecture: Refined and Categorized, arXiv: 1203.2182 [hep-th]
- [21] Futer D., Kalfagianni E., Purcell J.: Guts of surfaces and the colored Jones polynomial, Lecture Notes in Math. (Springer) 2069 (2013)
- [22] Futer D., Kalfagianni E., Purcell J.: Jones polynomials, volume and essential knot surfaces: a survey, arXiv: 1110.6388
- [23] Futer D., Kalfagianni E., Purcell J.: Quasifuchsian state surfaces, arXiv: 1209.5719
- [24] Garoufalidis T. : Quantum knot invariants, arXiv:1201.3314

- [25] Gramain A.: Sur le groupe fondamental de l'espace des noeuds, Ann. Inst. Fourier 27 (1977) 29-44
- [26] Goussarov M., Polyak M., Viro O.: Finite type invariants of classical and virtual knots, Topology 39 (2000) 1045-1068
- [27] Hatcher A. : Topological moduli spaces of knots, arXiv: math.GT/9909095
- [28] Jones V.: Hecke algebra representations of braid groups and link polynomials, Ann. of Math. 126 (1987) 335-388
- [29] Kashaev R.: The hyperbolic volume of knots from the quantum dilogarithm, Lett. Math. Phys. 39 (1997) 269-275
- [30] Kashaev R., Korepanov I., Sergeev S.: Functional tetrahedron equation, Theoret. and Math. Phys. 117 (1998) 1402-1413
- [31] Kauffman L. : Knots and Physics, World Scientific, Singapore (1991)
- [32] Kauffman L. : Virtual knot theory, European J. Comb. 20 (1999) 663-690
- [33] Kauffman L., Vogel P.: Link polynomials and a graphical calculus, J. Knot Theory Ramif. 1 (1992) 59-104
- [34] Ko K.H., Los J., Song W.T.: Entropy of braids, J. Knot Theory Ramif. 11 (2002) 647-666
- [35] Kolev B.: Entropie topologique et représentation de Burau, C.R. Acad. Sci. Paris Sér. I Math. 309 (1989) 835-838
- [36] Kolev B.: Dynamique topologique en dimension 2. Orbites périodiques et entropie topologique. Thèse de doctorat de l'Université de Nice (1991)
- [37] Kontsevich M.: Vassiliev's knot invariants, Adv. in Sov. Math. 16 (1993) 137-150
- [38] Thang T. Q. Le : The colored Jones polynomial and the A-polynomial for knots, Adv. Math. 207 (2006) 782-804

- [39] Mortier A.: Finite-type 1-cocycles of knots given by Polyak-Viro formulas, sites.google.com/site/mortier2x0/home/publications-thesis-and-preprints
- [40] Morton H.R.: Infinitely many fibred knots having the same Alexander polynomial, *Topology* 17 (1978) 101-104
- [41] Murakami H., Murakami J.: The colored Jones polynomials and the simplicial volume of a knot, *Acta Math.* 186 (2001) 85-104
- [42] Polyak M., Viro O.: Gauss diagram formulas for Vassiliev invariants, *Internat. Math. Res. Notes* 11 (1994) 445-453
- [43] Polyak M., Viro O.: On the Casson knot invariant, *J. Knot Theory Ramif.* 10 (2001) 711-738
- [44] Przytycki J.: Skein modules of 3-manifolds, *Bull. Polish Acad. Sci. Math.* 39 (1991) 91-100
- [45] Sakai K.: An integral expression of the first non-trivial one-cocycle of the space of long knots in \mathbb{R}^3 , *Pacific J. Math.* 250 (2011) 407-419
- [46] Thurston W.: *The Geometry and Topology of Three-Manifolds*, <http://www.msri.org/publications/books/gt3m/>
- [47] Turchin V. : Computation of the first non-trivial 1-cocycle in the space of long knots, (Russian) *Mat. Zametki* 80 (2006), no. 1, 105-114; translation in *Math. Notes* 80 (2006), no. 1-2, 101-108.
- [48] Turaev V. : The Yang-Baxter equation and invariants of links, *Invent. Math.* 92 (1988) 527-553
- [49] Turaev V.: The Conway and Kauffman modules of a solid torus, *J. Soviet. Math.* 52 (1990) 2799-2805
- [50] Vassiliev V. : Cohomology of knot spaces // in: *Theory of Singularities and its Applications*, *Advances in Soviet. Math.* 1 (1990) 23-69

- [51] Vassiliev V. : Combinatorial formulas of cohomology of knot spaces, Moscow Math. Journal 1 (2001) 91-123
- [52] Volic I.: On the cohomology of spaces of links and braids via configuration space integrals, arXiv: 1002.2467
- [53] Witten E.: Quantum field theory and the Jones polynomial, Comm. Math. Phys. 121 (1989) 351-399

Institute de Mathématiques de Toulouse
Université Paul Sabatier
118, route de Narbonne
31062 Toulouse Cedex 09, France
fiedler@math.univ-toulouse.fr